2011

Characterization of the Impact of Process Variables on the Densification of Corn Stover

Curtis Peder Thoreson
Iowa State University

Characterization of the impact of process variables on the densification of corn stover

by

Curtis Peder Thoreson

A thesis submitted to the graduate faculty
in partial fulfillment of the requirements for the degree of
MASTER OF SCIENCE

Major: Agricultural Engineering (Advanced Machinery Engineering)

Program of Study Committee:
Matthew J. Darr, Major Professor
Stuart J. Birrell
Brian L. Steward
Thomas J. Brumm

Iowa State University
Ames, Iowa
2011

Dedication

I dedicate this thesis to my parents, Jon and Gail Thoreson. Without their patience, understanding, support, and most of all love, the completion of this work would not have been possible.

Table of Contents

List of Figures

List of Tables

List of Equations

Acknowledgments

I would like to thank the North Central Regional Sun Grant Center for providing funding for this work. I would also like to thank Dr. Matt Darr for his direction, assistance, and guidance throughout this entire project. I also wish to thank Dr. Steven Hoff and Dr. Stuart Birrell for their assistance during the development of the densification test bench.

Special thanks should also be given to my student colleagues who helped me in many ways. To Keith Webster, Jeremiah Johnson, Robert McNaull, and Jon Roth for their support with the test bench development, fabrication, and validation. To Eric Fredrickson, Kent Thoreson, Mark Nie, Matt Kenyon, and Kyle Degener for their assistance with conducting the experiments. Finally, I would like to express my gratitude to Amber Thoreson, my wife, for her encouragement and assistance. Without the generous help of these individuals, this research would not have been possible.

Abstract

The bulk density of corn stover poses a major obstruction to its large scale viability as a biomass feedstock. Corn stover has a low bulk density which limits transportation and storage containers based on volume rather than weight, creating large inefficiencies during the harvest, transport, and storage phases of corn stover production. Producing a densified stover product during the harvest phase of production could reduce the overall production cost of corn stover.

Corn stover can currently be densified by grinding, baling, briquetting, or pelleting methods. Grinding systems do not produce an adequate bulk density to optimize transportation requirements alone, and are often used as a pre-processing operation for other densification systems. Baling can provide an improved bulk density at low energy requirements, but faces a logistical challenge associated with handling individual bales. Pelleting and briquetting systems generally require grinding as an initial process, and provide a high quality densified stover product at low mass flow rates and very high energy requirements. All of these factors drive up the production cost of densified corn stover for each system.

This research investigated a densification method that produced a large, tapered and cylindrical, densified stover product. This research differentiated itself from previous briquetting and pelleting work because these briquettes were produced at field harvested particle sizes and lower compression pressures. While this produced a lower quality and density briquette than traditional briquetting and pelleting processes, the energy requirement was significantly reduced. This type of densified corn stover product could be suitable for in-field single-pass corn stover harvesting systems where the material is harvested and stored until further processing (the densified product is not the final product).

Chapter 1. Introduction

1.1. Background

Corn stover is a widely available biomass resource for use as a feedstock for biofuel production. In 2005, the USDA estimated that approximately 75 million dry tons of corn stover were available annually for a biomass industry (DOE, 2005). Depending on the agricultural setting and feedstock use, corn stover can be harvested in various fractions and amounts to minimize negative soil impacts and material moisture content, and maximize feedstock potential for processing. The low bulk density of corn stover poses a major obstruction to its large scale acceptance as a biomass feedstock. The loose bulk density of chopped corn stover ranges from 40 to 80 kg/m^3 (2.5-5 lb/ft^3) (Knutson & Miller, 1982) which is low enough to create large inefficiencies during the harvest, transport, and storage phases of production. These inefficiencies are created because transportation vehicles loaded with corn stover are restricted by volume capacity rather than weight capacity. A cost-effective means of increasing corn stover bulk density during the harvest phase will be critical to the feasibility of large-scale production.

Ideally, a densification system would densify the material in-field in order to minimize in-field transport wagons and trips, and maximize over-the-road truck loading potential. Current production self-unloading trailers suitable for transporting densified biomass have volumes of 65 to 90 m^3 (2300-3200 ft^3). Minimum bulk densities of a briquetted biomass to fully load these trailers range from 270 to 370 kg/m^3 (17-23 lb/ft^3) (limited by legal weight restrictions of 36290 kg (80000 lb) for tractor-trailer combinations, and accounting for the weight of the tractor and trailer). Current production in-field carts that are suitable for stover collection currently reach a maximum volume capacity of about 31 m^3 (1100 ft^3), and will require multiple trips to fully load a large truck. In-field cart sizes, however, are not strictly governed with a maximum weight limit like trucks are, so cart sizes can be catered to maximize in-field logistical efficiency.

1.2. Densification Techniques

Several methods can be used to densify corn stover including grinding, baling, briquetting, and pelleting. Grinding operations involve reducing the particle size of a

material, which increases bulk density. Baling operations utilize a reciprocating plunger to compress material into a chamber, and then wrap the compressed material with strings to hold it in a densified form. Briquetting and pelleting operations apply extreme pressure, and in many cases, heat energy to the input material to compress it into a specific shape that can be retained without additional binding mechanisms.

Grinding biomass is a common technique that has been commercialized for many different materials and purposes, is readily available, and can provide bulk density increases to a variety of materials. Studies of a tub-grinding biomass system showed that corn stover bulk densities of 50-100 kg/m^3 (3-6 lb/ft^3) (Kaliyan et al., 2009b) are possible with a single grinding operation. Hammer mill performance with corn stover has also been quantified, with the output bulk density ranging from 130 to 160 kg/m^3 (8-10 lb/ft^3), at a specific energy requirement range of 25 to 122 MJ/t (11-52 BTU/lb) (Mani et al., 2002). While grinding operations can increase the bulk density of stover, this operation by itself does not provide enough gain to maximize hauling efficiency. Grinding operations are also energy intensive, so a densification system should attempt to minimize the amount of grinding used within a densification process.

Baling biomass is another common technique that is commercialized today for the production of livestock feed and bedding. A study of single-pass large square baled corn stover in the fall 2009 and 2010 harvest at the Agricultural Engineering Farm at Iowa State University in Ames, IA showed baled corn stover wet bulk densities ranging from 180 to 230 kg/m^3 (11-14.5 lb/ft^3) (140-180 kg/m^3 (8.5-11.5 lb/ft^3) dry bulk density) from various fractions of stover. Multi-pass round baling systems were also tested in the surrounding area from Iowa State University, and showed that wet bulk densities of 140 to 160 kg/m^3 (120 to 140 kg/m^3 dry) could be achieved with corn stover. Baling studies conducted at the University of Wisconsin—Madison during the fall 2002 corn harvest indicated wet baled bulk densities ranging from 180 to 250 kg/m^3 (11-15.5 lb/ft^3) (Shinners et al., 2003) could be produced. While baling offers an increased bulk density over loose stover, it presents issues associated with bale handling, which complicates transportation logistics and drives up unit production costs.

A third technique that has been investigated for biomass production is briquetting/pelleting. Conventional systems first grind the biomass to a small particle size (<25 mm (1 in)), and then briquette or pellet it to produce the final product. Many of these systems induce heat to the input material either by convection or by machine friction during the process to enhance the binding characteristics. Studies of both roll-press briquetting and ring-die pelleting mills were conducted at the University of Minnesota over the past several years. Output bulk density ranged from 420 to 480 kg/m^3 (26-30 lb/ft^3) on the roll-press briquetting machine, and 550 to 610 kg/m^3 (34-38 lb/ft^3) at a specific energy requirement of 189 to 262 MJ/t (173.3-178.0 BTU/lb) on the ring-die pelleting machine (Kaliyan et al., 2009a). When compared with the mass flow outputs of a class 8 combine harvesting corn (2-5 kg/sec depending on corn stover fraction), the ring-die pelleting machine requires approximately 500-1500 kW (700-2000 Hp) to produce pellets at in-field capacities. This power requirement is well beyond the range of engine power commonly used in mobile agricultural production equipment today. While these systems offer great bulk density and product durability compared with baling and grinding systems, they require many operations and high energy input to complete, and are not feasible to accomplish in-field at common harvesting rates.

Table 1.1 shows a summary of the densification processes from the literature, and their energy requirements with respect to the average energy content of corn stover. (Pordesimo et al., 2003) reported the gross energy content of corn stover to be 16750-20930 MJ/t. Table 1.1 compares the methods below using the average gross energy content as a metric (18840 MJ/t).

Table 1.1. Previous densification research summary

Densification Method	Output Product Form	Wet Bulk Density (kg/m^3)	Specific Energy (MJ/t)	Specific Energy (% of stover)
None	Chopped Corn Stover	40-80	0	0%
Hammermill	Ground Corn Stover	130-160	25-122	0.1-0.6%
Large Square Baling	0.9 x 1.2 x 2.4 m bale	180-230	37	0.2%
Round Baling	1.8 m diameter x 1.5 m wide bale	140-160	NA	NA
Roll-Press Briquetting	Almond Shaped, 40 mm long	420-480	NA	NA
Ring-Die Pelleting	Cylindrical Shaped, 25 mm long, 10 mm diameter	550-610	189-262	1.0-1.4%

Chapter 2. Research Objectives

With the U.S. government mandating increased biofuel production from cellulosic feedstocks in the coming years, viable feedstocks and production systems need to be developed to meet a rising demand. Currently, about 36 million hectares (88 million acres) of corn are produced annually, providing a large amount of potential feedstock for cellulosic ethanol production (NASS, 2011). For a viable large scale corn stover supply to become a reality, several details affecting harvest, transportation, and storage must be addressed, including corn stover bulk density. The low bulk density of corn stover adversely affects in-field harvest logistics, and transportation and storage efficiency.

Long term, this research seeks to improve the cost and efficiency of corn stover production by developing a densification (briquetting) method that is feasible for in-field operations with current single-pass corn stover harvesting systems. Research has previously been conducted on potential pelleting and briquetting densification systems, but the majority of the systems researched required a very small input material particle size and had very high specific energy requirements. Reducing these specific energy requirements will reduce the specific cost of corn stover densification. This work sought to develop and test a densification system that did not require as much particle size reduction or energy as the previous systems. Three specific objectives were derived to accomplish the main objective of this research:

- Objective #1: Develop and test a small scale system to produce a densified corn stover product at large particle sizes (up to 102 mm) and at feasible energy requirements (require less than 370 kW to densify material at field capacity) for in-field densification systems. Test and quantify pertinent process variables to determine the basic system requirements (pressure, energy) and outputs (density) for densification of corn stover produced using single-pass harvesting technology.
- Objective #2: Determine the durability of the densified stover product, and compare results with other densified stover products.

- Objective #3: Determine optimal process variable treatment conditions for corn stover densification. Using these conditions, estimate the machine requirements for a large-scale densification system for use in a single-pass corn stover harvesting system. Compare estimated machine requirements with other single-pass densification technologies being researched for corn stover production.

This research differentiates itself from previous densification work in many ways. Focusing on testing densification characteristics of corn stover produced from real harvesting scenarios involving chopped particle sizes and field-harvested moisture contents allows this work to produce a better indication of the feasibility of this method for in-field densification systems. Testing this process under energy and power requirements which are feasible for traditional agricultural equipment allows this process to be scaled for in-field operation. Only corn stover fractions that can be produced using harvesting technology currently available are tested in this research. All of these factors combine to produce research that is well aligned with current corn stover crop and harvesting systems.

Chapter 3. Test Bench Development

3.1. Introduction

To meet the objectives described in chapter 2, an experimental corn stover densification system was developed that could densify corn stover at different material and mechanical settings. Some of the flexibility requirements of this experiment setup included:

- Must be capable of applying a variable compression pressure from 0-17 MPa (0-2500 psi). Previous research indicated that this compression pressure range could produce feasible energy and power requirements for scaled up densification processes, so this work focused on determining the capabilities of a densification system within this compression range.
- Densification region must be large enough to feed and densify a material particle size up to 102 mm particle length. This facilitated densification of field-harvested chopped corn stover without additional size reduction operations.
- Design must be flexible enough to facilitate quick mechanical modifications. Due to the experimental nature of this research, it was possible that early experiment observations would motivate design changes to the system. Designing the system to be easily modified would facilitate quicker design changes, if necessary.
- System must be able to log pertinent densification process data including pressure, power, and energy. This provided data used in determining densification energy and mechanical requirements.

3.2. Materials & Methods

3.2.1. Densification Bench – General Design

A bench based densification system was developed to meet the requirements from section 3.1. This bench was designed to vary critical machine settings, and could densify different material types, moisture contents, and particle sizes. The CAD model of the bench is shown in figure 3.1. This bench utilized a uni-axial piston cylinder to densify biomass by pressing the material into a tapered die (figure 3.2). Material was loaded into the cylinder from the opening at the top, and then pressed into the die using a plunger actuated by a

hydraulic cylinder. This process was repeated until a desired material compression pressure was reached, upon which the briquette was ejected from the die using a separate ejection press.

The piston-cylinder densification test machines illustrated in the literature all plunged material into a straight, cylindrical die. The dies were very small (<25 mm diameter), and thus the test machines were limited to small material particle sizes (Mani et al., 2004), (Kaliyan & Morey, 2006). The densification bench for this research utilized a larger diameter, tapered cylindrical die. A tapered cylindrical die exerts up to 20% more axial force from the die wall to the material than a straight cylindrical die (for the die taper angles tested in this research). This additional force could provide enough resistance to densify the material without the need for a cap on the die, potentially allowing the die to flow a densified product. The die had a 127 mm (5 in) inlet diameter, a 203 mm (8 in) length, and was easily removable to allow dies with different taper angles to be installed. The 127 mm (5 in) diameter material chamber had a plunger distance of 280 mm (11 in) to compress material into the die. The plunger could apply a maximum of 267 kN (60,000 lb) of compression force on the material, which met the compression pressure goal stated in section 3.1.

Preliminary testing of the tapered die showed that material variability did not allow a densified product to consistently flow through the machine. Different mechanical and material inputs would cause the machine to shift from flowing a non-densified stover product, to choking flow and producing a densified stover product. For the purposes of this research, an instrumented cap was added to the end of the die to stop material flow and measure the force distribution for different process variable combinations. This helped to quantify the different flow characteristics of the different process variables to determine if this system could be modified to consistently flow a densified product.

Figure 3.1. CAD model of the densification test bench

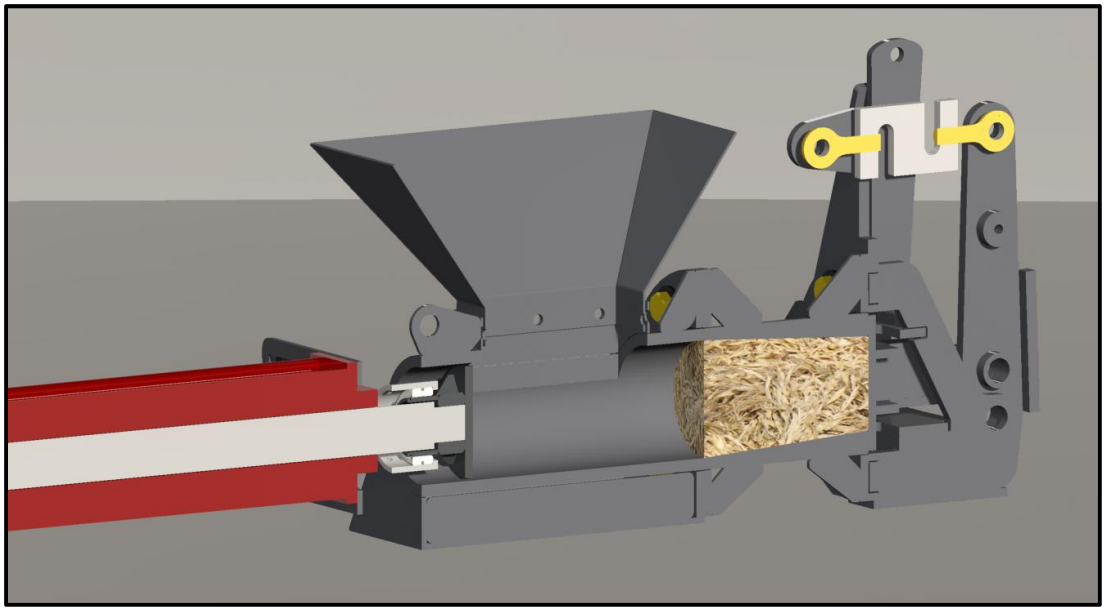

Figure 3.2. CAD model of the piston-cylinder region

The free body diagram of a briquette and die during a compression cycle is shown in figure 3.3. During a compression cycle, the plunger exerted a positive axial force (x-direction) on the material, while forces resulting from the die taper angle, die friction, and

end cap combined to return that force. During compression, the material attempted to expand in the radial direction, causing an outward force to be exerted on the die wall. The balance of these forces is shown in equations 3.1 and 3.2.

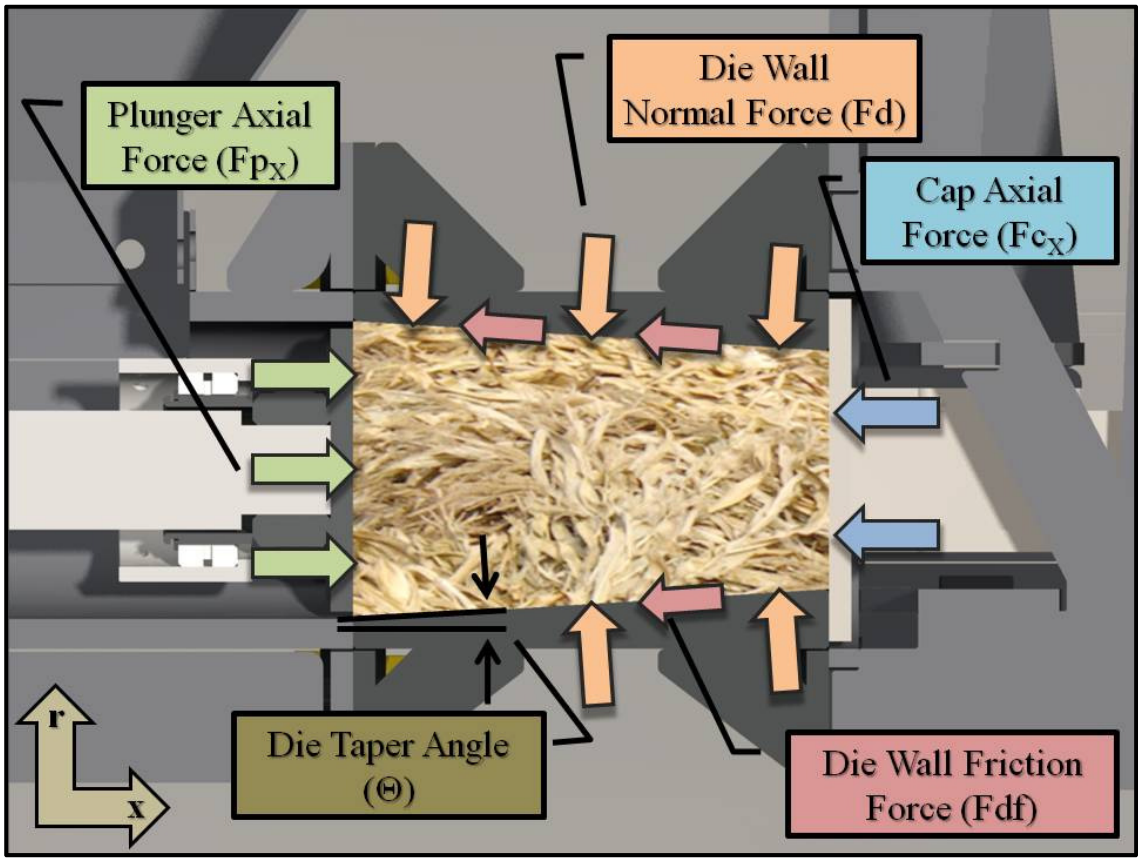

Figure 3.3. Free body diagram of the briquette during a compression cycle

Equation 3.1. The sum of all axial forces on the material in the die

$$\sum F_x = 0 = Fp_x - Fc_x - Fd_x - Fdf_x$$

where

F_x = Axial forces

Fp_x = Plunger axial force (The plunger acts in the x-direction)

Fc_x = Die cap axial force (The die cap acts in the x-direction)

Fd_x = Die axial force component (the x-component of Fd)

Fdf_x = Material to die friction axial force component (the x-component of Fdf)

Equation 3.2. The sum of all radial forces on the material in the die.

$$\sum F_r = 0 = Fm_r - Fd_r + Fdf_r$$

where

F_r = Radial forces

Fm_r = Material radial force on the die

Fd_r = Die force radial component (the r-component of Fd)

Fdf_r = Friction force radial component (the r-component of Fdf)

Material under compression exerted a radial force on the die wall based on Poisson's Ratio, which relates the axial strain to the radial strain for different material types. For the purposes of this calculation, it was assumed that the die wall is a fixed surface (i.e. it did not strain during densification), which meant that the material did not expand at all in the radial direction during compression. Rearranging and substituting terms on Poisson's ratio led to equation 3.3 which related input plunger force to radial stress and radial force:

Equation 3.3. Relationship between radial stress, radial force, and axial force (based on Poisson's Ratio)

$$\sigma_r = \frac{Fm_r}{A_{SA}} = \frac{v * Fp_x}{A_{IN}}$$

where

σ_r = Briquette radial stress

Fm_r = Briquette radial force

A_{SA} = Radial briquette surface area

v = Poisson's Ratio

A_{IN} = Die inlet area

Based on these equations, knowledge of the plunger axial force and cap axial force allowed the material to die wall coefficient of friction to be estimated. Changing material properties could change the material to die wall coefficient of friction, so estimating it provided benefit to determining the densification characteristics of changing process variables.

3.2.2. Hydraulic Design

The bench utilized a hydraulic cylinder to actuate the plunger head, and required hydraulic power to be externally supplied. A solenoid operated, open-centered directional control valve was used to control cylinder position. The schematic for the complete bench system is shown in figure 3.4, and the individual components are listed below.

1. Adjustable Hydraulic Pressure Relief Valve: Prince in-line pressure relief valve model RV-2H, 10-21 MPa pressure relief range
2. Directional Control Valve: Eaton-Vickers model DG4V-3 double-solenoid control valve
3. Hydraulic Cylinder: Red Lion double-acting hydraulic cylinder model 50TL18-200. 127 mm bore, 51 mm rod, 460 mm stroke
4. Manual Pressure Gage: 0-34 MPa pressure range
5. Electronic Pressure Transducer: Omega pressure transducer model PX309-5KG5V, 0-34 MPa pressure range

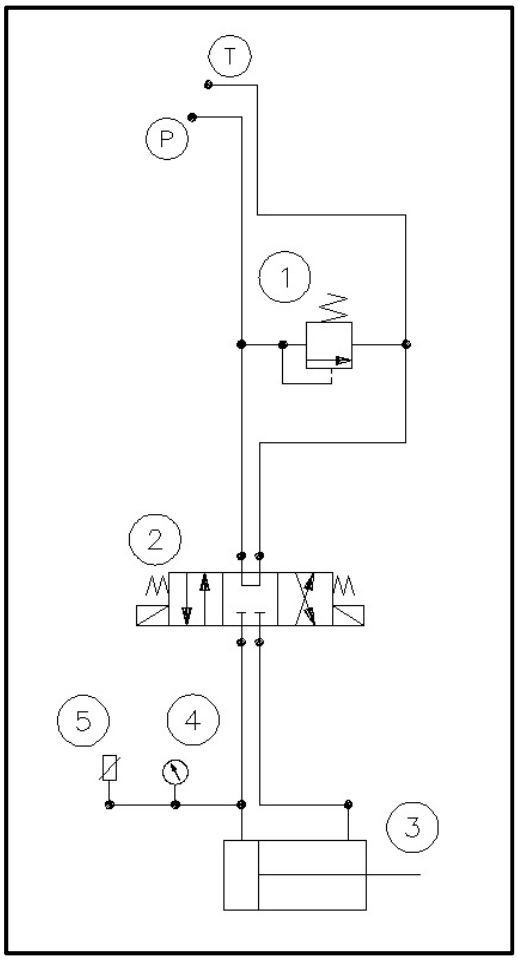

Figure 3.4. Bench hydraulic schematic

The pressure port (P) flowed oil in parallel to the adjustable-pressure relief valve, and to the directional control valve. During operation, oil flowed from the directional control valve to the hydraulic cylinder, and returned to the hydraulic power supply at port (T). The hydraulic pressure gages were located on the piston end of the cylinder to measure the hydraulic pressure required during the compression cycles.

Hydraulic power was supplied by a modified Positech hydraulic power pack. This system was powered by 460VAC electric motor and provides adjustable hydraulic flow up to 19 lpm (5 gpm) at 21 MPa (3000 psi).

3.2.3. Control Design

A macro-embedded Microsoft Excel user interface on a personal computer was used for densification bench control and data logging purposes. The PC interfaced with a Measurement Computing 1408-FS PMD (figure 3.5) via a USB connection to read the sensors and control the outputs. The 1408-FS was outfitted with 16 channels of digital I/O pins, 4 channels of double ended 14 bit A/D converters, and provided 5V excitation voltage to the sensors.

Figure 3.5. USB-1408FS (Photo courtesy of Measurement Computing)

A flowchart of the basic control logic design is shown in figure 3.6. The sensors illustrated in the flowchart are described in further detail in section 3.2.4. Once the densification sequence was started, the program informed the user of the test settings, and required initial material weights to be entered. It then began the main control loop where it actuated the cylinder, read all sensors, and calculated energy use at approximately 10 Hz. This cycle was ended if the operator's hands were removed from the safety switches, or if the cycle was completed. These cycles were repeated with added material until the desired compression pressure was reached. Once a briquette was completed, the software prompted the user for final material weights, made final calculations, and exported the data. Summary data including total energy consumption and briquette density was stored on an Excel spreadsheet and exported as a text file, while the complete data including sensor data from every program cycle was only exported as a text file.

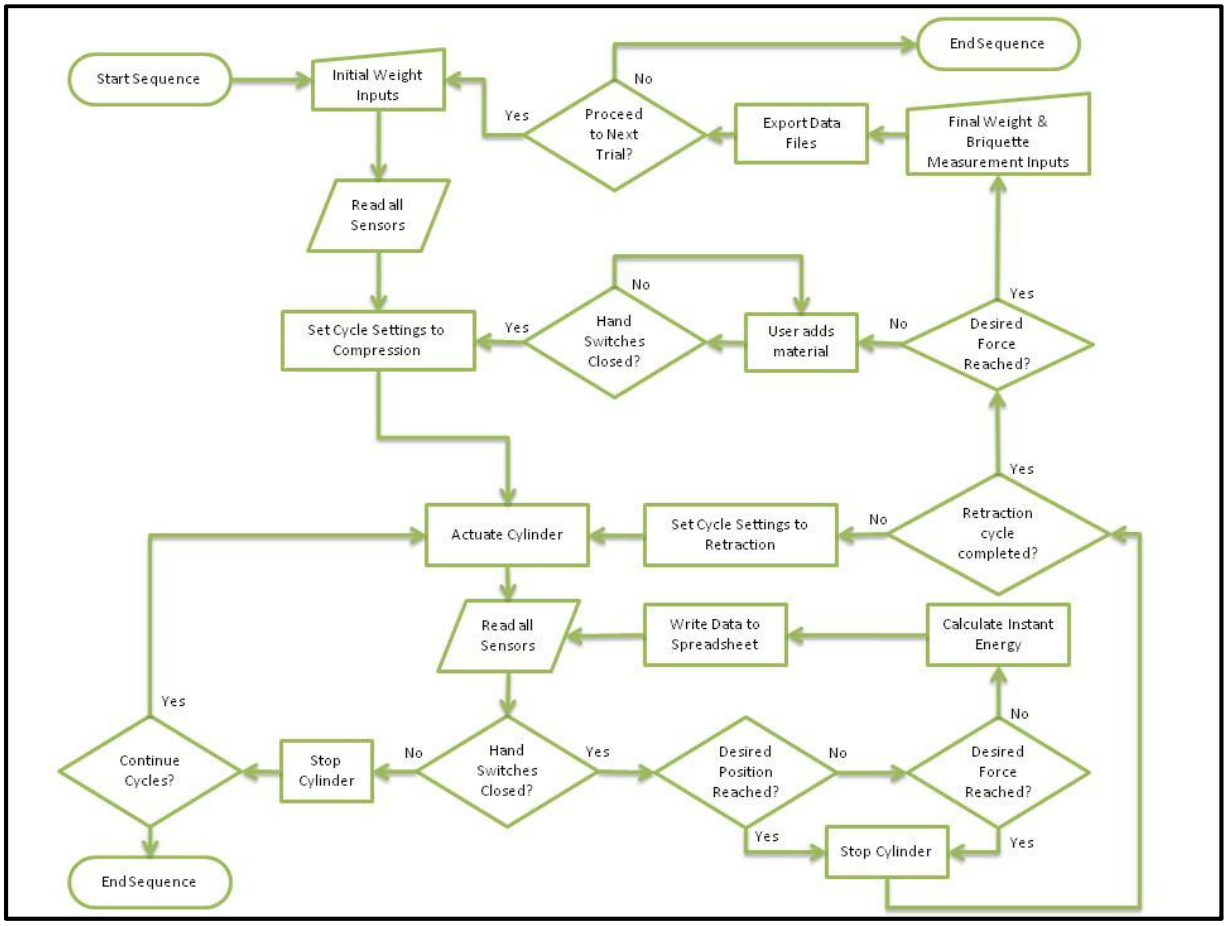

Figure 3.6. Bench control system flow cart

3.2.4. Sensor Design

To meet the control and data logging requirements of the densification bench, the following sensors were added to the system (letters are referenced to the locations shown in figure 3.7):

- Plunger Force Sensor – S-Type Axial Load Cell (A)
- Plunger Position Sensor – String Potentiometer (B)
- Hydraulic Pressure Sensor (On cylinder piston end) – Pressure Transducer (C)
- Die Cap Force Sensor – S-Type Axial Load Cell (D)

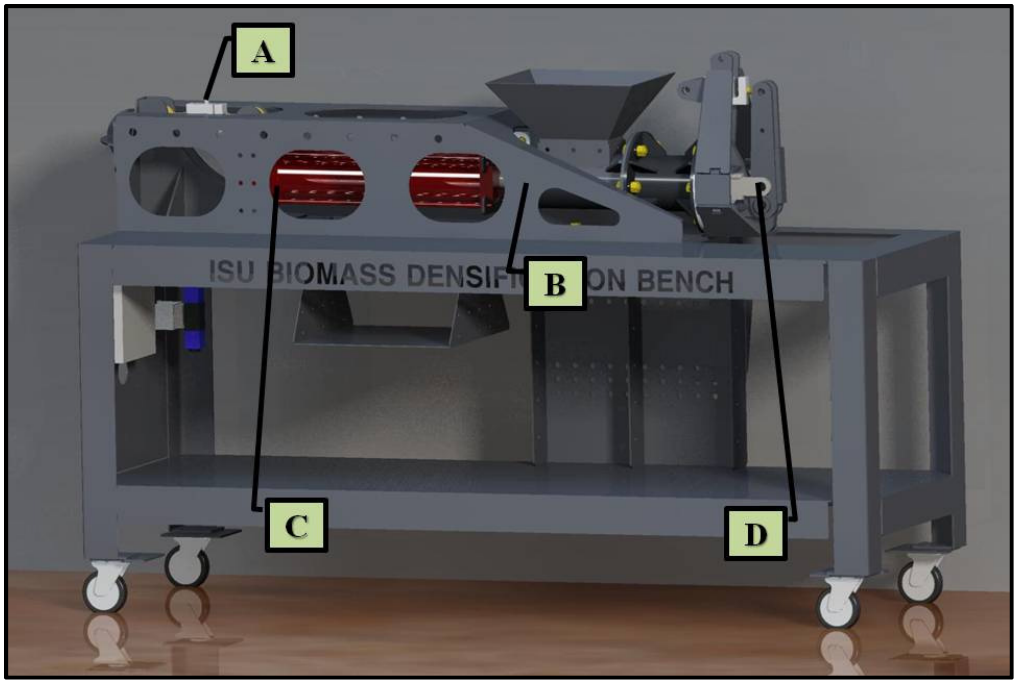

Figure 3.7. Bench sensor locations

Plunger Force Sensor

An Axial S-Type load cell was used to measure the plunger force exerted on the material (Fp_x from equation 3.1). This information was required to control compression pressure, estimate the coefficient of friction, and to calculate the mechanical energy consumed during the process. Based on the compression pressure requirements of the bench, a load cell would be required to measure up to 267 kN (60,000 lbs) if it acted directly on the plunger cylinder. S-Type axial load cells of this load rating are expensive and difficult to find, so this design was not considered. Instead, an Omega LC101-20K was selected to measure plunger force. It is an S-type, strain gage based load cell with a load capacity of 89 kN (20,000 lbs). To limit the force transmitted to the load cell while allowing the measurement of maximum plunger force, a lever linkage was developed. This linkage was dimensionally designed to provide a 3:1 force reduction ratio (figure 3.8). 33% of the axial force is transmitted to the load cell, while the remaining 67% is transmitted to the bench structure. This design allows the full 267 kN (60,000 lb) plunger force to be measured with a 3:1 reduction in resolution.

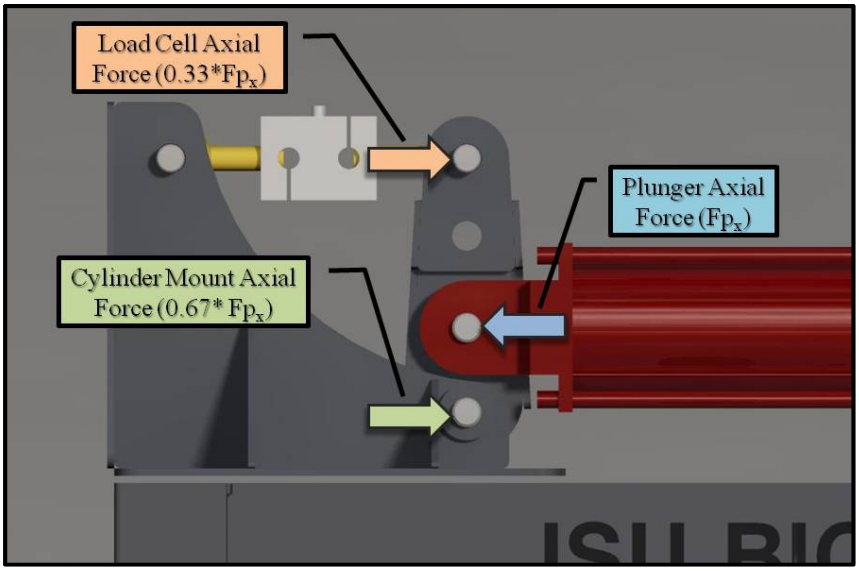

Figure 3.8. Free body diamgram of the plunger load cell force reduction linkage.

At maximum load, the load cell outputted 3 mVDC/VDC excitation. The power supply for the bench controller provided 5 VDC of excitation voltage to the load cell, which led to a maximum voltage output of 15 mVDC from the load cell at maximum axial load. Accounting for the 3:1 force reduction lever arm on the load cell, the system provided a marginal resolution of 0.056 mVDC/kN (0.00025 mVDC/lb), or 10.9 kN/bit (2444 lb/bit) at the 14-bit A/D converter on the PMD. This design was also inefficient, because it did not use the full range of the -5 VDC to +5 VDC on the A/D converter. To remedy this problem, a Maxim 495 operational amplifier was installed in series with the load cell output voltage signal with a voltage gain of 134. The gain was verified using a controlled power supply to input a variable voltage to the operational amplifier, and a multi-meter to read the output. This improved the voltage resolution to 7.52 mVDC/kN (0.0335 mVDC/lb), or 0.081 kN/bit (18.24 lb/bit) at the A/D converter.

Die Cap Force Sensor

Die cap force (the Fc_x term from equation 3.1) was measured to facilitate estimation of the material to die wall coefficient of friction. While it was unlikely that the full 267 kN (60000 lb) of available plunger force would be transmitted to the die cap during the densification process, the die cap was designed to measure the maximum potential force. This was done for calibration purposes between the plunger and die cap force sensors. A

similar lever linkage and signal conditioning design was utilized on the cap force transducer (to the design used on the plunger force sensor), however, it used an Industrial Commercial Scales TD-112-10K S-Type load cell, instead of the Omega model used on the plunger. This load cell was rated for a maximum load of 44.5 kN (10,000 lb). The system used the same style lever linkage design, but was designed to provide a 6:1 force reduction ratio, limiting the load cell force to 17% of the input cap force (figure 3.9). This allowed cap forces up to 267 kN (60,000 lb) to be measured with a smaller load cell, but with a resolution reduction of 6:1.

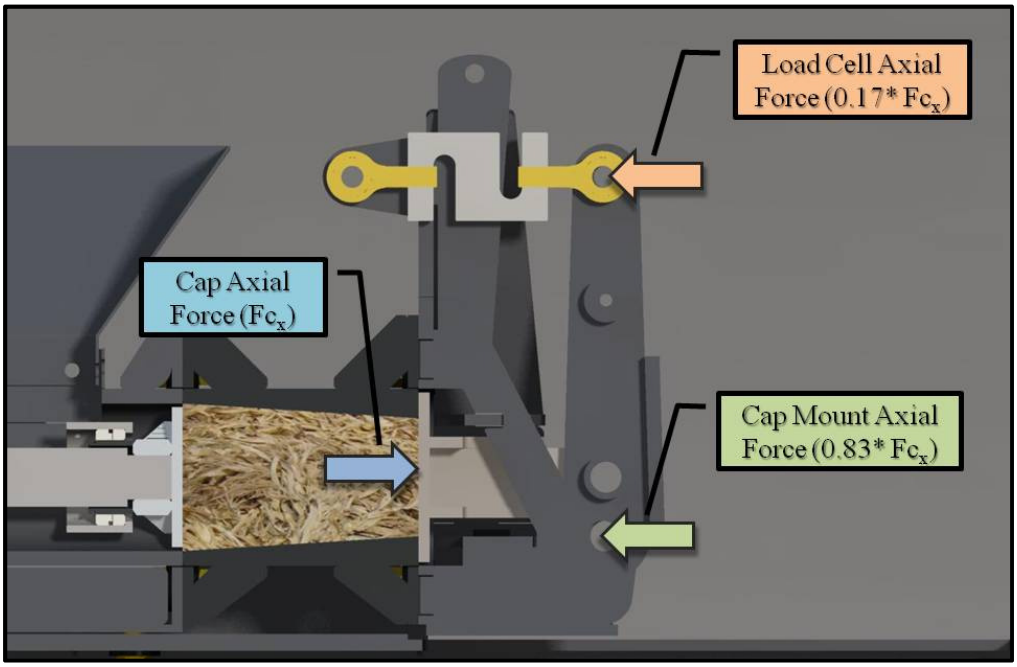

Figure 3.9. Load cell force reduction linkage on cap force transducer.

A similar load cell amplification design was used to measure axial force on the die cap. The cell outputted 3 mVDC/VDC excitation at maximum load, and was applied 5VDC excitation. A Burr-Brown INA118 Instrumentation Amplifier was installed in line with the output voltage signal with a voltage gain of 278.8, and was verified in the same manner as described for the plunger force sensor. With the excitation voltage of 5 VDC, this load cell provided a voltage resolution of 15.7 mVDC/kN (0.0697 mVDC/lb). The binary resolution at the 14 bit A/D converter on the 1408-FS was 0.0390 kN/bit (8.76 lb/bit).

Hydraulic Pressure Transducer

Hydraulic pressure on the piston end of the cylinder provided a second metric to determine plunger force, and was used to verify calibrations. Hydraulic pressure was also used as a secondary means to control compression pressure in the event that the plunger force sensor failed. Pressure was measured using an Omega model PX309-5KG5V pressure transducer (figure 3.10). The transducer required a 5 VDC excitation voltage, had a pressure range of 0-35.4 MPa (0-5000 psi), and outputted a linear voltage of 0-5 VDC with respect to pressure. The voltage resolution of this transducer was 145 mVDC/MPa (1 mV/psi), or when quantized with the 14 bit A/D converter, 0.0042 MPa/bit (0.6104 psi/bit). For the purposes of this research, this resolution was adequate without further signal conditioning.

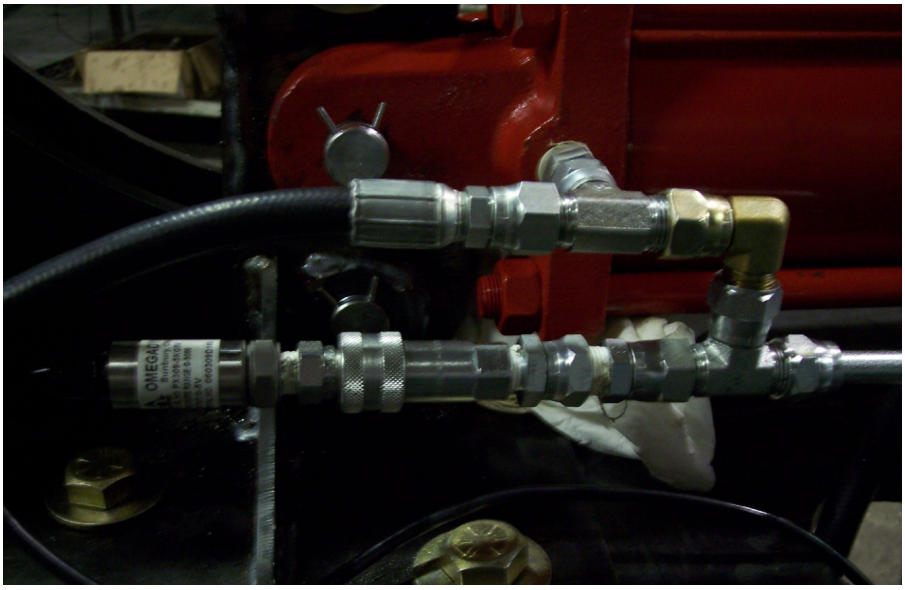

Figure 3.10. Hydraulic pressure transducer installed on cylinder

String Potentiometer for Plunger Position Sensing

To provide positional feedback control, log position data, and calculate energy throughout the process, the plunger position was sensed using a Unimeasure model PX-HA-60 string potentiometer. The installation is shown in figure 3.11, with the base of the potentiometer mounted to the cylinder body, and the string routed out to the plunger. The potentiometer outputted a linear voltage signal with respect to input voltage and string position (16.28 mVDC/(VDC*in). With this type of transducer, the position to voltage resolution increases with an increasing input voltage. A 12 VDC excitation voltage was used

(instead of the 5 VDC excitation used on the other sensors), which provided a voltage resolution of 7.69 mVDC/mm (195.4 mVDC/in). Using the 14 bit A/D converter on the PMD, this provided a binary resolution of 0.079 mm/bit (0.0031 in/bit).

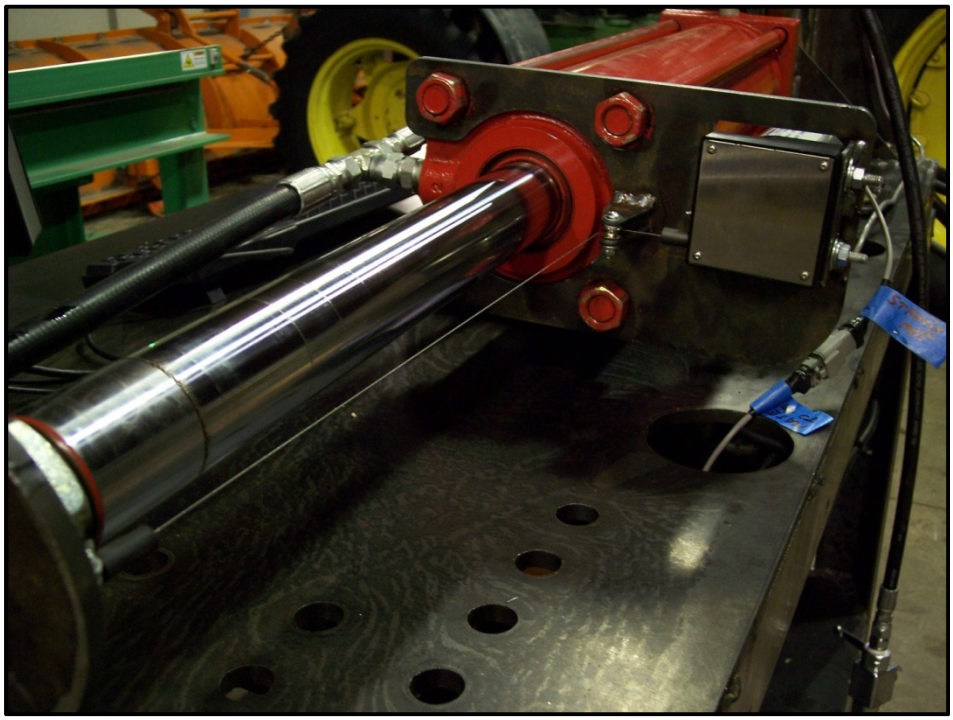

Figure 3.11. String potentiometer installed on plunger (die and material chamber are removed to show sensor)

3.3. Results

3.3.1. Process Variable Ranges

Mechanical Variables

The mechanical process variable ranges are limited to the capabilities of the bench, hydraulic power supply, and the dies produced for these experiments. Table 3.1 lists the mechanical process variable settings within the capabilities of the entire system.

Table 3.1. Densification bench mechanical process variable value ranges

Process Variable Ranges				
Process Variable	Interval	Value Range	Units	Controlling Means
Compression Speed	Continuous	0-5.0	m/min	Hydraulic Flow from Power Source
Compression Pressure	Continuous	0-17	MPa	Bench Controller
Die Geometry	Discrete	3.6, 7.2	deg	User-Installed Die

Material Feed Rate

Material feed rate was controlled by the bench operator during the briquetting process. While the material properties dictated the maximum material feed rate, generally no more than 0.3 kg (0.7 lb) of stover could be briquetted per compression cycle with this bench design. The user had to manually add material to the densification chamber in between plunging cycles, so the material was metered to the chamber by observing the scale reading on the input material container. The average material flow rate was calculated at the end of each briquetting cycle, and the test was accepted if the actual average material feed rate was within 0.05 kg (0.1 lb) of the desired feed rate.

Material Particle Size

Material particle size was determined and controlled prior to the briquetting experiments. ASABE Standard S424.1 was used to determine the geometric mean particle size of the input stover sample. Due to the varying nature of particle size from corn stover samples of different moisture content and material fractions, the different material particle sizes were statistically analyzed based on the method used to reduce the material particle size, as opposed to the absolute particle size of each sample. The geometric mean particle size is reported with all data, but it was not used for statistical analysis. The numbering convention below was used to indicate the particle size reduction method. These numbers are used in charts and tables to indicate the particle size reduction method.

- 1: “As Received”: No particle size reduction was done beyond what was done in the combine during harvest. Particles in this category passed through an integrated chopper on the combine, but saw no further size reduction.

- 2: “Vermeer HG200”: Particles in this category are the same as those from category 1, but have one additional processing step. All particles in this category were conditioned using a Vermeer HG200 chipper with the screen combination shown in figure 3.12. The two screens used in parallel for this conditioning had opening sizes of 70 mm and 111 mm.
- 3: “Hammer mill”: Particles in this category are the same as those from category 1, but have one additional step. All particles in this category were conditioning using an Arts-Way 60HP stationary hammer mill with a 19 mm screen (figure 3.13).

Figure 3.12. Vermeer HG200 grinder and screens

Figure 3.13. Arts-Way 60Hp hammer mill

Material Moisture Content

Material moisture content was determined using ASABE S358.2. Samples were dried at 60^{O} C for 72 hours, and final weights were measured immediately following drying. Moisture content values are reported on a wet basis, and the formula is shown in equation 3.4:

Equation 3.4. Wet basis moisture content

$$\%MCwb = \frac{(WW - DW)}{WW} * 100$$

where

%MCwb = Percent moisture content on a wet basis

WW = Weight of wet material

DW = Weight of dry material

Some of the experiments conducted required specific material moisture contents that were not directly available at the time of the experiment, so moisture conditioning was required. A procedure for adding moisture was developed and is described in appendix B.

Material Type

Material type was controlled by the setup used on the combine harvester. Different header and attachment configurations yielded different corn stover outputs from the machine. The three material types tested in this research are described below.

- Corn Stover: This material was harvested with a standard 'all crop' header which cuts the material at a certain height (generally just below the corn ear) and harvests all material above the cut point. This material consists of approximately 18% cob, 61% leaf and husk, and 21% stalk (by weight).
- MOG (Material other than grain): This material was harvested using a conventional corn header which generally harvests just the ear and husk. The exact material fractions for MOG are not known, however, the material composition falls in between the composition of corn stover and pure cobs.
- Pure Cobs: This material was harvested using a conventional corn header and combine with a secondary attachment for output material processing. Output material consists of approximately 80% cob and 20% stalk/leaf/husk (by weight).

3.3.2. Sensor Calibrations

String Potentiometer

The string potentiometer was provided with a factory calibration that was dependent on excitation voltage. This calibration was used after verifying the excitation voltage using an electrical multi-meter and calculating the true calibration value. The calibration was verified at the plunger extremities using a tape measure prior to conducting experiments, and throughout the testing period.

Plunger & Cap Force Load Cells

During operation, the plunger load cell measures force in compression, while the die cap force load cell measures force in tension. The plunger load cell was provided with a tension calibration certificate, however, that calibration was not valid in compression. The cap load cell was provided with a tension calibration certificate, so it was used as the standard for calibrating the plunger load cell prior to testing. With the cap force sensor

installed, the plunger head was pressed against the sensor at ten different compression forces to establish a calibration line. This procedure was executed throughout the testing period to verify plunger accuracy. The relationship between the two sensors after the calibration values were established is shown in figure 3.14.

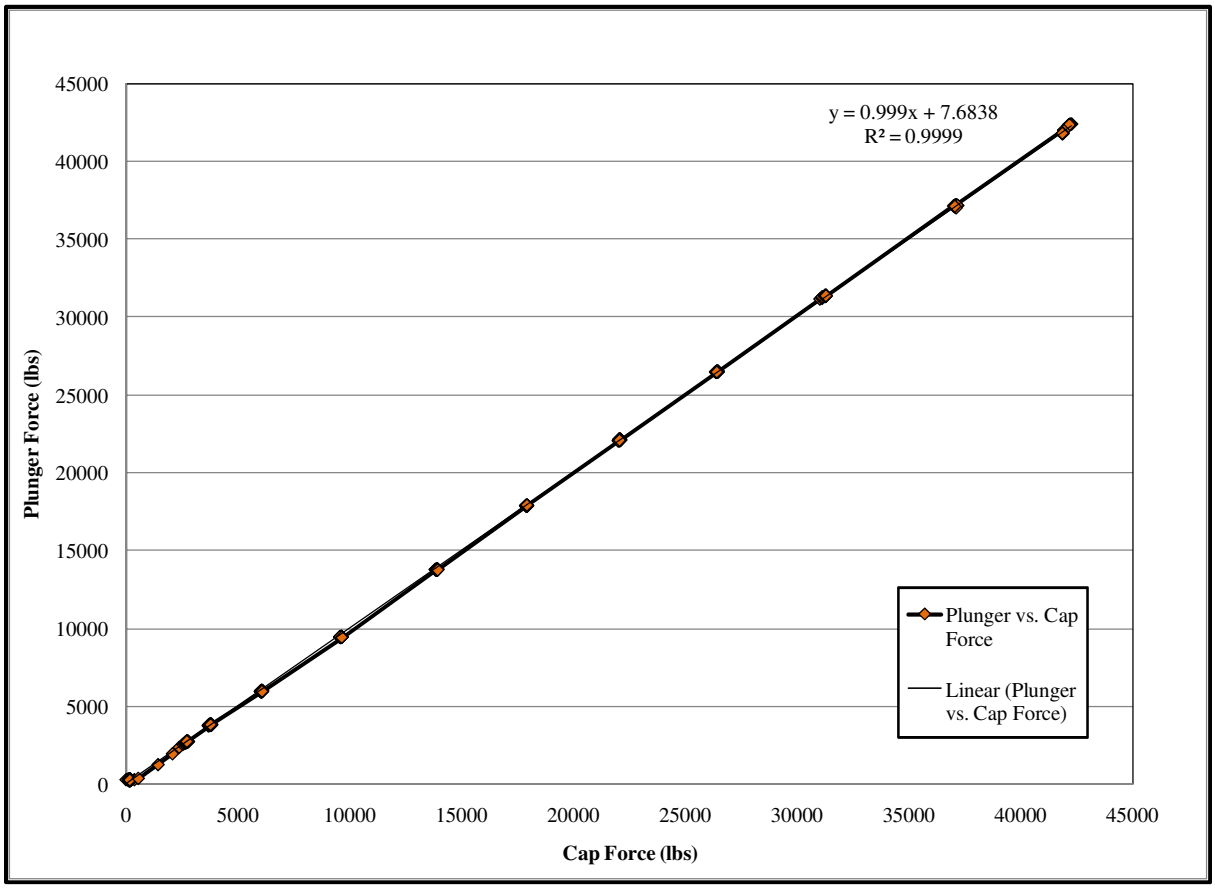

Figure 3.14. Plunger force calibration data

Pressure Transducer

The pressure transducer was provided with a calibration certificate, which was used to directly calculate the piston end cylinder pressure. The calibration was verified visually by observing the readings from the manual pressure dial and checking them against the pressure transducer values found on the user interface.

3.3.3. Output Calculations

The following is a description of how all of the output values reported in the results sections were calculated.

Particle Density

Particle density was calculated in two forms in the raw data; wet particle density and dry particle density. Wet particle density is the actual density of the briquette produced on the bench, while dry particle density is the density of only dry material in the briquette. Dry particle density is the measure that is reported in all of the results sections. Density of any form is calculated using the basic equation shown in equation 3.5.

Equation 3.5. Briquette density

$$D_{BRICK,WET} = \frac{W_{BRICK}}{V_{BRICK}}$$

where

$D_{BRICK,WET}$ = Briquette density

W_{BRICK} = Briquette wet weight

V_{BRICK} = Briquette volume

Briquette weight was directly measured during the briquetting procedure outlined in section 13.1, but volume was not (because of the time required to directly measure particle volume). During preliminary bench testing, the end diameters of the briquettes after ejection were not significantly different than the end diameters of the die used during the process (i.e. very little radial briquette expansion was observed). Significant briquette axial expansion was observed after ejection. Based on those observations, two assumptions were defined to facilitate briquette volume measurement:

- Every briquette was assumed to be shaped as a frustum of a cone.
- The end diameters of the cone frustum are assumed to be the same diameters as the die entry and exit.

With those assumptions and the knowledge of the die dimensions used to produce the briquette, the volume was calculated by measuring the axial length of the ejected briquette using equation 3.6:

Equation 3.6. Briquette volume

$$V_{BRICK} = \frac{\pi * L_{BRICK}}{3} * \{(D_1/2)^2 + [(D_1/2) * (D_2/2)] + (D_2/2)^2\}$$

where

V_{BRICK} = Briquette volume

L_{BRICK} = Briquette length (measured)

D_1 = Die inlet diameter

D_2 = Die outlet diameter

Using the briquette weight and volume, equation 3.5 was used to calculate the wet particle density of the output briquettes. To calculate the dry particle density the briquette weight, volume, and moisture content must be known. The equation to calculate dry particle density is shown in equation 3.7.

Equation 3.7. Dry briquette density

$$D_{BRICK,DRY} = \frac{W_{BRICK} * \left(1 - \frac{\%MCwb}{100}\right)}{V_{BRICK}}$$

where

$D_{BRICK,DRY}$ = Dry briquette density

Specific Energy

Similarly to particle density, the specific energy of briquetting was calculated in two forms in the raw data; wet specific energy, and dry specific energy. The specific energy of a briquetting process is calculated by dividing the total mechanical energy to densify the material by the material weight. Mechanical energy is calculated by multiplying force by distance. Every time the control software cycled the program recorded values from the plunger force load cell and plunger position string potentiometer. This allowed the program to calculate the energy consumed each time the program cycled, and sum that energy value throughout the plunging cycles and briquetting process. The basic formula to calculate the total mechanical energy required to produce a briquette is shown in equation 3.8:

Equation 3.8. Total mechanical energy to produce a briquette

$$E_{BRICK} = \sum_{i=1}^{r} \left\{ \sum_{j=1}^{c_i} \left| Fp_{ij} * \left(P_{ij} - P_{i(j-1)} \right) \right| \right\}$$

where

E_{BRICK} = Total energy consumed to produce a briquette

r = Total plunging cycles executed to produce a briquette

c_i = Total program execution cycles required to complete a plunging cycle

Fp_{ij} = Plunger force during a specific plunging and execution cycle

P_{ij} = Plunger position during a specific plunging and execution cycle

$P_{i(j-1)}$ = Plunger position during the previous execution cycle from P_{ij}

To calculate the wet specific energy of the briquette, the total energy must be scaled to the briquette weight. Equation 3.9 shows the formula to calculate the wet specific energy of an individual briquette:

Equation 3.9. Briquette wet specific energy

$$SE_{BRICK,WET} = \frac{E_{BRICK}}{W_{BRICK}}$$

where

$SE_{BRICK,WET}$ = Briquette wet specific energy

Dry specific energy was calculated in the same manner as wet specific energy, but it accounted for the dry weight of the briquette, not the total weight. Equation 3.10 shows the calculation for dry specific energy:

Equation 3.10. Briquette dry specific energy

$$SE_{BRICK,DRY} = \frac{E_{BRICK}}{W_{BRICK} * \left(1 - \frac{\%MCwb}{100}\right)}$$

where

$SE_{BRICK,DRY}$ = Briquette dry specific energy

Material to Die Wall Coefficient of Friction

The coefficient of friction between the input material and the die wall can be estimated using data from an individual briquette and a few assumptions. Solving the free body diagram system of equations from section 3.2.1 allows the user to estimate the material to die wall coefficient of friction for an assumed Poisson's Ratio. No data was found for the Poisson's Ratio of corn stover, so for the purposes of this analysis, Poisson's Ratio was assumed to be 0.3. This was a valid assumption for this estimate because the value of Poisson's Ratio did not mathematically affect the relative differences (percentage based) of the coefficient of friction between process variable treatment levels. Poisson's ratio did affect the actual coefficient of friction value, however, so these estimations should not be taken as a statement of the true coefficient of friction. The system was also assumed to be in a static state of motion. All equations were calculated using maximum observed values for plunger and die cap axial force. While these assumptions may not have produced accurate data on the exact coefficient of friction between the material and the die wall, they provided a valid comparison among the different treatment variables tested in this research.

The coefficient of friction can be calculated using the static sum-of-forces equations from the die and briquette under a compression cycle. Relating the axial force components of friction and die wall force to the die taper angle and coefficient of friction, and substituting them into equation 3.1 yields equation 3.11:

Equation 3.11. The sum of all axial forces on the material in the die (rearranged)

$$Fp_x - Fc_x = \mathrm{Fd}(\mu_s * \cos\theta + \sin\theta)$$

where

μ_s = Coefficient of friction between the material and the die wall

Fd = Die normal force

Θ = Die taper angle

A similar approach was used on the radial sum of forces equation. Relating the radial component forces of die wall and friction force to the die taper angle and the coefficient of friction yields what is shown in equation 3.12.

Equation 3.12. Equation 3.2 solved for Fm_r

$$Fm_r = \mathrm{Fd} * (-\mu_s * \sin\theta + \cos\theta)$$

Both equations have die normal force and coefficient of friction as unknown variables, allowing them to be solved simultaneously. Solving for Fd in equation 3.12 and substituting it into equation 3.11 produces an equation that can be solved explicitly for the coefficient of friction (equation 3.13). This equation was used to estimate the material to die wall coefficient of friction for each briquette that was produced using the instrumented die cap.

Equation 3.13. Equations 3.11 and 3.12 simultaneously solved for μ_s

$$\mu_s = \frac{\left(\left(\mathrm{Fp_x} - \mathrm{Fc_x}\right) * \cos\theta - Fm_r * \sin\theta\right)}{\left(Fm_r * \cos\theta + \left(\mathrm{Fp_x} - \mathrm{Fc_x}\right) * \sin\theta\right)}$$

Briquette Axial Expansion

The axial expansion of the briquette was quantified to illustrate the effects of certain process variables on the elastic behavior of the output briquette. Briquette axial expansion is reported as a percent of the compressed briquette length, and the formula is shown in equation 3.14.

Equation 3.14. Briquette percent axial expansion

$$AE_{\%} = \left(\frac{L_{BRICK} - L_{BRICK,COMP}}{L_{BRICK,COMP}}\right) * 100$$

where

$AE_{\%}$ = Briquette percent axial expansion

$L_{BRICK,COMP}$ = Compressed briquette length (216 mm)

3.3.4. Data Output

Bench Output

Data generated from the densification bench provided plots and relationships that closely describe the process. Figure 3.15 shows a plot of plunger force, plunger position, and total energy consumption over time. Each force peak represents an additional compression cycle, while the valleys represent the time period of adding stover to the chamber. The green line shows the plunger position (no units) throughout the process. The red line shows the

continuous summation of mechanical energy over time. This particular briquette reached the desired compression pressure in 7 compression cycles and required approximately 27 kJ of mechanical energy to complete the process.

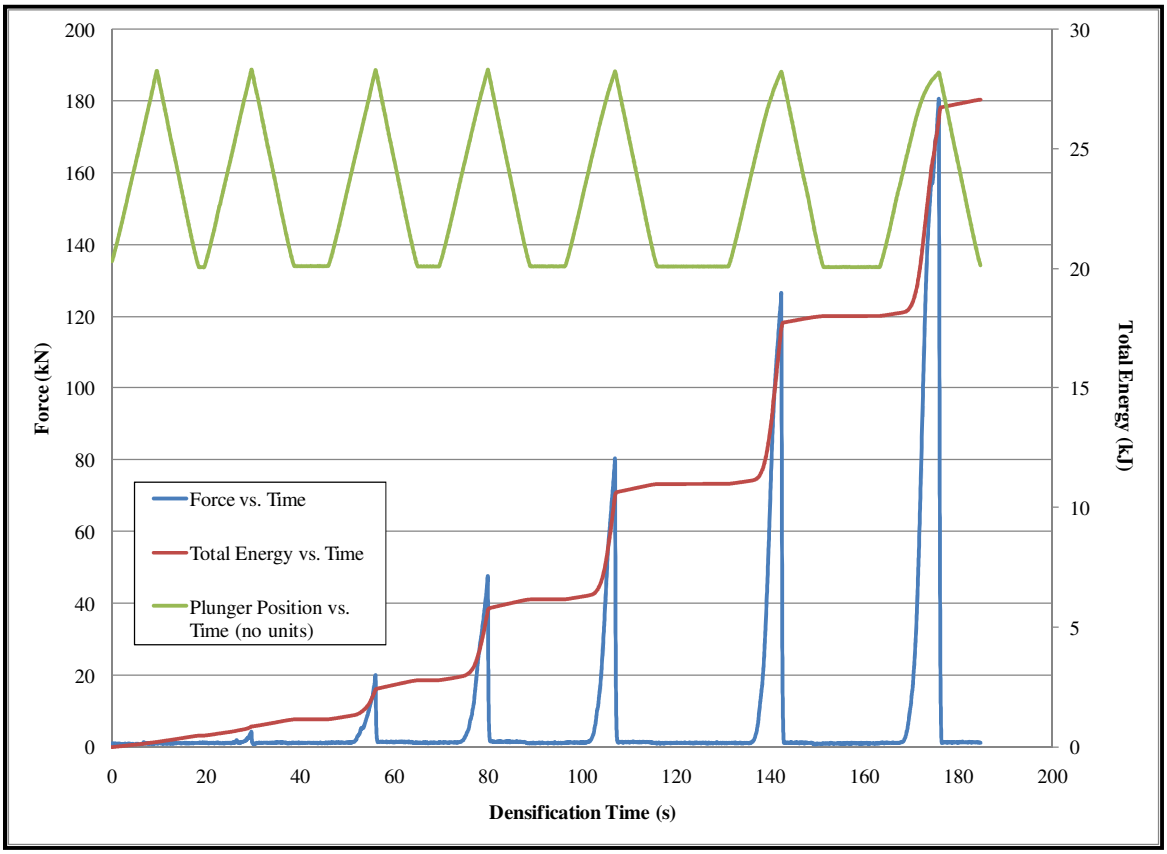

Figure 3.15. Plunger force and energy plot

Statistical Analysis

All statistical tests were conducted using Minitab software. All experiments discussed utilized full-factorial experiment designs, which allowed the use of the factorial analysis tool (ANOVA) to determine the variation caused by each treatment factor. Factorial ANOVA was used to determine the significance of each treatment variable on the selected output factor. Confidence interval plots were used to determine if significant differences were present between treatment variable levels. The confidence intervals assume a normal distribution of the data and use critical values following a t-distribution. Treatments were reported to be significantly different if the confidence intervals do not overlap.

3.4. Conclusions

The densification bench design facilitated small-scale densification of combine-chopped corn stover for research purposes. Tapered cylindrical briquettes weighing 0.9-2.0 kg were produced on this bench to determine the densification characteristics of different material conditions and mechanical settings. The bench was instrumented to facilitate mechanical variable measurement and control, and energy consumption measurement. This machine provided a suitable platform for testing densification process variables, and producing densified corn stover samples for other analyses.

Chapter 4. Compression Speed Experiment

4.1. Objectives

While compression speed was a key mechanical variable and could have large implications on the design of a large-scale densification machine, it did not intuitively appear that it would induce large impacts on particle density or specific energy. This experiment was developed to determine what impact compression speed had on the densification process. The hypothesis behind this experiment was that within a 95% confidence interval (α=0.05), compression speed within a range of 0.8-4.6 m/min would not affect dry particle density or dry specific energy. To test that hypothesis, the objective of this experiment was to determine the effect of compression speed on the dry particle density and dry specific energy.

4.2. Experiment Design

This was the first experiment conducted on the bench after the initial verification tests, and not all of the sensing equipment was developed at the time of this experiment. Tests conducted in this experiment did not utilize an end cap to stop material flow and sense cap force, so initially material would flow from the end of the die. After several compression cycles, material flow would cease and compression pressure would build until the desired pressure was reached. From there, the briquette was ejected as described in appendix A. The hydraulic power supply described in section 3.2.2 could not provide adequate flow to conduct the high speed portion of this experiment, so a John Deere 8245R tractor was utilized as the hydraulic power source for this experiment. The tractor provided variable hydraulic flow at 21 MPa (3000 psi) up to 75 lpm (20 gpm). Corn stover for this experiment was sampled from the fall 2009 corn harvest in the Ames, IA region. All material was sampled from the same location, harvest date, and variety, however, these properties for this material are not known. Only material at 9%MCwb was available as field harvested material, so all experiments using stover at 48%MCwb used stover that had the moisture content artificially increased. The procedure for adding moisture content to the material is found in appendix B.

Values of compression speed were tested with different treatments of compression pressure, material particle size, and material moisture content. The compression speed values

were selected to test the outer limits of the densification bench capabilities. This was done to provide the highest chance of demonstrating significant differences caused by compression speed. The complete experiment design is shown in table 4.1. The intent was to determine if compression speed would demonstrate any main or interaction effects on particle density or specific energy, but not to draw a complete effects matrix between all process variables. This led to the use of an 'incomplete' factorial design where compression speed treatments were tested at two levels of the other three variables. No other combinations were used beyond those treatments. Eight individual treatments were replicated three times for a total of 24 observations in this experiment.

Table 4.1. Treatment design for compression speed experiment

Compression Speed Experiment

Constants

Variable	Value	Units
Material Type	Corn Stover	
Die Taper Angle	3.6	deg
Material Feed Rate	0.23	kg/plunge
Plunging Distance	280	mm

Variables

Treatment	Compression Pressure	Material Moisture Content	Particle Size Reduction Method		Compression Speed
(#)	(MPa)	(%wb)	(method)	(mm)	(m/min)
1	10.5	9.3	1	43	0.8
2	10.5	9.3	1	43	4.6
3	10.5	9.3	3	5	0.8
4	10.5	9.3	3	5	4.6
5	17.6	9.3	1	43	0.8
6	17.6	9.3	1	43	4.6
7	10.5	47.6	1	43	0.8
8	10.5	47.6	1	43	4.6

Total Treatments	8
Replicates	3
Total Observations	24

4.3. Results

4.3.1. Dry Particle Density

As predicted, the factorial analysis on dry particle density accepted the hypothesis of no main or interaction effects from compression speed. It rejected the hypothesis for the other three process variables, indicating that some potentially significant variation was present. An incomplete factorial design was used for the three significant treatment variables, so those results will not be discussed. The complete ANOVA table of all main and interaction effects from the compression speed experiment is shown in table 4.2.

Table 4.2. Compression speed experiment factorial ANOVA for dry particle density

Dry Bulk Density (kg/m^3)						
Source	DF	Seq SS	Adj SS	Adj MS	F	P
Particle Size Reduction Method	1	104811	7715	7715	36.67	0.000
Material Moisture Content (%wb)	1	1083926	604648	604648	2873.67	0.000
Compression Pressure (MPa)	1	61547	61547	61547	292.51	0.000
Compression Speed (m/min)	1	1584	323	323	1.54	0.233
Particle Size Reduction Method * Compression Speed (m/min)	1	342	99	99	0.47	0.502
Material Moisture Content (%wb) * Compression Speed (m/min)	1	148	148	148	0.7	0.415
Compression Pressure (MPa) * Compression Speed (m/min)	1	11	11	11	0.05	0.826
Error	16	3367	3367	210		
Total	23	1255736				

4.3.2. Dry Specific Energy

The factorial analysis for dry specific energy (table 4.3) accepted the hypothesis of no main or interaction effects from compression speed. It rejected the hypothesis for compression pressure and particle size reduction method, indicating significant effects on dry specific energy could be caused by those variables. Again, those potentially significant results will not be discussed.

Table 4.3. Compression speed experiment factorial ANOVA for dry specific energy

Dry Specific Energy (MJ/t)						
Source	DF	Seq SS	Adj SS	Adj MS	F	P
Particle Size Reduction Method	1	562.08	265.03	265.03	15.21	0.001
Material Moisture Content (%wb)	1	138.33	13.78	13.78	0.79	0.387
Compression Pressure (MPa)	1	167.61	167.61	167.61	9.62	0.007
Compression Speed (m/min)	1	211.88	39.26	39.26	2.25	0.153
Particle Size Reduction Method * Compression Speed (m/min)	1	0.43	1.25	1.25	0.07	0.792
Material Moisture Content (%wb) * Compression Speed (m/min)	1	0.33	0.06	0.06	0	0.953
Compression Pressure (MPa) * Compression Speed (m/min)	1	2.24	2.24	2.24	0.13	0.725
Error	16	278.79	278.79	17.42		
Total	23	1361.69				

4.4. Conclusions

Compression speed was tested at two different levels of 0.8 and 4.6 m/min at different levels of compression pressure, material particle size, and material moisture content. This was done to ensure both main and interaction effects with compression speed were properly accounted. During this experiment, briquettes were produced with an average dry particle density of 400-420 kg/m^3 at dry specific energy requirements of 27-33 MJ/t. As hypothesized, compression speed did not have any significant main or interaction effects on either dry particle density or dry specific energy for α=0.05. Based on this data, all further experiments were designed without compression speed as a variable.

Chapter 5. 3-Way Interaction Experiment

5.1. Objectives

Based on a review of literature on previous densification research, it appeared that compression pressure, material moisture content, and material particle size would be responsible for the most variation in dry particle density and dry specific energy. The objective of this experiment was to determine the main and interaction effects of these process variables with the outputs expressed as dry particle density, dry specific energy, and material to die wall coefficient of friction.

5.2. Materials & Methods

A full factorial experiment design was utilized in this experiment with three levels of compression pressure, two levels of material moisture content, and three levels of material particle size. With 18 total treatments replicated three times, this experiment tested 54 total briquettes. This experiment design was selected to provide strong resolution of main and two-way interaction effects. A complete table of this experiment design is shown in table 5.1. The material moisture content levels were selected to represent the outer boundaries of possible field-harvested corn stover moisture contents. The compression pressure values were selected in the upper half of the pressure capabilities of the bench, because initial shakedown experiments showed briquettes produced at compression pressures lower than 7 MPa had unacceptably low density and durability. The particle size reduction methods were selected to represent a wide spectrum of coarse grinding operations, and compare them against field-harvested particle sizes.

A trial version of this experiment conducted prior to this iteration demonstrated a difference in the force distribution in the die between materials of high and low moisture contents. This provided motivation to develop an instrumented cap to quantify those force distribution differences. Consequently, this was the first experiment that tested material using the die cap force instrumentation. Corn stover from multiple dates during the fall 2010 corn harvest at Iowa State University was used to produce multiple moisture contents, and the experiment was conducted in two separate events to accomplish this. The wet material was harvested in the first week of September 2010, while the dry material was harvested during

the second week of October 2010. The exact corn varieties, harvest dates, and locations for these materials are not known.

Table 5.1. Treatment design for 3-way interaction experiment

3-Way Interaction Experiment

Constants

Variable	Value	Units
Material Type	Corn Stover	
Die Taper Angle	3.6	deg
Material Feed Rate	0.23	kg/plunge
Plunging Distance	280	mm
Compression Speed	1.5	m/min

Variables

Treatment (#)	Compression Pressure (MPa)	Material Moisture (%wb)	Material Particle Size (method)	(mm)
1	7.0	8.3	3	19
2	10.5	8.3	3	19
3	14.0	8.3	3	19
4	7.0	8.3	2	22
5	10.5	8.3	2	22
6	14.0	8.3	2	22
7	7.0	8.3	1	42
8	10.5	8.3	1	42
9	14.0	8.3	1	42
10	7.0	54.5	3	23
11	10.5	54.5	3	23
12	14.0	54.5	3	23
13	7.0	54.5	2	35
14	10.5	54.5	2	35
15	14.0	54.5	2	35
16	7.0	54.5	1	40
17	10.5	54.5	1	40
18	14.0	54.5	1	40

Total Treatments	18
Replicates	3
Total Observations	54

5.3. Results

5.3.1. Dry Particle Density

Based on the factorial ANOVA, data from the 3-way interaction experiment rejected the hypothesis of no effect from all three treatment factors, and an interaction effect from moisture content and compression pressure on dry particle density (table 5.2). Material moisture content was responsible for the most variability in the whole experiment by a large margin, with the other three effects accounting for smaller amounts of variation.

Table 5.2. 3-way interaction factorial ANOVA for dry particle density

Dry Particle Density (kg/m^3)						
Source	DF	Seq SS	Adj SS	Adj MS	F	P
Compression Pressure (MPa)	2	37913	37692	18846	54.5	0.000
Particle Size Reduction Method	2	3826	2346	1173	3.39	0.045
Material Moisture Content (%wb)	1	373961	373578	373578	1080.3	0.000
Compression Pressure (MPa) * Particle Size Reduction Method	4	1658	1706	427	1.23	0.314
Compression Pressure (MPa) * Material Moisture Content (%wb)	2	15323	15304	7652	22.13	0.000
Particle Size Reduction Method * Material Moisture Content (%wb)	2	1809	1853	926	2.68	0.083
Compression Pressure (MPa) * Particle Size Reduction Method * Material Moisture Content (%wb)	4	4234	4234	1058	3.06	0.029
Error	35	12103	12103	346		
Total	52	450827				

While the factorial ANOVA showed a potential relationship between particle size reduction method and dry particle density, only two significant treatment differences were observed between particle size treatments levels during the experiment ($\alpha = 0.05$). Figure 5.1 shows a plot of the data means and confidence intervals for each individual treatment combination on dry particle density. The particle size treatments only had significant effects at 54.5%wb moisture content, and at 10.5 MPa compression pressure.

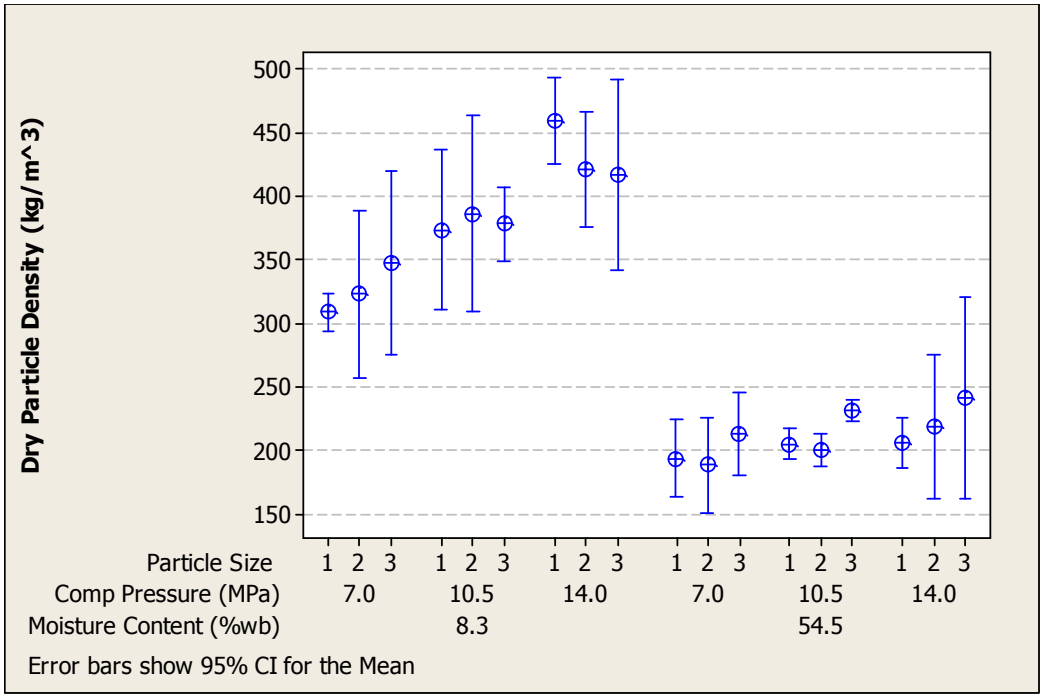

Figure 5.1. Treatment variable effects on dry particle density (3-way interaction experiment)

Figure 5.2 shows the effects of compression pressure and moisture content averaged over all particle sizes on dry particle density. At 8.3%MCwb, compression pressure showed a significant, positive, and linear relationship with output particle density ranging from 330 – 430 kg/m^3 across 7-14 MPa. This was caused by an increase in briquette weight (from the additional compression cycles with added material) with no significant increase in briquette axial expansion (figure 5.3). No significant differences were found between the compression pressure treatment levels at 54.5%MCwb on dry particle density ($\alpha = 0.05$).

The most significant effect on dry particle density was caused by material moisture content. Increasing moisture content from 8.3 to 54.5%wb decreased the mean dry particle density by about 45% from 380 to 210 kg/m^3 (averaged over all treatment levels of compression pressure and material particle size). The significant decrease in dry particle density caused by material moisture content can be attributed to two main factors that were observed during this experiment; briquette dry weight and briquette axial expansion (figure 5.3). While increasing moisture content increased the wet weight of a briquette, the weight was offset by the large amount of moisture present in the briquette, so the overall dry briquette weight was reduced. The elastic behavior of the briquette was also negatively altered with increased moisture content, as evidenced by the significant increase in briquette

axial expansion over increasing moisture content. Both of these factors directly contributed to reducing dry particle density at increased material moisture contents.

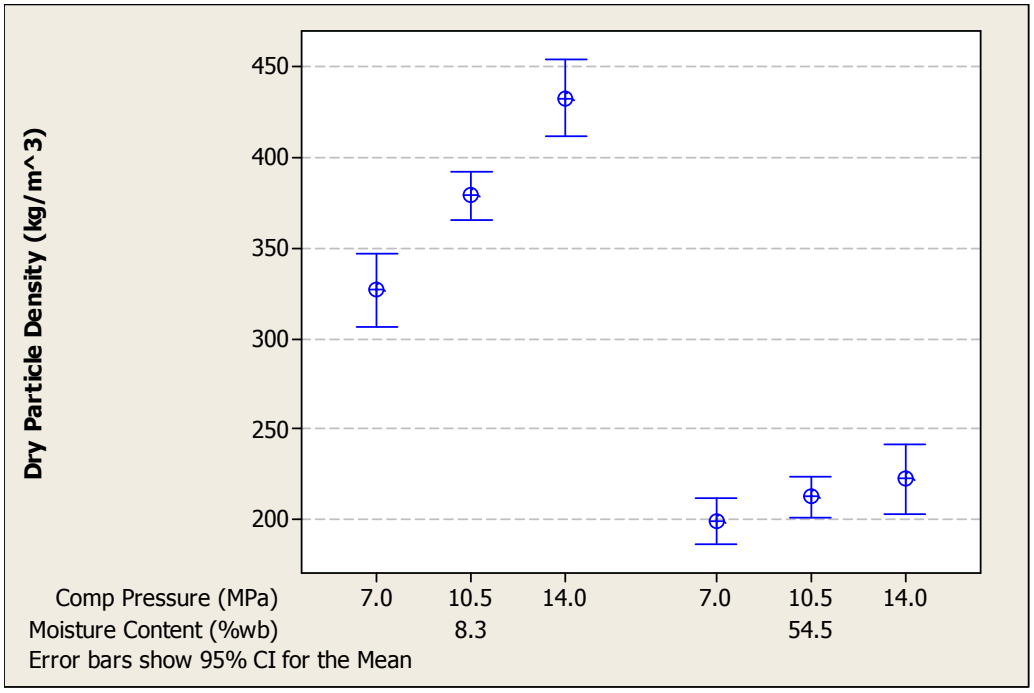

Figure 5.2. Compression pressure and material moisture content effects on dry particle density (3-way interaction experiment)

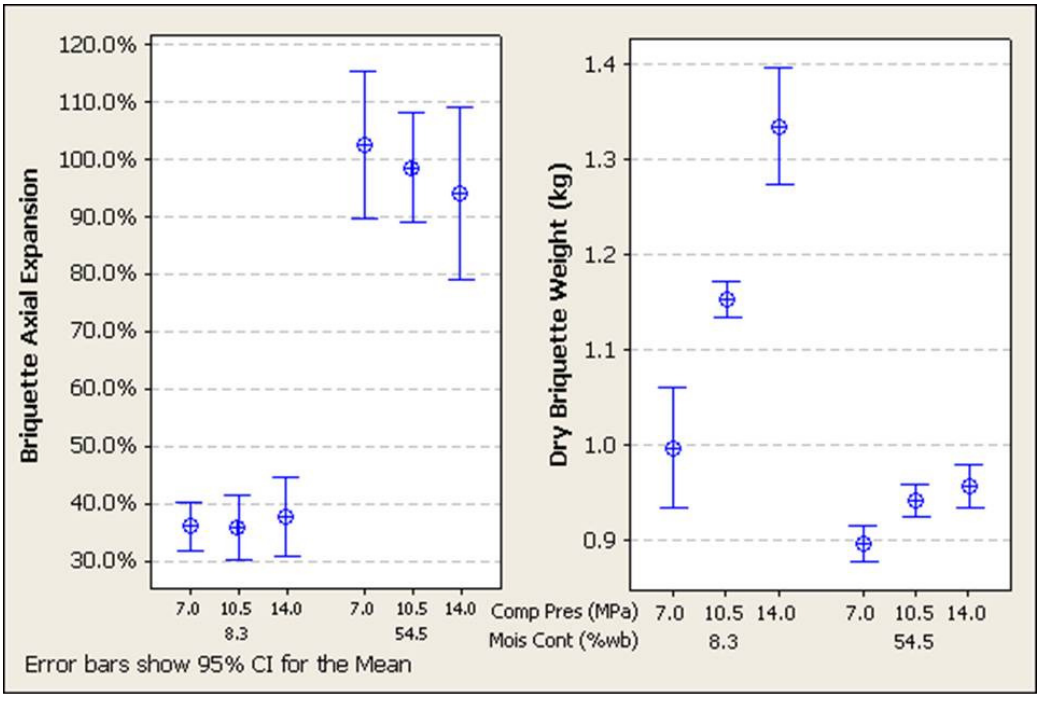

Figure 5.3. Treatment factor effects on dry briquette weight and briquette axial expansion (3-way interaction experiment)

Based on the data collected in this experiment, a regression equation was developed to determine the dry particle density of corn stover briquettes based on compression pressure and material moisture content. Material particle size was not used in the regression, because during the regression analysis, the coefficient produced based on material particle size had a P-value exceeding 0.05. This regression produced the following equation for determining the dry particle density of corn stover briquettes:

Equation 5.1. Regression equation for determining dry particle density

$$PD = 313 - 3.64 * \%MCwb + 9.21 * CP$$

where

PD = Dry particle density (kg/m^3)

%MCwb = Percent moisture content (wet basis)

CP = Compression Pressure (MPa)

Figure 5.4 shows a contour plot of this regression equation. The main effect of compression pressure is reduced in magnitude at increasing material moisture content levels. At 8.3%MCwb, particle density increased by 32% from 7-14 MPa, but at 54.5%MCwb, that increase was reduced to 12%.

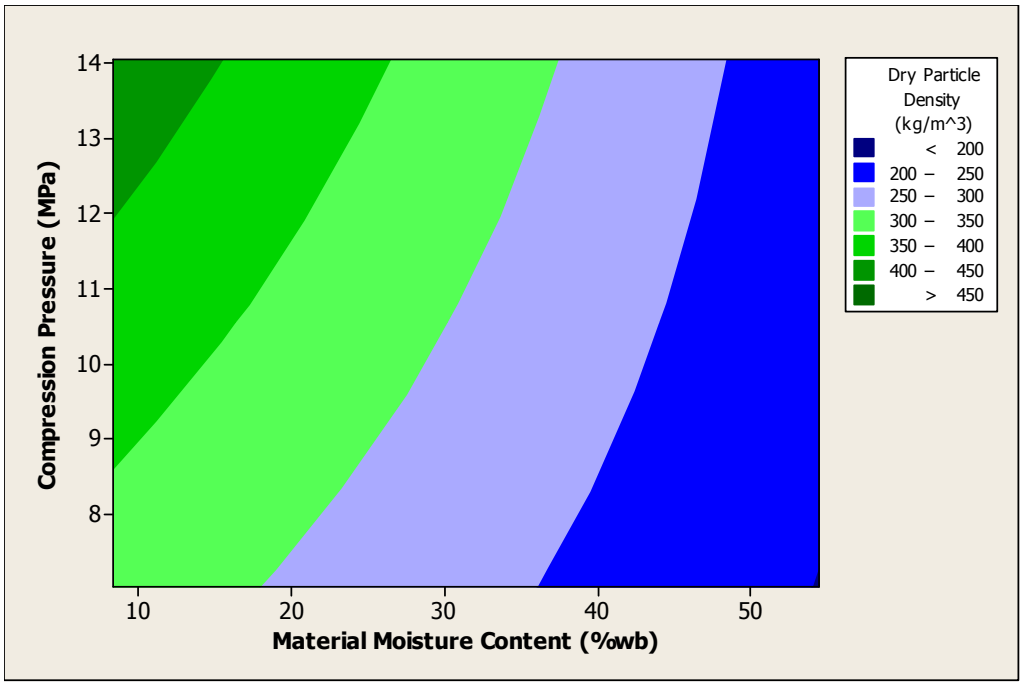

Figure 5.4. Contour plot of the regression equation for dry particle density (3-way interaction experiment)

5.3.2. Dry Specific Energy

The factorial ANOVA of this experiment on dry specific energy could not reject the hypothesis of no main effect caused by any of the treatment factors (table 5.3). Similarly to dry particle density, material moisture content was responsible for the most variation on dry specific energy, and compression pressure and particle size had a small amount of potentially significant variation.

Table 5.3. 3-way interaction factorial ANOVA for dry specific energy

Dry Specific Energy (MJ/t)						
Source	DF	Seq SS	Adj SS	Adj MS	F	P
Compression Pressure (MPa)	2	466.33	462.8	231.4	14.17	0.000
Particle Size Reduction Method	2	155.18	110.75	55.38	3.39	0.045
Material Moisture Content (%wb)	1	3852.26	3843.4	3843.4	235.34	0.000
Compression Pressure (MPa) * Particle Size Reduction Method	4	75.78	68.49	17.12	1.05	0.396
Compression Pressure (MPa) * Material Moisture Content (%wb)	2	14.56	15.4	7.7	0.47	0.628
Particle Size Reduction Method * Material Moisture Content (%wb)	2	41.89	36.35	18.17	1.11	0.340
Compression Pressure (MPa) * Particle Size Reduction Method * Material Moisture Content (%wb)	4	43.63	43.63	10.91	0.67	0.619
Error	35	571.6	571.6	16.33		
Total	52	5221.22				

Based on 95% confidence interval plots ($\alpha = 0.05$) of each treatment variable combination, all material particle size treatment levels reflected no significant difference in the dry specific energy (figure 5.5). Averaging the effects of compression pressure and material moisture content over all levels of material particle size produces the interval plot shown in figure 5.6. Similar to dry particle density, compression pressure had a significant effect on dry specific energy at 8.3%MCwb, but not at 54.5%MCwb. At 8.3%MCwb, the mean dry specific energy requirement increased by approximately 40% (15.6 to 22.2 MJ/t) from 7-14 MPa. As expected, this increase was caused by a significant increase in the amount of compression cycles required to reach a desired compression pressure (figure 5.7).

Moisture content showed a very strong positive trend with respect to dry specific energy. From 8.3 to 54.5%MCwb, the dry specific energy requirement increased approximately 90% (19.2 to 36.4 MJ/t) (averaged over all levels of compression pressure and material moisture content). This increase can be partially attributed to the same factors that negatively affected dry particle density. As mentioned in section 5.3.1, the dry briquette weight significantly dropped as moisture content increased, which negatively impacted the dry specific energy. The second factor that affected the dry specific energy was the number of compression cycles required to reach the desired compression pressure (figure 5.7). Averaged over all levels of compression pressure and material particle size, briquettes with a 54.5%MCwb averaged 4.5 more compression cycles than briquettes at 8.3%MCwb. Every compression cycle adds more energy to the process, so increasing the cycle count by about 60% had a negative effect on dry specific energy.

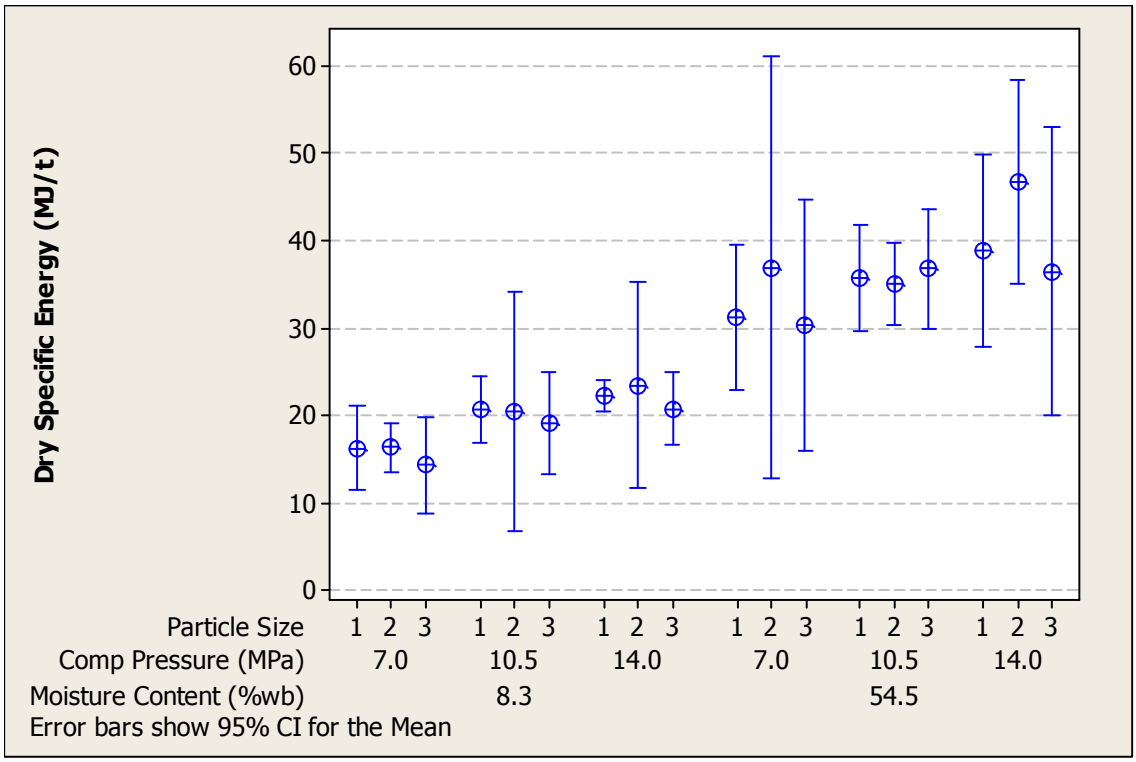

Figure 5.5. Treatment factor effects on dry specific energy (3-way interaction experiment)

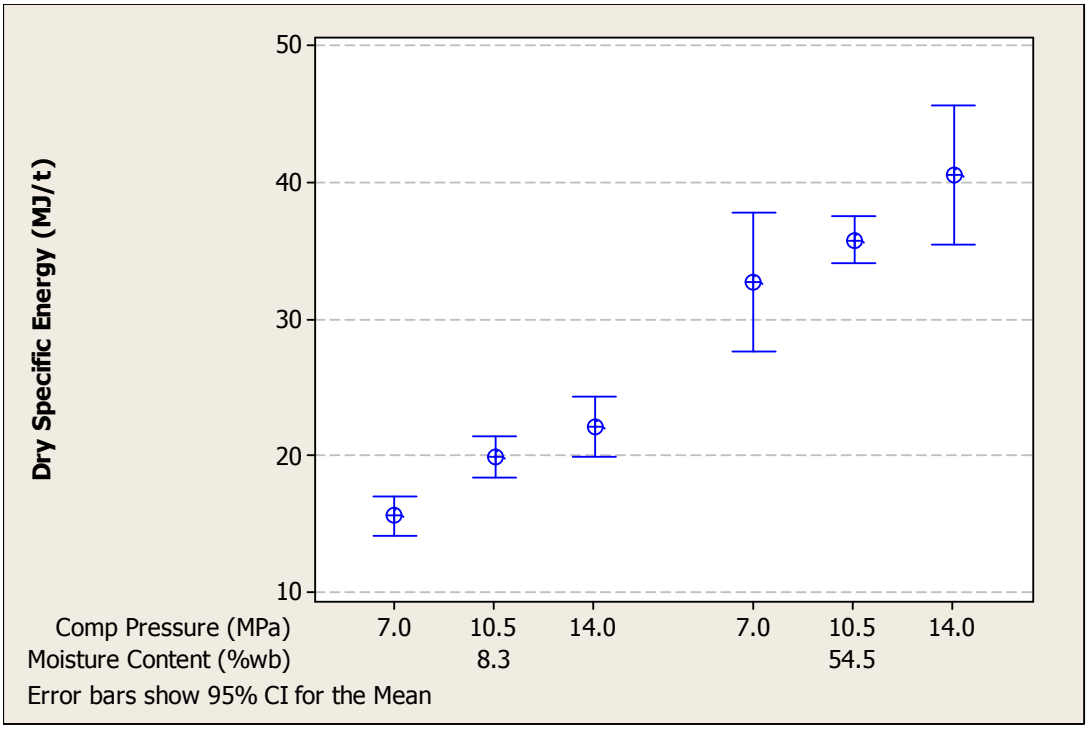

Figure 5.6. Material moisture content and compression pressure effects on dry specific energy (3-way interaction experiment)

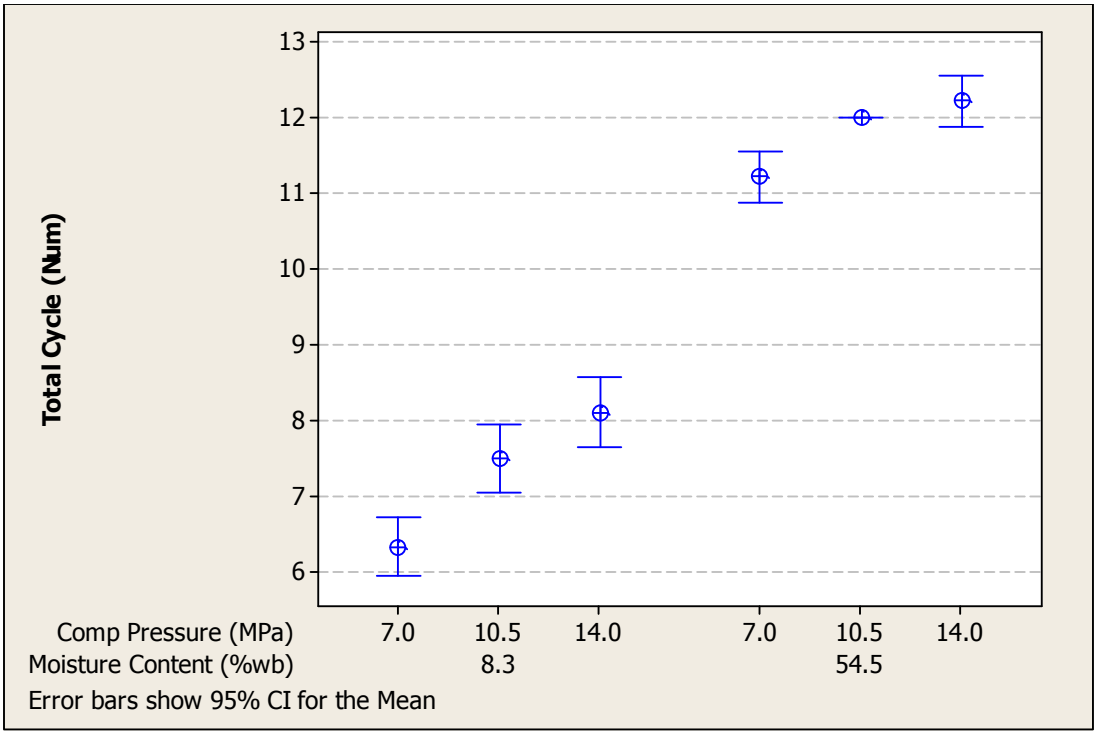

Figure 5.7. Moisture content main effect on total compression cycle count (3-way interaction experiment)

5.3.3. Material to Die Coefficient of Friction

The factorial ANOVA showed no effect on the coefficient of friction from material particle size, but could not prove there was no main or interaction effect from compression pressure and material moisture content (table 5.4). As expected, material moisture content accounted for the most variation, while compression pressure had a fairly small amount.

Table 5.4. 3-Way interaction factorial ANOVA for coefficient of friction

Material to Die Coefficient of Friction						
Source	DF	Seq SS	Adj SS	Adj MS	F	P
Compression Pressure (MPa)	2	0.0057	0.00614	0.00307	4.64	0.016
Particle Size Reduction Method	2	0.0037	0.0039	0.00195	2.94	0.066
Material Moisture Content (%wb)	1	0.34168	0.33811	0.33811	510.67	0.000
Compression Pressure (MPa) * Particle Size Reduction Method	4	0.00082	0.00081	0.0002	0.3	0.873
Compression Pressure (MPa) * Material Moisture Content (%wb)	2	0.00593	0.00592	0.00296	4.47	0.019
Particle Size Reduction Method * Material Moisture Content (%wb)	2	0.00436	0.00426	0.00213	3.21	0.052
Compression Pressure (MPa) * Particle Size Reduction Method * Material Moisture Content (%wb)	4	0.00233	0.00233	0.00058	0.88	0.486
Error	35	0.02317	0.02317	0.00066		
Total	52	0.38768				

Figure 5.8 shows the 95% confidence interval plot of the effects of compression pressure and material moisture content on the coefficient of friction. The effects of the different compression pressure treatments were not significant on a 95% confidence interval. Moisture content, however, had large and significant effects on the coefficient of friction. From 8.3 to 54.5%MCwb, (averaged over all levels of compression pressure and material particle size) the mean coefficient of friction decreased by about 40% (0.41 to 0.25).

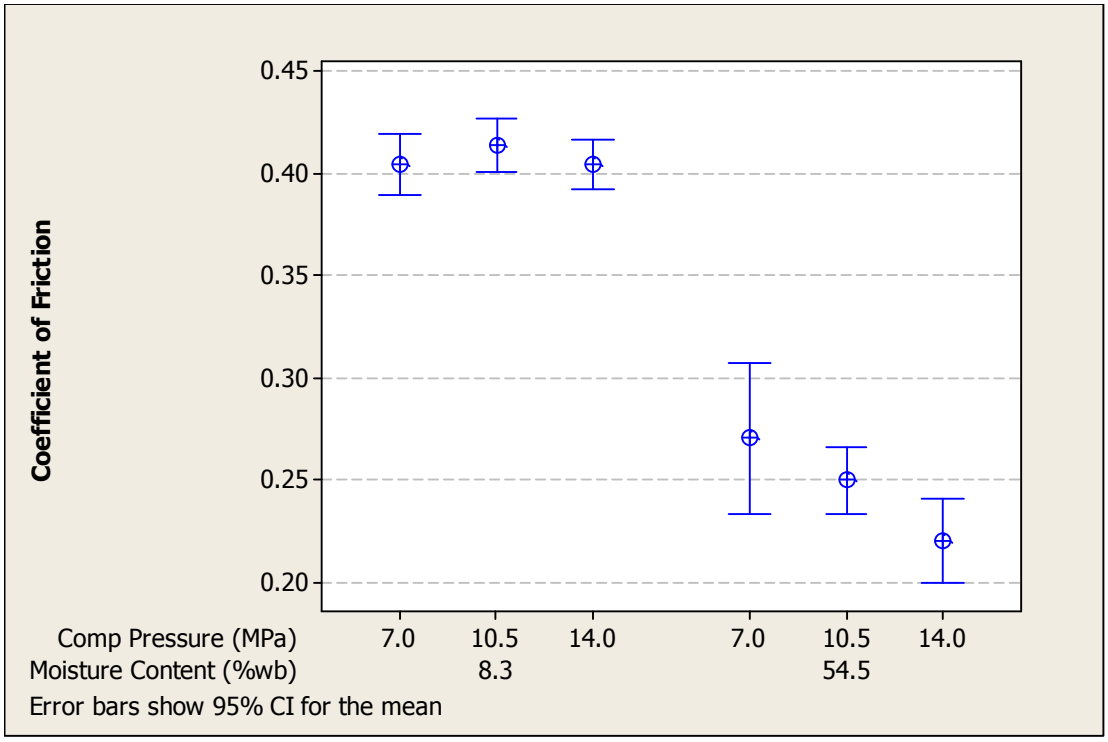

Figure 5.8. Moisture content and compression pressure effects on the coefficient of friction (3-way interaction experiment)

5.3.4. Qualitative Effects

The effect of compression pressure on the output briquette quality can be observed by visual inspection. Figure 5.9 shows a briquette produced at 7 MPa, while figure 5.10 shows one produced at 14 MPa (both are produced with 'as received' corn stover and at 8.3% MCwb). While the overall size and shape of the briquettes was about the same, the surface texture of the high pressure briquette is much smoother than the low pressure version. The individual flakes tended to hold together more readily on the high pressure briquettes than the low pressure versions, and this is reflected in the durability discussions in chapter 9.

Figure 5.9. Briquette produced during the 3-way interaction experiment. (7 MPa compression pressure, 8.3% MCwb, 42 mm particle size)

Figure 5.10. Briquette produced during the 3-way interaction experiment. (14 MPa compression pressure, 8.3% MCwb, 42 mm particle size)

The difference between the tested particle size reduction methods is visually noticeable. Figures 5.11, 5.12, and 5.13 show briquettes made with 'as received', Vermeer HG200 ground, and hammer milled corn stover respectively. The change in particle size is apparent by looking at the briquette surfaces. The hammer milled briquette shows a bit more flake separation, whereas the other two briquettes appear to be more uniform across the briquette length. Briquette surface stiffness was also significantly reduced for smaller particle sizes.

Figure 5.11. Briquette produced during the 3-way interaction experiment. (14 MPa compression pressure, 8.3% MCwb, 42 mm particle size)

Figure 5.12. Briquette produced during the 3-way interaction experiment. (14 MPa compression pressure, 8.3% MCwb, 22 mm particle size)

Figure 5.13. Briquette produced during the 3-way interaction experiment. (14 MPa compression pressure, 8.3% MCwb, 19 mm particle size)

5.4. Conclusions

During this experiment, briquettes were produced with a dry particle density range of 170-470 kg/m^3 at dry specific energy requirements of 12-52 MJ/t. Material moisture content was responsible for the most significant effects on dry particle density, dry specific energy, coefficient of friction, and briquette quality. Compression pressure demonstrated predictable effects on low moisture content material, but had no significant effects on high moisture content material. Material particle size demonstrated little to no quantitative impact on the output factors, and based on visual inspection, generated a lower quality briquette as particle size decreased.

Dry particle density was most affected by the associated effects of material moisture content, and in a highly negative manner. Significant axial expansion and lower dry weights occurred at increasing moisture contents, causing the overall dry particle density to significantly decrease. Compression pressure had a positive linear effect on dry particle density at low material moisture content (8.3%wb).

Similar to dry particle density, material moisture content demonstrated the largest effect on dry specific energy. Increasing the moisture content from 8.3 to 54.5%wb increased the dry specific energy of the densification process by about 90%. Reduced dry briquette weights and increased cycle count to reach a desired compression pressure are primarily responsible for this trend. A greater number of compression cycles to produce a lighter dry weight briquette was a very obvious reason for the large change in dry specific energy requirement. Similarly to dry particle density, compression pressure also had a positive linear effect on dry specific energy that was only significant at low moisture contents.

Material moisture content also was primarily responsible for changes in the material to die coefficient of friction. Increasing moisture content from 8.3 to 54.5%wb changes the material properties enough to decrease the coefficient of friction by about 40%. This means that if a scaled-up continuous flow densification machine were to be developed based from this bench, flexibility to control densified material flow would be required. Materials with higher moisture contents would flow much easier than materials with less moisture, making it more difficult to maintain a specified compression pressure.

While material moisture content was the only factor consistently significant on a 95% confidence interval to affect all of the output factors, qualitative differences between the briquettes based on the treatment values were quite noticeable, and could have a large impact on briquette quality. Increasing compression pressure increased the strength between flakes, which greatly improves durability during basic handling after densification. This effect was also seen with material particle sizes, where smaller sizes would result in less flake adherence, making them less durable to handle. Increasing moisture contents from 8.3%wb to 54.5%wb led to briquettes that not only had poor density and high energy requirements, but had very poor adherence between flakes, making them essentially impossible to handle as a single particle after densification.

Chapter 6. Moisture Effects Experiment

6.1. Objectives

This experiment was developed following the 3-way interaction experiment to further investigate the effects of material moisture content. Material moisture content demonstrated very significant effects across two widely spaced levels during the 3-way interaction experiment, so this experiment sought to improve the resolution of the analysis on moisture content. The objective of this experiment was to determine the main and interaction effects of compression pressure, material moisture content, and die taper angle. The outputs were expressed as dry particle density, dry specific energy, and the material to die wall coefficient of friction.

6.2. Materials & Methods

This experiment followed a similar design to the 3-way interaction experiment, however, it provided a more precise view of the effects of moisture content by testing three levels of moisture content instead of two. Corn stover for this experiment was sampled from the fall 2009 corn harvest in the Ames, IA region. This material was only available at a field harvested moisture content of 13.0%wb, so the materials tested at 24.8 and 47.6%MCwb had the moisture content artificially increased using the procedure from appendix B. All material was sampled from the same location, harvest date, and variety, however, these properties for this material are not known.

A full factorial design was used for this experiment with two levels of compression pressure, three levels of material moisture content, and two levels of die taper angle. This experiment was replicated three times for a total of 36 briquettes produced (table 6.1). Compression pressure was included in this experiment to determine if some of the trends that were observed but not significant during the 3-way interaction experiment could be significant in this setting. Die taper angle was included to determine if it had any direct effects on the output factors, and to provide a second replicate of data that would theoretically have the same coefficient of friction, but a different cap force because of the changing geometry.

Table 6.1. Treatment design for the moisture effects experiment

Moisture Effects Experiment		
Constants		
Variable	Value	Units
Material Type	Corn Stover	
Material Particle Size	40	mm
Material Feed Rate	0.23	kg/plunge
Plunging Distance	280	mm
Compression Speed	1.5	m/min

Variables			
Treatment (#)	Compression Pressure (MPa)	Material Moisture (%wb)	Die Taper Angle (deg)
1	8.8	13.0	3.6
2	14.0	13.0	3.6
3	8.8	24.8	3.6
4	14.0	24.8	3.6
5	8.8	47.6	3.6
6	14.0	47.6	3.6
7	8.8	13.0	7.2
8	14.0	13.0	7.2
9	8.8	24.8	7.2
10	14.0	24.8	7.2
11	8.8	47.6	7.2
12	14.0	47.6	7.2

Total Treatments	12
Replicates	3
Total Observations	36

6.3. Results

6.3.1. Dry Particle Density

Based on the factorial ANOVA for dry particle density, no significant mean differences were found for the die taper angle main or interaction effects. The hypothesis that the compression pressure and material moisture content treatments had no mean differences, however, was rejected (Table 6.2).

Table 6.2. Moisture effects experiment factorial ANOVA for dry particle density

Dry Particle Density (kg/m^3)						
Source	DF	Seq SS	Adj SS	Adj MS	F	P
Material Moisture Content (%wb)	2	76654.8	78633.1	39316.6	44.53	0.000
Compression Pressure (MPa)	1	15945.2	16026.6	16026.6	18.15	0.000
Die Taper Angle (deg)	1	1033.7	1021.4	1021.4	1.16	0.293
Material Moisture Content (%wb) * Compression Pressure (MPa)	2	8684.6	7515	3757.5	4.26	0.027
Material Moisture Content (%wb) * Die Taper Angle (deg)	2	1423.2	1669	834.5	0.95	0.403
Compression Pressure (MPa) * Die Taper Angle (deg)	1	119.5	64.3	64.3	0.07	0.790
Material Moisture Content (%wb) * Compression Pressure (MPa) * Die Taper Angle (deg)	2	2882.8	2882.8	1441.4	1.63	0.217
Error	23	20305.4	20305.4	882.8		
Total	34	127049				

Compression pressure demonstrated similar effects to those observed during the 3-way interaction experiment. Increasing levels of compression pressure produced significant dry particle density gains at moisture contents at and below 24.8%MCwb (figure 6.1). This trend was not significant at increased moisture contents (47.6%wb).

Following a similar trend to that displayed during the 3-way interaction experiment, material moisture content had a significant negative effect on dry particle density. Figure 6.2 shows the 95% confidence interval plot for the effects of material moisture content on dry particle density (averaged over all levels of compression pressure and die taper angle), which indicates a negative, linear relationship. From 13.0 to 47.6%MCwb, dry particle density decreased by approximately 35%. While the final relationship between moisture content and dry particle density was about the same between the 3-way interaction and moisture effect experiments, the reasoning behind the relationship was different.

Examining the briquette dry weight and axial expansion numbers can explain why the density was reduced at higher moisture contents. Figure 6.3 shows the mean briquette axial expansion and dry briquette weights for each moisture content level. An increase in dry briquette weight was observed between 13.0 and 24.8%MCwb, followed by a slight decrease at 47.6%MCwb. The weight increases were small (33% increase between 13.0 and

24.8%MCwb) in comparison to the changes in briquette axial expansion over different moisture contents. A sharp trend was observed between 13.0 and 47.6%MCwb where axial expansion increased by 360%, which completely negated the density gains the increased dry particle weight offered. This indicates that while certain moisture content levels might allow more dry material weight to be densified, any density gained in that manner will be lost upon ejection due to the increased elasticity of briquettes made from increased moisture content.

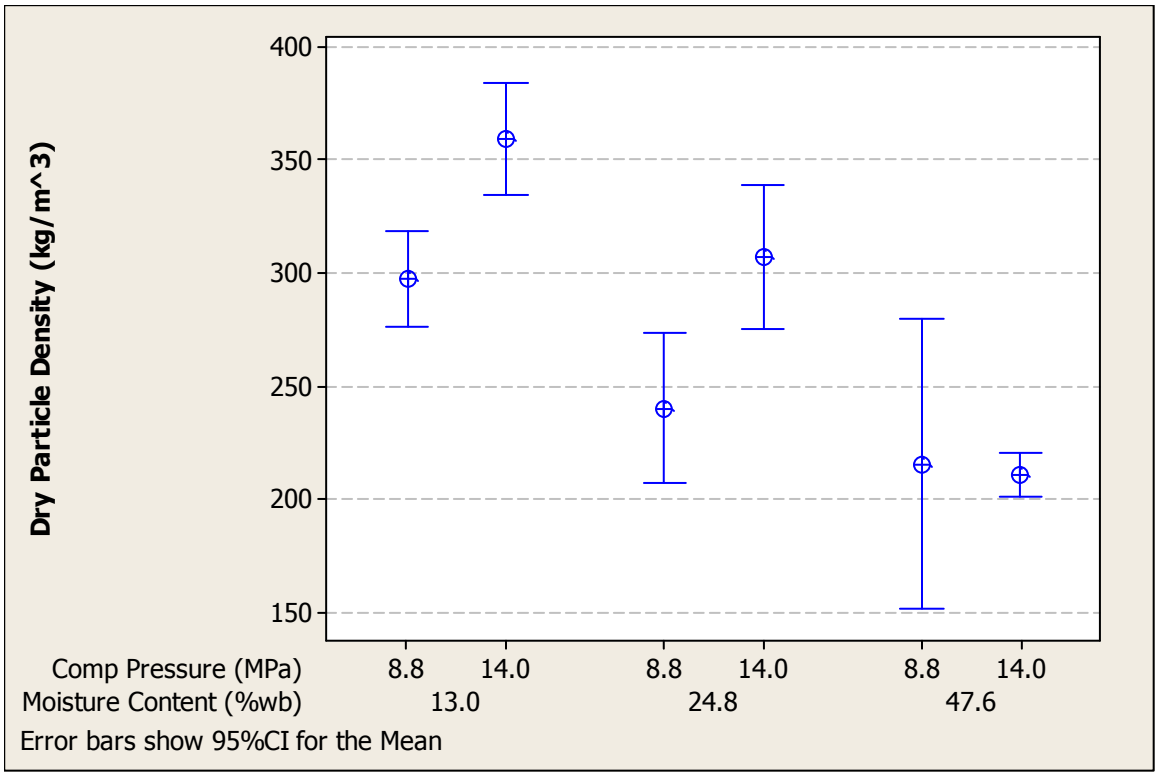

Figure 6.1. Compression pressure and material moisture content effects on dry particle density (moisture effects experiment)

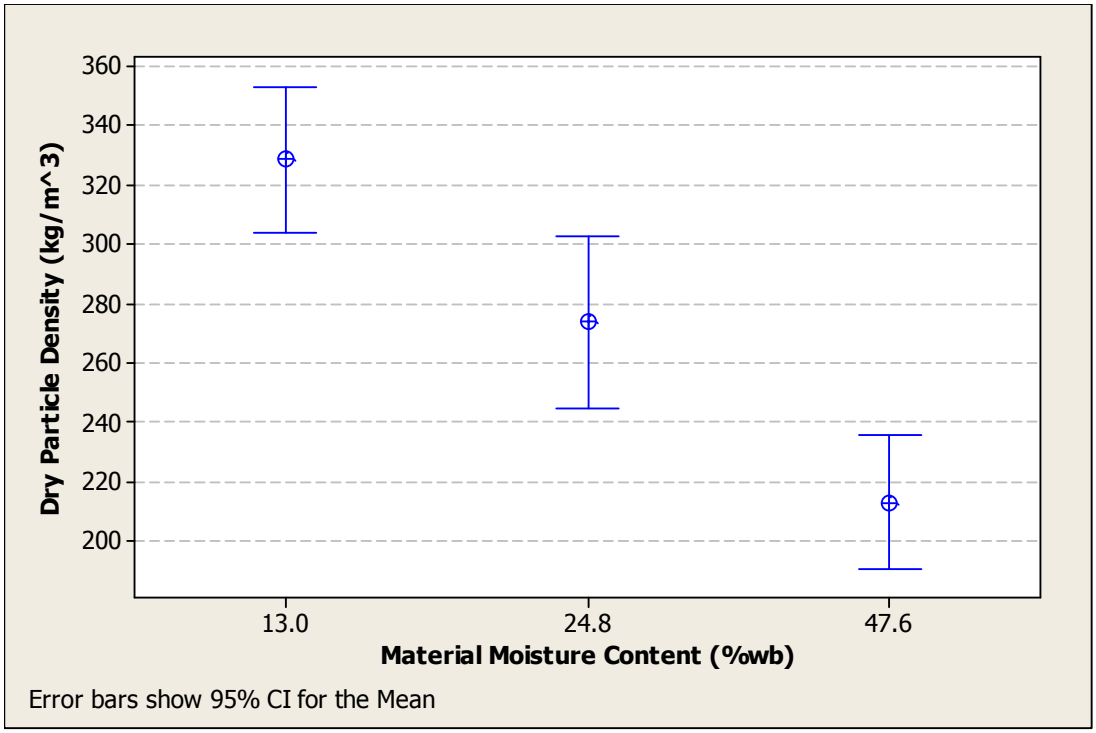

Figure 6.2. Moisture content main effect on dry particle density (moisture effects experiment)

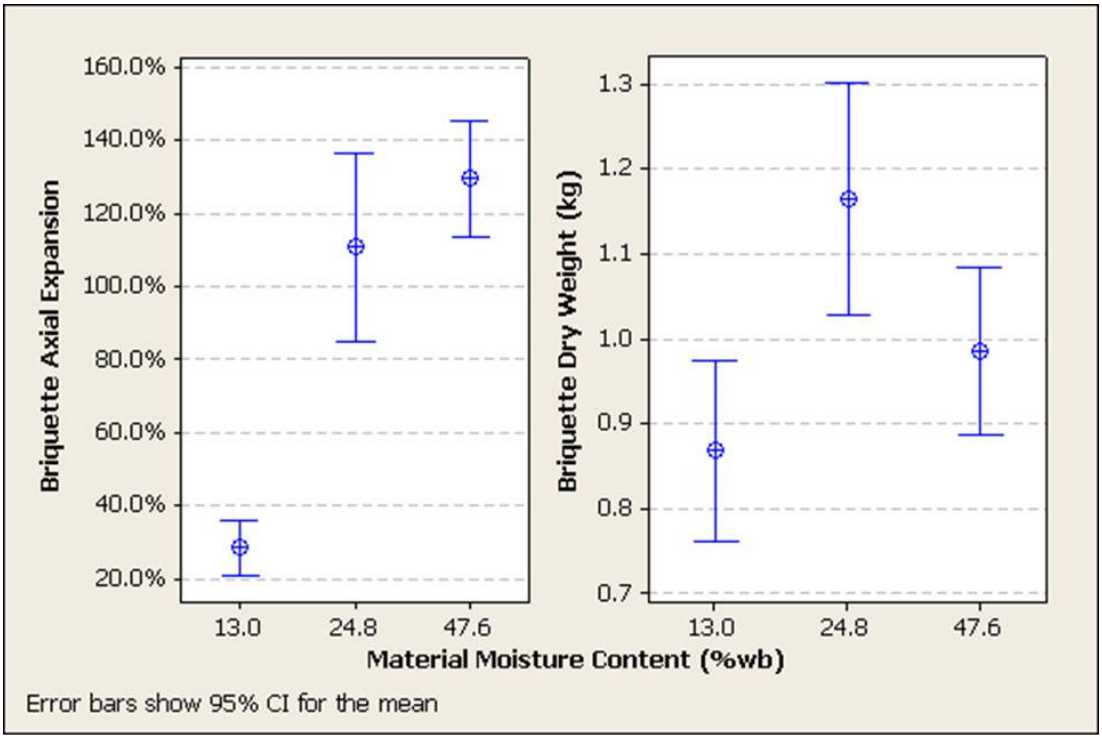

Figure 6.3. Moisture content main effect on dry briquette weight and briquette axial expansion (moisture effects experiment)

6.3.2. Dry Specific Energy

The factorial ANOVA rejected the hypothesis that compression pressure and material moisture content had no difference in group means (table 6.3), and accepted the hypothesis of no change in energy from die taper angle or any interaction factors. Contrary to what the 3-way interaction experiment determined, compression pressure demonstrated more variation than material moisture content on dry specific energy.

Table 6.3. Moisture effects experiment factorial ANOVA for dry specific energy

Dry Specific Energy (MJ/t)						
Source	DF	Seq SS	Adj SS	Adj MS	F	P
Material Moisture Content (%wb)	2	175.089	156.99	78.495	8.55	0.002
Compression Pressure (MPa)	1	432.81	419.45	419.45	45.71	0.000
Die Taper Angle (deg)	1	0.327	0.594	0.594	0.06	0.801
Material Moisture Content (%wb) * Compression Pressure (MPa)	2	9.595	7.307	3.654	0.4	0.676
Material Moisture Content (%wb) * Die Taper Angle (deg)	2	20.315	21.432	10.716	1.17	0.329
Compression Pressure (MPa) * Die Taper Angle (deg)	1	17.381	16.897	16.897	1.84	0.188
Material Moisture Content (%wb) * Compression Pressure (MPa) * Die Taper Angle (deg)	2	21.187	21.187	10.593	1.15	0.333
Error	23	211.042	211.042	9.176		
Total	34	887.744				

As expected, compression pressure demonstrated a significant and positive main effect on the dry specific energy requirement (figure 6.4). Increasing the compression pressure from 9.0 to 14.0 MPa significantly increased the dry specific energy at 24.8 and 47.6%wb moisture content. At these higher moisture content treatments, a 60% increase in compression pressure added about 40% to the specific energy requirement (which increased dry particle density by about 0-30%). The ratio is not 1:1 because the extra compression pressure allows more material weight to be briquetted as well. The overall energy requirement was increased by about 55% to increase the compression pressure, but the individual briquette weight was increased by about 15%. Contrary to what the 3-way

interaction experiment demonstrated, moisture content did not have a significant effect on dry specific energy (α=0.05).

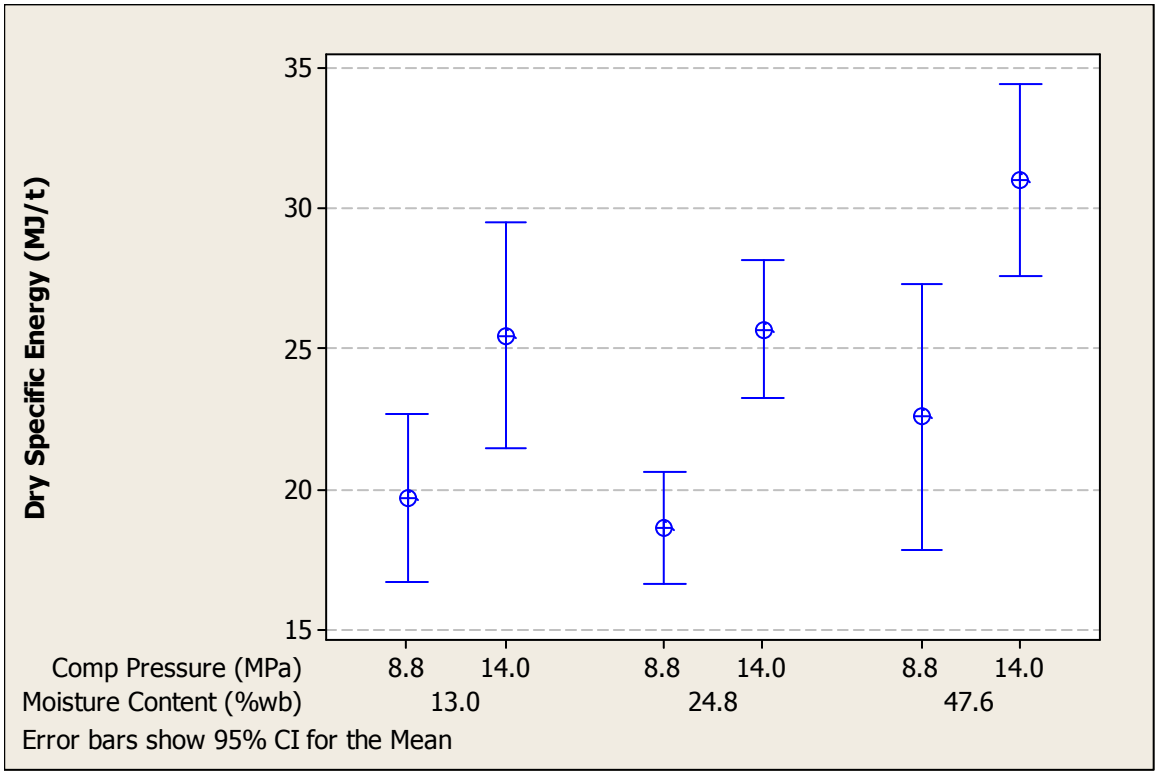

Figure 6.4. Material moisture content and compression pressure effects on dry specific energy (moisture effects experiment)

6.3.3. Coefficient of Friction

The factorial ANOVA for the coefficient of friction was only able to accept the hypothesis of no difference in group means for two interaction factors. Compression pressure did not show any difference in treatment levels when compared using 95% confidence intervals. Die taper angle and material moisture content demonstrated significant main and interaction effects at the 95% confidence level.

Table 6.4. Moisture effects experiment factorial ANOVA for coefficient of friction

Coefficient of Friction						
Source	DF	Seq SS	Adj SS	Adj MS	F	P
Material Moisture Content (%wb)	2	0.07668	0.07733	0.03867	165.96	0.000
Compression Pressure (MPa)	1	0.00242	0.00198	0.00198	8.5	0.008
Die Taper Angle (deg)	1	0.03163	0.03095	0.03095	132.84	0.000
Material Moisture Content (%wb) * Compression Pressure (MPa)	2	0.00702	0.00632	0.00316	13.57	0.000
Material Moisture Content (%wb) * Die Taper Angle (deg)	2	0.01146	0.01077	0.00539	23.11	0.000
Compression Pressure (MPa) * Die Taper Angle (deg)	1	0.00037	0.00042	0.00042	1.82	0.190
Material Moisture Content (%wb) * Compression Pressure (MPa) * Die Taper Angle (deg)	2	0.00078	0.00078	0.00039	1.68	0.209
Error	23	0.00536	0.00536	0.00023		
Total	34	0.13571				

Figure 6.5 shows an interval plot of the effects of moisture content and die taper angle on the coefficient of friction. Moisture content had significant main effects that were similar to those observed during the 3-way interaction experiment. At a 3.6^{o} taper angle, increasing moisture content from 13.0 to 47.6%wb decreased the average coefficient of friction by about 36% (0.45 to 0.28). This effect was less pronounced when using a 7.2^{o} taper angle die; the coefficient of friction only decreased by about 13% across the same moisture content range. At both die taper angles, the slope of the trend increased for increasing moisture content levels, indicating a potentially non-linear trend.

Unexpectedly, die taper angle demonstrated a significant main effect and an interaction effect with material moisture content on coefficient of friction ($\alpha = 0.05$) Changing die taper angles from 7.2^{o} to 3.6^{o} decreased the coefficient of friction by 14% (averaged over all levels of material moisture content and compression pressure). This was not anticipated because the die taper angle does not affect the input material properties. No further data was collected to explain this change between die taper angles. It could indicate a more complex force relationship between the plunger, material, and die than the calculations in this research have accounted. It could also indicate the changing material behavior as the corn stover transitions through plastic deformation from loose material to a single briquette.

A solid briquette would have a different die wall force value than a loose material, and the changing die taper angle would impact that force.

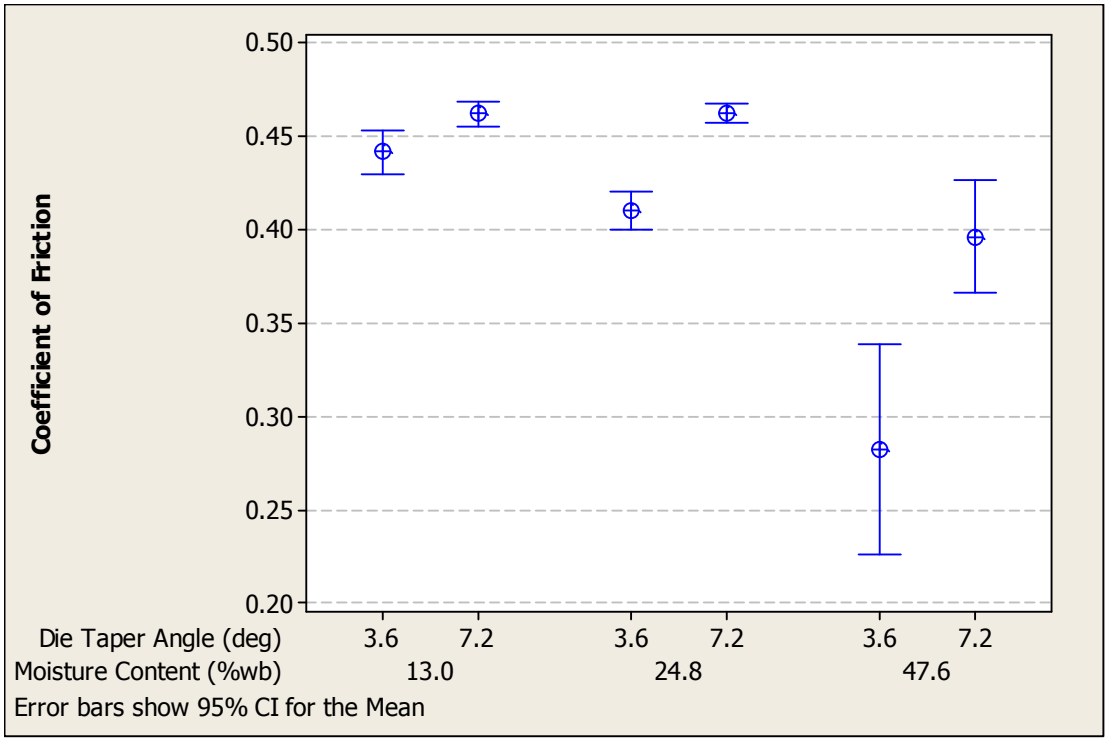

Figure 6.5. Moisture content main effect on material to die coefficient of friction (moisture effects experiment)

6.3.4. Qualitative Effects

A potential explanation for the effect of moisture content on the coefficient of friction can be observed during the briquetting process. Figure 6.6 shows the remaining material in the compression chamber after a briquette was produced at 47.6%MCwb and 14 MPa compression pressure. During the densification process, water was 'squeezed' from the material and formed puddles underneath the die. The water that did not exit the die moved to the perimeter of the die and chamber, as indicated by the arrows. This would artificially increase the moisture content of the material at the surface. If the trend of decreased coefficient of friction continues past 47.6%MCwb, and this moisture movement occurs consistently at increasing moisture contents, then this explains why there is a non-linear effect that increases the rate of change of coefficient of friction with respect to material moisture content.

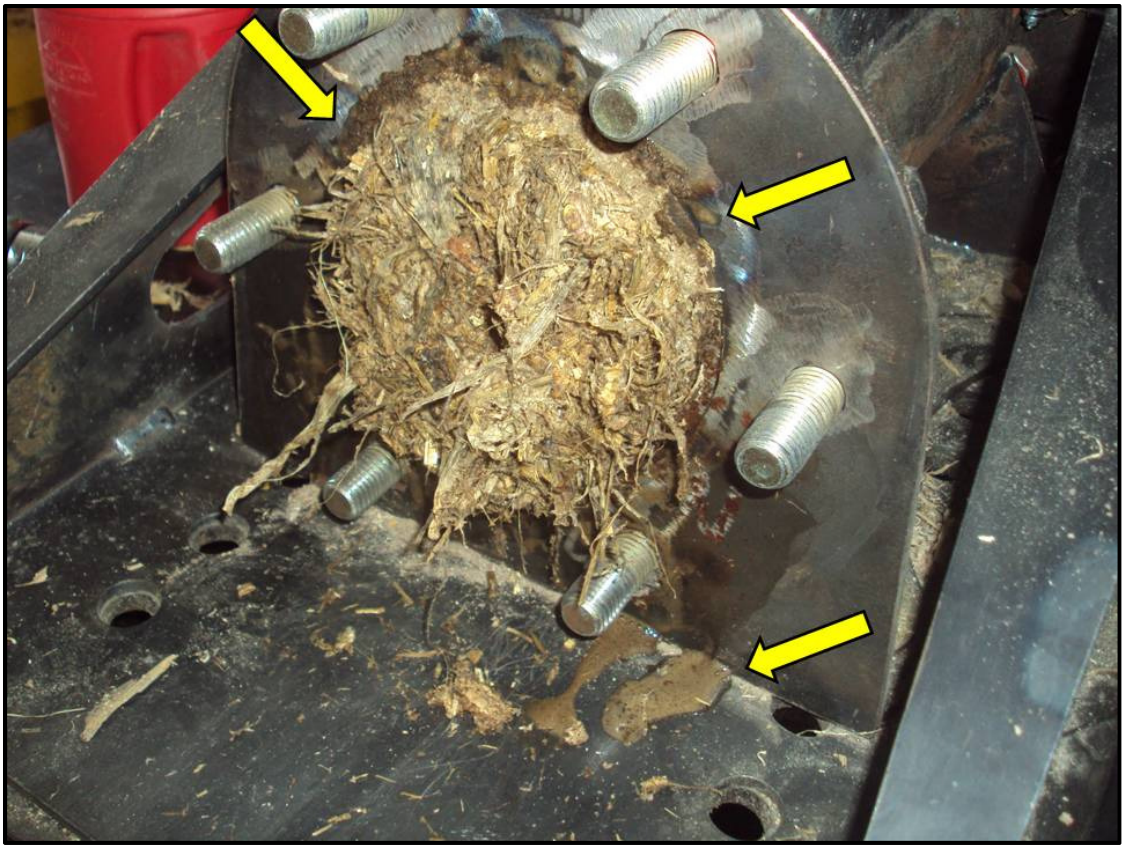

Figure 6.6. Compression chamber with die removed after producing a high moisture briquette

The effect of material moisture content on briquette quality can easily be visually observed. Figures 6.7, 6.8, and 6.9 show briquettes produced at 13.0, 24.8, and 47.6%MCwb, respectively (all other treatment variables are equal). The obvious visual difference is the amount of axial expansion observed on the high moisture briquette. Other differences include very low handling durability between the moisture contents. Dry briquettes like the example in figure 6.7 can be handled (by hand) without falling apart, while wet briquettes (like the one in figure 6.9) cannot be moved without completely supporting the briquette. Without support, it completely falls apart and handles like loose corn stover.

Figure 6.7. Briquette produced during the moisture effects experiment. (14 MPa compression pressure, 13.0%MCwb, 3.6^{o} die taper angle)

Figure 6.8. Briquette produced during the moisture effects experiment. (14 MPa compression pressure, 24.8%MCwb, 3.6^{o} die taper angle)

Figure 6.9. Briquette produced during the moisture effects experiment. (14 MPa compression pressure, 47.6%MCwb, 3.6° die taper angle)

It is easy to visually tell the difference between the two die taper angles tested in this experiment when the briquettes do not demonstrate a high level of axial expansion. Figure 6.10 shows a briquette produced using the 3.6° die, while figure 6.11 shows one produced using the 7.2° die (but otherwise with the exact same treatment levels as the other). High moisture briquettes produced with the two different dies are difficult to distinguish because of the large amount of expansion. There were no other visual or handling differences observed between the two die taper angles.

Figure 6.10. Briquette produced during the moisture effects experiment. (9 MPa compression pressure, 13.0%MCwb, 3.6° die taper angle)

Figure 6.11. Briquette produced during the moisture effects experiment. (9 MPa compression pressure, 13.0%MCwb, 7.2° die taper angle)

6.4. Conclusions

This experiment revealed very similar results regarding material moisture content as the 3-way interaction experiment, but with more resolution. Dry particle density was negatively affected by increasing moisture content levels due to a large change in material elasticity which caused large amounts of briquette axial expansion after ejection from the die. Specific energy was not significantly affected by moisture content during this experiment. The coefficient of friction responded similarly to the 3-way interaction experiment, where a negative relationship was observed between material moisture content and the coefficient of friction. This relationship increased in slope with an increasing moisture content indicating a non-linear relationship.

As anticipated, increasing compression pressure increased the total energy consumption, and also increased the briquette weight. The energy increase outweighed the increased briquette weight which caused a specific energy increase of about 35% when increasing compression pressure from 9.0 to 14.0 MPa (averaged over all treatment variable combinations). Similarly to the 3-way interaction experiment results, compression pressure had a positive effect on dry particle density at mid to low material moisture contents.

Die taper angle did not have a significant effect on either dry particle density or dry specific energy. Unexpectedly, die taper angle had significant effects on the coefficient of friction. While the die geometry did not directly affect the input material properties, it did

affect the force distribution of briquette and die system under compression cycles. While this relationship was not explained by the calculations used for this research, is does indicate that these changes in die angle will have very significant impacts on the material flowability in a continuous flow process. It could be explained by a true material friction change, or possibly by the shift in material behavior when transitioning from a loose to solid briquette.

Chapter 7. Material Types Experiment

7.1. Objectives

The objective of this experiment was to determine the main effects of material type, and the interaction of material type with particle size and compression pressure on the densification process characteristics. The material types tested in this experiment represent potential harvesting fractions of corn stover being researched today. These corn stover fractions could have different densification characteristics, so this experiment was designed to determine what differences could be found. The outputs were expressed as dry particle density, dry specific energy, and material to die wall coefficient of friction.

7.2. Materials & Methods

The different material types tested in this experiment included corn stover, MOG, and pure cobs. All material types are produced using a conventional combine harvester, but the headers and chaff processing attachments are different. Those differences are described in section 3.3.1. A full factorial design was utilized for this experiment with two levels of compression pressure, three different material types, and two different particle size reduction methods. Table 7.1 shows the complete experiment design. Particle sizes for a given size reduction method (hammer milled, or as received) were not the same due to the different nature of each material type. Different harvesting setups yielded different particle sizes, and different materials in the hammer mill produced different particle sizes as well. The actual particle size of each treatment is shown on the right-hand column. Corn stover for this experiment was sourced from multiple dates in various locations around the Ames, IA region during the fall 2010 harvest. The exact corn varieties, harvest dates, and locations for these materials are not known.

Table 7.1. Treatment design of material types experiment

Material Types Experiment				
Constants				
Variable		Value	Units	
Material Moisture Content		10-20%	%wb	
Die Taper Angle		3.6	deg	
Material Feed Rate		0.23	kg/plunge	
Plunging Distance		280	mm	
Compression Speed		1.5	m/min	
Variables				
Treatment (#)	Compression Pressure (MPa)	Material Type	Material Particle Size (method)	(mm)
1	7.0	Corn Stover	3	17
2	14.0	Corn Stover	3	17
3	7.0	Corn Stover	1	33
4	7.0	Corn Stover	1	33
5	7.0	MOG	3	12
6	14.0	MOG	3	12
7	7.0	MOG	1	31
8	14.0	MOG	1	31
9	7.0	Pure Cobs	3	2
10	14.0	Pure Cobs	3	2
11	7.0	Pure Cobs	1	39
12	14.0	Pure Cobs	1	39
Total Treatments	12			
Replicates	3			
Total Observations	36			

7.3. Results

7.3.1. Dry Particle Density

The factorial ANOVA showed no significant main effect from material type on dry particle density, however, it rejected the hypothesis of no difference from the interaction effect of material type and material particle size (table 7.2). The largest amount of variation was caused by compression pressure, which was expected because compression pressure was

always the second highest source of variation behind material moisture content in all of the other experiments with respect to dry particle density.

Table 7.2. Material types experiment factorial ANOVA for dry particle density

Dry Particle Density (kg/m^3)						
Source	DF	Seq SS	Adj SS	Adj MS	F	P
Material Type	2	3732	1371	686	2.01	0.154
Compression Pressure (MPa)	1	103604	102011	102011	298.66	0.000
Particle Size Reduction Method	1	4556	3790	3790	11.09	0.003
Material Type * Compression Pressure (MPa)	2	391	467	234	0.68	0.513
Material Type * Particle Size Reduction Method	2	3198	3032	1516	4.44	0.022
Compression Pressure (MPa) * Particle Size Reduction Method	1	27	40	40	0.12	0.734
Material Type * Compression Pressure (MPa) * Particle Size Reduction Method	2	7696	7696	3848	11.27	0.000
Error	27	9222	9222	342		
Total	38	132426				

Figure 7.1 shows the data means and confidence intervals of the dry particle density for each treatment variable combination during this experiment. No significant dry particle density differences were caused by material type ($\alpha = 0.05$). Similar to the previous experiments, the effect of material particle size was not consistent across each material type and compression pressure treatment, however, particle size did have a significant effect on pure cob materials at 14.0 MPa compression pressures. At this treatment, hammer milling the cobs resulted in an 11% increase in dry particle density.

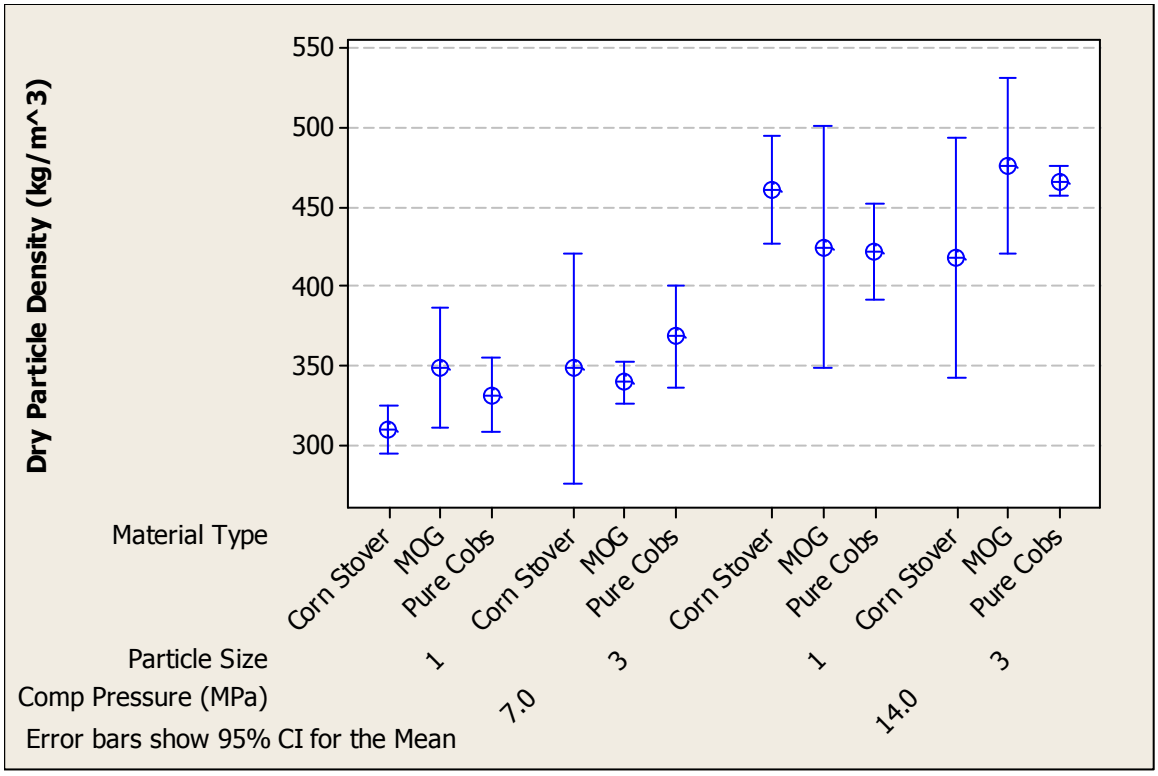

Figure 7.1. Treatment factor effects on dry particle density (material types experiment)

Compression pressure was the only variable that demonstrated consistently significant differences between treatment levels on a 95% confidence interval and rejected the factorial ANOVA null hypothesis. Figure 7.2 shows the interval plot for dry particle density at different compression pressure levels (averaged across every material type and particle size reduction method). In general, increasing compression pressure from 7 to 14 MPa increased the dry particle density by 30%. This can be directly attributed to a 30% increase in briquette weight, with essentially no change in the briquette axial expansion. This is expected because all materials tested in this experiment were at 5-15%MCwb, which showed very little axial expansion in previous experiments.

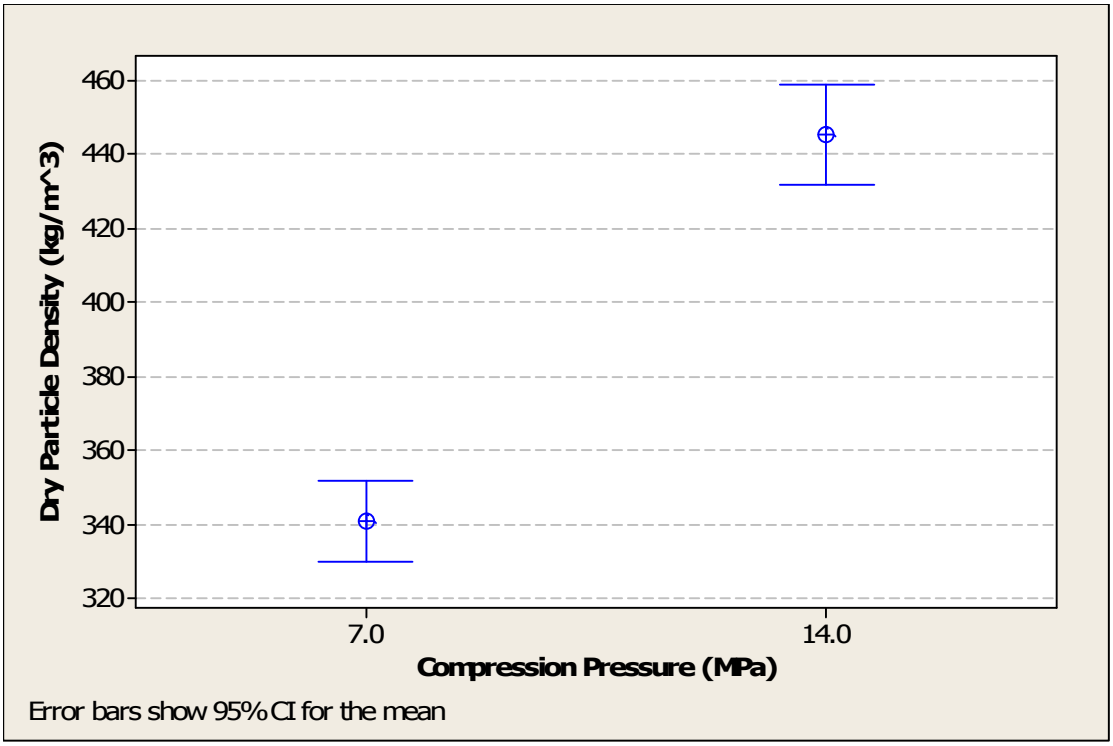

Figure 7.2. Compression pressure main effect on dry particle density (material types experiment)

7.3.2. Dry Specific Energy

The factorial ANOVA rejected the null hypothesis of no change in data means for all groups except two of the interactions (table 7.3). Again, compression pressure contributed the most variability to dry specific energy by a large margin.

Table 7.3. Material types experiment factorial ANOVA for dry specific energy

Dry Specific Energy (MJ/t)						
Source	DF	Seq SS	Adj SS	Adj MS	F	P
Material Type	2	39.49	35.99	17.99	5.19	0.012
Compression Pressure (MPa)	1	876.47	881.45	881.45	254.25	0.000
Particle Size Reduction Method	1	192.85	173.35	173.35	50	0.000
Material Type * Compression Pressure (MPa)	2	53.12	54.24	27.12	7.82	0.002
Material Type * Particle Size Reduction Method	2	33.01	30.2	15.1	4.36	0.023
Compression Pressure (MPa) * Particle	1	14.42	13.6	13.6	3.92	0.058
Material Type * Compression Pressure (MPa) * Particle Size Reduction Method	2	9.45	9.45	4.72	1.36	0.273
Error	27	93.61	93.61	3.47		
Total	38	1312.4				

Figure 7.3 shows the effects of all three treatment variables on dry specific energy. Material type demonstrated only a single significant effect on dry specific energy. For briquettes produced using an ‘as received’ particle size at 14.0 MPa compression pressure, pure cobs had approximately a 27% higher specific energy requirement than corn stover. No other treatment variable combinations demonstrated significant differences based on material type, indicating a weak relationship overall between material type and dry specific energy.

Similar to the effect of material type, particle size reduction method had only isolated significant effects on dry specific energy. MOG briquettes produced at 7.0 MPa, and pure cob briquettes produced at 14.0 MPa had similar significant effects caused by the particle size reduction method. In both of those treatments, ‘as received’ particle sizes had approximately a 30% higher specific energy requirement than hammer milled treatments. Compression pressure demonstrated approximately the same trend on dry specific energy it showed during the moisture effects experiment. Averaged over all particle size reduction methods and material types, increasing the compression pressure from 7.0-14.0 MPa increased the dry specific energy by about 65% (14.7-24.3 MJ/t). This is due to the additional compression cycles that are run to increase the applied compression pressure. These

additional cycles consume more energy than material weight added to the briquette which increased the overall dry specific energy.

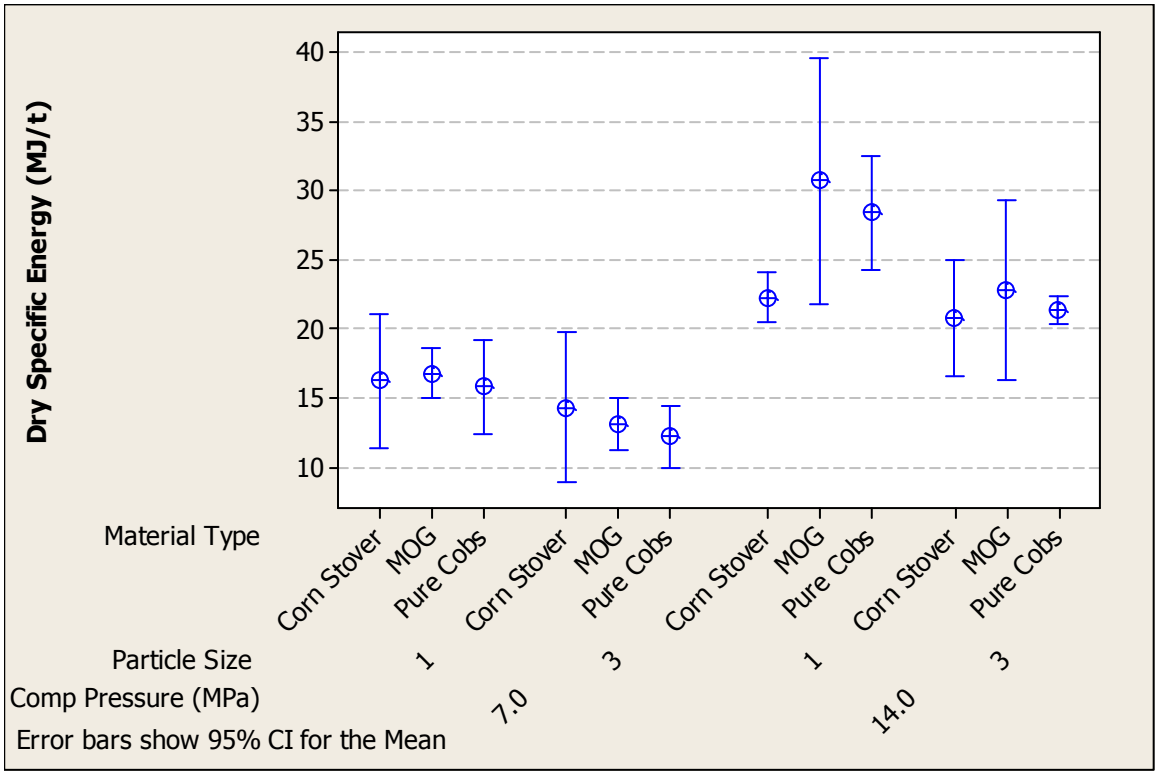

Figure 7.3. Treatment factor effects on dry specific energy (material types experiment)

7.3.3. Coefficient of Friction

The factorial ANOVA for coefficient of friction (table 7.4) rejected the no effect null hypothesis for all of the main effects and two interaction effects. Compression pressure and material particle size had small and isolated effects on the coefficient of friction, but were not consistent across all treatment combinations. These effects will not be discussed in this writing. Material type was responsible for the most variability, and was the only variable that had significant mean differences at a 95% confidence interval when averaged over all treatments.

Table 7.4. Material types experiment factorial ANOVA for coefficient of friction

Coefficient of Friction						
Source	DF	Seq SS	Adj SS	Adj MS	F	P
Material Type	2	0.061082	0.062038	0.031019	139.7	0.000
Compression Pressure (MPa)	1	0.001784	0.002406	0.002406	10.83	0.003
Particle Size Reduction Method	1	0.003779	0.001377	0.001377	6.2	0.020
Material Type * Compression Pressure (MPa)	2	0.001455	0.002029	0.001015	4.57	0.021
Material Type * Particle Size Reduction Method	2	0.006343	0.006313	0.003157	14.22	0.000
Compression Pressure (MPa) * Particle Size Reduction Method	1	0.000081	0.000017	0.000017	0.08	0.782
Material Type * Compression Pressure (MPa) * Particle Size Reduction Method	2	0.001504	0.001504	0.000752	3.39	0.051
Error	24	0.005329	0.005329	0.000222		
Total	35	0.081356				

Figure 7.4 shows the effect of material type on the coefficient of friction when averaged over all levels of compression pressure and particle size reduction method. The coefficient of friction showed a decreasing trend with respect to increasing cob content of material (from corn stover, to MOG, to pure cobs). While the coefficient of friction of the MOG material was not significantly different from pure cobs ($\alpha = 0.05$) the means indicated a steady decreasing trend with respect to increasing cob content. This trend is similar to the trend displayed for increasing moisture content, however, the increasing cob content does not share the same negative relationship with dry particle density as increasing material moisture content does. This indicates that the changing frictional relationship is not always consistent with the changing density relationship.

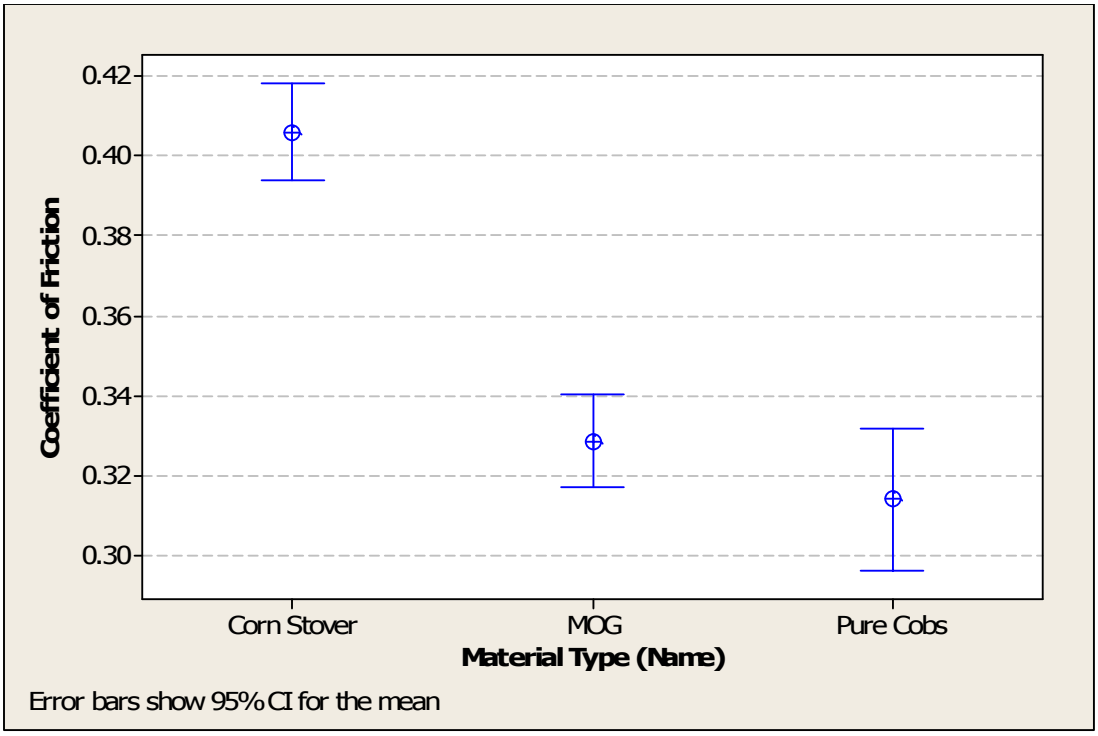

Figure 7.4. Material type main effect on coefficient of friction (material types experiment)

7.3.4. Qualitative Effects

Figures 7.5, 7.6, and 7.7 show briquettes made from corn stover, MOG, and pure cobs, respectively. The surface texture of MOG and pure cobs was significantly smoother and stiffer than the surface of the corn stover product. As with all tests involving corn stover, it was not hard to find the flake divisions, however that was less true with MOG and nearly impossible with the pure cob briquettes. MOG and pure cobs seemed to form more of a single unit briquette compared with corn stover, which likely impacts the briquette durability which is described in detail in chapter 9.

Figure 7.5. Briquette produced during the material types experiment. (14 MPa compression pressure, 13%MCwb, corn stover)

Figure 7.6. Briquette produced during the material types experiment. (14 MPa compression pressure, 11%MCwb, MOG)

Figure 7.7. Briquette produced during the material types experiment. (14 MPa compression pressure, 10%MCwb, pure cobs)

7.4. Conclusions

While material type demonstrated no consistently significant effects on dry particle density or dry specific energy, significant qualitative differences could be observed. Output product quality was significantly improved with an increased cob content in terms of flake-to-flake strength and surface smoothness and stiffness. Significant decreases in the material to die coefficient of friction were observed based on material type; it decreased 25% going from corn stover to pure cob treatments. Material type did demonstrate a significant increase in specific energy from corn stover to pure cobs during the densification of 'as received' material at 14.0 MPa.

Compression pressure demonstrated significant effects on both dry particle density and dry specific energy very similar to the effect observed during the 3-way interaction and the moisture effects experiment. Material particle size showed significant effects on both dry particle density and dry specific energy during the densification of pure cobs at 14.0 MPa. Reducing the particle size of pure cobs using the hammer mill produced briquettes with 11% greater dry particle density at 25% less the specific energy requirement.

Chapter 8. Bulk Density Experiment

8.1. Objectives

All of the previous experiments reported density in terms of particle density. Particle density is not a true representation of the bulk density of a material, so this experiment was conducted to determine the relationship between particle density and bulk density. The previous experiments had shown that varying moisture content created the largest variance in the particle density of the briquette, so the objective of this experiment was to test the effect of moisture content on the dry bulk density of the product.

8.2. Materials and Methods

This experiment was conducted without performing any of the measurements illustrated in the briquetting procedure (Appendix A) because those measurements were not of interest in this experiment. The procedure was modified to only include the necessary steps to produce a briquette. Briquettes were produced and filled into 189 l (50 gal) barrels until the barrels were approximately 60% full. No care was taken to stack the briquettes into the barrels to optimize space utilization, they were simply 'tossed' into the barrel in order to avoid data biasing for filling efficiency. Measurements were then taken on the volume and weight of the sample in the barrel to produce bulk density data for a particular barrel. This method was selected over other standardized methods like ASTM Standard E873-82 because of the physical limitations of the standard. ASTM E873 specifies the density be measured in a 305 x 305 x 305 mm (12 x 12 x 12 in) box. This box does not have large enough physical dimensions to accommodate the efficient filling of these briquettes, so a larger vessel was required. The 189 l (50 gal) drums were being used for densified corn stover storage research, so it was convenient to test the density using them as a container.

This experiment tested material moisture content at two different levels, and was replicated three times for a total of six briquette-filled barrels. The experimental unit in this test was a barrel full of briquettes of a particular treatment (as opposed to an individual briquette) because the desired output was bulk density instead of particle density. The complete experiment design is shown in table 8.1. All other treatment variables were conducted at 'ideal' levels to optimize particle density to provide information on the best

density this current system can produce for given moisture contents. The corn stover used for this experiment was taken from the same samples used in the 3-way interaction experiment (multiple dates during the fall 2010 harvest). The exact corn varieties, harvest dates, and locations for these materials are not known.

Table 8.1. Treatment design of bulk density experiment

Bulk Density Experiment		
Constants		
Variable	Value	Units
Compression Pressure	14	MPa
Die Taper Angle	3.6	deg
Material Feed Rate	0.23	kg/plunge
Plunging Distance	280	mm
Compression Speed	1.5	m/min
Material Type	Corn Stover	
Material Particle Size	40-42	mm
Variables		
Treatment (#)	Material Moisture Content (%wb)	
1	8.3%	
2	54.5%	
Total Treatments	2	
Replicates	3	
Total Observations	6	

8.3. Results

Figure 8.1 shows the bulk density results from the two treatments of the bulk barrels experiment alongside the average particle density values for the same treatments. Similar to dry particle density, a significant decrease in dry bulk density was observed from 8.3 to 54.5%MCwb. As expected, a large decrease was also observed between dry particle density and dry bulk density. For 54.5%MCwb stover, the dry density decreased approximately 70% going from particle to bulk density while the 8.3%MCwb stover had a decrease of approximately 60%. The dry material had a mean dry bulk density of 190 kg/m^3 (wet bulk density = 210 kg/m^3), while the wet material had a dry bulk density of 64 kg/m^3 (wet bulk

density = 141 kg/m^3), marginally improved from a non-densified material sample. This inefficiency in translating particle density to bulk density was created by large void spaces between the particles, creating a large amount of storage space taken by air.

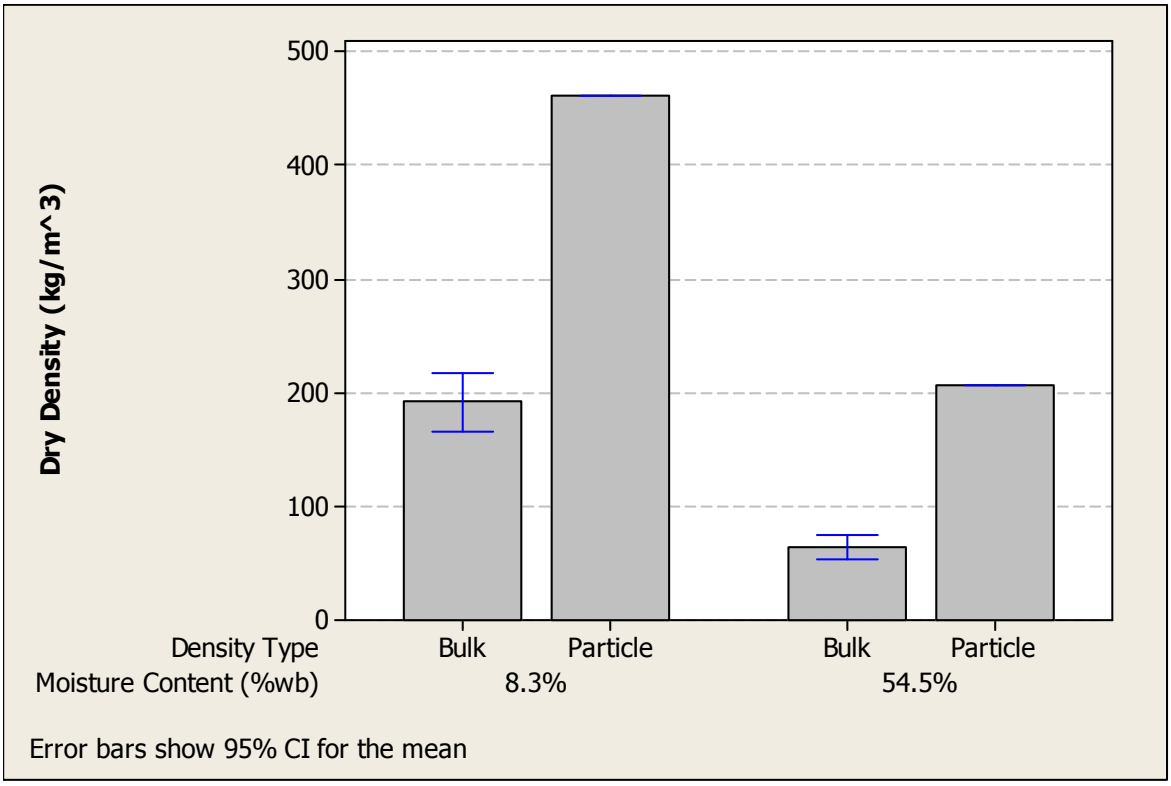

Figure 8.1. Moisture content main effect on dry bulk and particle density (bulk barrels experiment)

8.4. Conclusions

Briquettes produced in this densification setup lost a significant portion (60-70%) of their particle density when bulk loading these materials. This density loss can be used to estimate the bulk density of other briquette treatment combinations. The low moisture briquettes produced a bulk density of 190 kg/m^3 (wet bulk density = 210 kg/m^3), which is competitive with the bulk density of both round bales and large square bales, but falls short of the bulk density needed to optimize transportation efficiency discussed in section 1.

Based on maximum legal trailer dimensions (without a specialized permit), this densified corn stover product allows over the road trucks to theoretically haul approximately 18-19.5 metric tons using a single 16.1 m (53 foot) live bottom trailer. By comparison, up to

18-20 metric tons of large square bales (0.9 m x 1.2 m x 2.4 m) can be hauled using a single 16.1 m (53 foot) flatbed or drop deck trailer. 8.5-9.7 metric tons of round bales (1.8 m diameter x 1.5 m wide) can be legally hauled without an over-width permit, while up to 19.5 metric tons can be hauled with a specialized permit (to allow a bales to be stacked two-wide (3.1 m), which is over the 2.6 m width restriction). None of these systems fully utilize the maximum legal combined weight of 36.3 metric tons (Iowa DOT, 2011), so they are not optimized for over the road transport at these densities.

Chapter 9. Durability Analysis of Briquettes

9.1. Objectives

To further assess the practicality of the briquetting method in this research, durability testing was required. Previous experiments determined the output dry particle density and the dry specific energy requirement to produce a briquette. These metrics provided a means of determining the baseline outputs and engineering requirements, however, they did not provide a full indication of the product durability during handling operations.

The objective of this experiment was to determine briquette durability based on mechanical and material variables. The following specific objectives were derived based on ASABE S269.4 – Cubes, Pellets, and Crumbles – Definitions and Methods for Determining Density, Durability, and Moisture Content. Determine the effects of compression pressure, material particle size, material moisture content, and material type, and express the outputs as Durability Rating (DR) and Side Distribution Index (SDI).

9.2. Materials & Methods

9.2.1. ASABE S269.4

ASABE Standard S269.4 outlines a procedure for determining the durability of a 'cube', which is defined as "An agglomeration of unground ingredients in which some of the fibers are equal to or greater than the length of the minimum cross-sectional dimension of the agglomeration. The configuration of the agglomeration may take any form." The usage of this procedure was appropriate, because many of the briquettes produced on the densification bench include particles exceeding 76 mm, which is the smallest cross-section of a briquette produced using the 7.2^{o} die.

The procedure for determining the durability of cubes involved tumbling the briquettes at a specified rate and period of time in the durability tester shown in figure 9.1. After tumbling, the remaining particles are sorted based on final weight into different weight classes, and the weight of all materials in each weight class was used in calculating the output values.

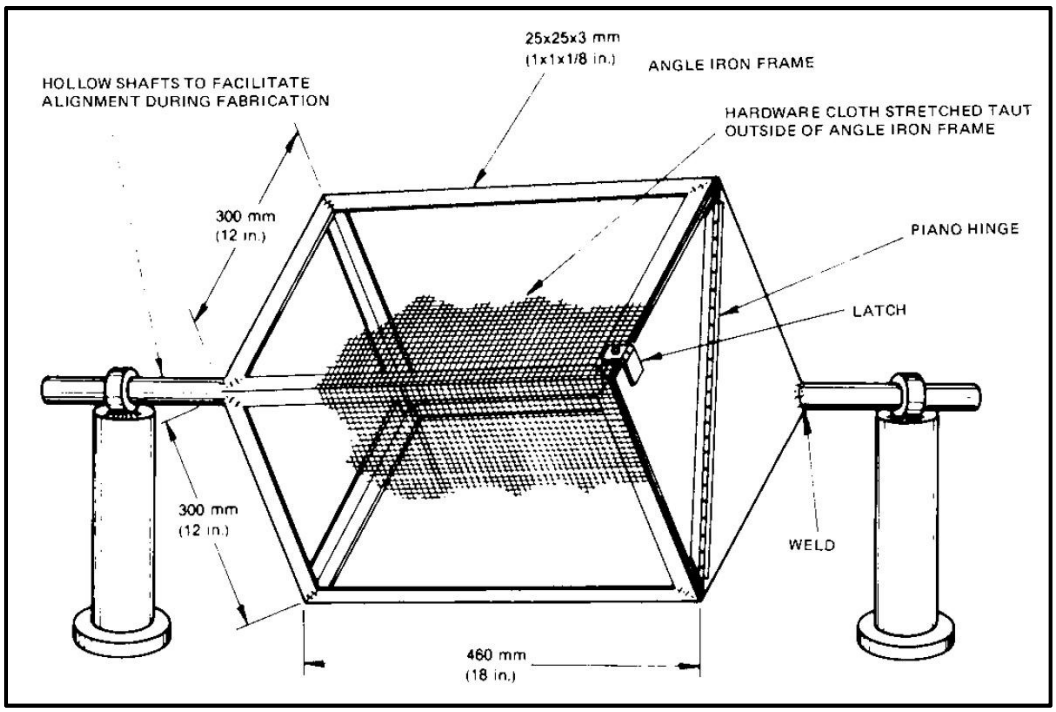

Figure 9.1. ASABE S269.4 durability tumbling apparatus for cubes

The standard tumbling apparatus is a 305 mm x 305 mm x 460 mm box rotating on a diagonal axis (across two planes). The box is covered in 12.7 mm mesh hardware cloth, and cube samples are tumbled for 3 minutes in the box at 40 rpm. After tumbling, particles weighing more than 20% of the average initial cube mass are separated out and designated cube size material (CSM). From there, the CSM particles are sorted into five weight classes, each class expressing 20% increments of the original average cube weight. The durability rating for cubes is defined as the percentage of total input material that qualifies as CSM after tumbling (or the percentage of material greater than 20% of the initial average cube weight). The formula is shown below in equation 9.1.

Equation 9.1. Durability rating for cubes

$$DR = \frac{M_{CSM}}{M_{INPUT}} * 100$$

where

DR: Durability rating

M_{CSM}: Weight of cube sized material (particles weighing more than 20% of the average initial briquette weight)

M_{INPUT}: Weight of input material

The size distribution index is used as an indication of the weight distribution of the particles remaining after the tumbling test. The formula is shown below in equation 9.2. The SDI ranges between 0 and 400 with 400 indicating a 'perfect' durability.

Equation 9.2. Size distribution index for cubes

$$SDI = 4 * M_{80-100\%} + 3 * M_{60-80\%} + 2 * M_{40-60\%} + 1 * M_{20-40\%}$$

where

SDI: Size distribution index

$M_{80\text{-}100\%}$: Percent of total particles weighing 80-100% of the average initial cube weight

$M_{60\text{-}80\%}$: Percent of total particles weighing 60-80% of the average initial cube weight

$M_{40\text{-}60\%}$: Percent of total particles weighing 40-60% of the average initial cube weight

$M_{20\text{-}40\%}$: Percent of total particles weighing 20-40% of the average initial cube weight

9.2.2. Durability Tumbler Development

Tumbler Capacity

The standard did not describe the volume range of a cube or offer any indication of the maximum volume the cubes should use in the tumbler box during a test. The standard did mention that a sample of ten cubes should be utilized for durability testing. With the box volume equal to 0.042 m^3, and the average volume of ten bricks being about 0.039 m^3 (91% of box capacity), the experimental setup would not work as defined in ASABE S269.4. This was because the briquettes produced on the ISU bench likely have a much larger volume than the cubes used to develop the standard.

To provide a more balanced volume ratio, the number of briquettes used in the box was reduced, and the outside dimensions of the box were modified to increase the overall volume capacity. The box dimensions were increased to 457 mm x 457 mm x 610 mm, which increased the volume to 0.127 m^3. The number of briquettes per test was reduced to three, which uses only 9% of the tumbler volume capacity.

Tumbler Speed

Due to the increase in overall size, the rotational radius of the tumbler box was changed. This required a change in rotational speed to keep the outside velocity of the

tumbler box the same as the standardized box. If the radius is assumed to be the width dimension of the box (305 mm on the standard box, 457 mm on the new box), then the velocity at that radius can be set equal between the two boxes to determine the necessary rotational velocity for the larger box. Table 9.1 shows the calculations for the modified rotational speed.

Table 9.1. Tumbler box rotational speed calculation.

	Value	Units
Standardized Box		
Rotational Speed	40	rpm
Box 'Radius'	305	mm
Velocity at Radius	77	m/min
Larger Box		
Box 'Radius'	457	mm
Velocity at Radius	77	m/min
Rotational Speed	27	rpm

Based on those calculations, the necessary shaft speed to drive the larger box at the same outside velocity as the standard box is 27 rpm. This speed was used for all durability experiments conducted in this project.

Tumbler Design

The final tumbler design (Pro/E CAD model) can be seen in figure 9.2. The catch pan (green) for any materials that fall from the tumbler box was removable for quick cleaning. A chain drive powered by a hydraulic gear motor was used to drive the box, and was located under the shield (red). Material was added and removed from the tumbler through the hinged door (white). Figure 9.3 shows the completed durability tumbler.

The tumbler required an external hydraulic power supply source with an adjustable flow of 4-8 lpm (1-2 gpm), and directional valving. Box rotational speed was controlled by varying the hydraulic flow to the motor. There was no means of reading box rotational speed automatically, so speed reading and control was done manually. The desired rotational speed (27 rpm) was slow enough that the operator could count the revolutions while timing with a

stop watch to determine speed, and adjust the hydraulic flow accordingly. These adjustments were made before the experiments began, and then verified during the tests.

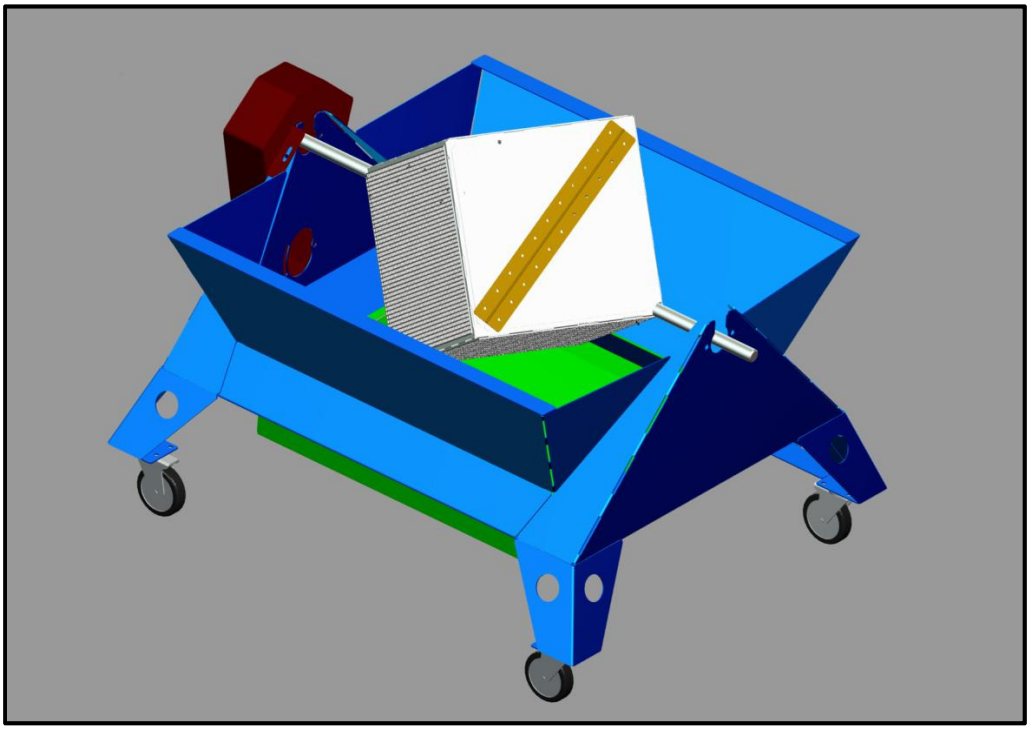

Figure 9.2. CAD model of the ISU durability tumbler.

Figure 9.3. Iowa State University durability tumbler.

9.2.3. Durability Testing Method

The durability testing procedure was almost identical to the procedure outlined in the standard, and is as follows:

1. Measure and record the weight of the empty tub for holding briquettes.
2. Measure and record the weights of all of the empty tubs used for sorting the particles into their mass classes.
3. Procure three briquettes of the specified treatment to be tested and place them in the empty briquette tub.
4. Measure and record the weight of the tub holding the three briquettes to be tested.
5. Ensure the durability tumbler is clean from material from previous experiments.
6. Open the hinged door (figure 9.4) and load the three briquettes into the tumbler, close the door, and tighten the locking hardware.

Figure 9.4. Tumbler Door.

7. Ensure that hydraulic power is properly connected to the control valve and the tumbler, and if so, engage the hydraulics such that the tumbler box rotates clockwise when facing the shield end of the tumbler at 27 rpm. At the same time, start the stop watch to keep track of the tumbling time.
8. After three minutes of tumbling time, disengage hydraulic flow to the tumbler.

9. Open the hinged tumbler door, and sort all particles into the appropriate tub according to mass. Reference the calculation spreadsheet to determine what weights the 20% increment classes are divided at, and sort the particles in the tumbler according to those classes. Having the scale on hand is helpful in checking particles that may be close to the weight class division.
10. Empty all material in the catch pan into the 0-20% weight class tub. (All particles that fall through the screen are assumed to be less than 20% of the average briquette weight.)
11. Measure and record the loaded weight of all of the weight class tubs.
12. Refer to end of the calculation spreadsheet to see the values for the Size Distribution Index and Durability Rating.

Durability Experiments

While the objectives of the durability test were to determine the effects of compression pressure, particle size, moisture content, and material type; not all combinations of the above variables were used in the tumbler test. Throughout the briquetting experiments, several combinations of the above variables showed no potential for any durability value. Qualities that were observed during the production of these zero durability briquettes included extensive axial expansion after ejection from die, excessive flake separation, and low flake stiffness. Many of these examples actually expanded almost back to the same appearance as the loose stover that was used in the input for densification.

The settings that drew obvious zero durability observations focused mainly on the compression pressure and moisture content variables. Any compression pressure below 10.5 MPa, and any moisture content above 25% MCwb (figure 9.5) had obvious durability problems. There were no observations of this nature with respect to particle size and material type.

Figure 9.5. Briquette produced at 54.5% moisture content.

The durability tumbling experiment was developed with those observations in mind. The only variables tested in the experiment were material type and particle size, at specified moisture contents and compression pressures that were observed to have a potential for non-zero durability values.

A factorial experiment was developed which tested three different material types, and two different material particle size reduction methods. Due to the different nature of each corn stover fraction, each material type did not have the same particle sizes for the same size reduction treatment, or the same moisture content. Table 9.2 shows of all treatment combinations tested in this experiment, along with the actual particle size and moisture content of each treatment. Each treatment was replicated three times, for a total observation count of 18. All durability tests were conducted within 24 hours of briquette production. Corn stover for this experiment was sourced from multiple dates in various locations around the Ames, IA region during the fall 2010 harvest. The exact corn varieties, harvest dates, and locations for these materials are not known.

Table 9.2. Treatment design for the durability experiment

Durability Experiment				
Constants				
Variable		Value	Units	
Compression Pressure		14.0	Mpa	
Moisture Content		As Received		
Die Taper Angle		7.6	deg	
Treatment	Material Type	Particle Size Reduction Method		Moisture Content
		(method)	(mm)	(%wb)
1	Corn Stover	3	17	8.3
2	MOG	3	12	12.0
3	Pure Cobs	3	2	10.0
4	Corn Stover	1	42	8.3
5	MOG	1	31	11.0
6	Pure Cobs	1	39	10.0

9.3. Results

9.3.1. Durability Rating and Standard Distribution Index

The tumbler experiments revealed strong main effects from both material type and particle size on the durability rating and size distribution index. Table 9.3 shows the ANOVA results for both the durability rating and size distribution index. The near-zero p-values show that both particle size control and material type demonstrate potentially significant main effects. The ANOVA also shows a potential interaction effect between particle size and material type, however, this can be neglected as the durability values for all hammer milled materials was the same. More treatments on particle size would be required to determine if a significant interaction actually occurred.

Table 9.3. Durability experiment factorial ANOVA for durability rating and size distribution index

Durability Rating

Source	DF	Seq SS	Adj SS	Adj MS	F	P
Material Type (Name)	2	717.44	717.44	358.72	15.83	0.000
Particle Size Reduction Method	1	3556.42	3556.42	3556.42	156.98	0.000
Material Type (Name)* Particle Size Reduction Method	2	717.44	717.44	358.72	15.83	0.000
Error	12	271.86	271.86	22.66		
Total	17	5263.15				

Size Distribution Index

Source	DF	Seq SS	Adj SS	Adj MS	F	P
Material Type (Name)	2	2179.5	2179.5	1089.8	32.36	0.000
Particle Size Reduction Method	1	5432.8	5432.8	5432.8	161.31	0.000
Material Type (Name)* Particle Size Reduction Method	2	2179.5	2179.5	1089.8	32.36	0.000
Error	12	404.1	404.1	33.7		
Total	17	10196				

Figures 9.6 and 9.7 show the plots of durability rating and size distribution index against the treatment variables. The plots show very strong main effects from both material type and material particle size, and a strong interaction effect between the two. Any briquette made from material that was hammer milled had a zero durability rating. The material type showed an increasing trend from corn stover and MOG to pure cobs. As indicated by the low values of the size distribution index, the remaining particles from any of the tests were much lighter than the original briquette, indicating that significant breakage occurred during the test regardless of the combination. Figure 9.6 shows the confidence interval for 'as received' MOG briquettes having a range below zero. This is not physically possible, as zero durability is the minimum possible value from this test. This is not accounted for in the statistical calculations, and it indicates that the data is not normally distributed, which is assumed when calculating the confidence intervals.

The durability improvement when moving from corn stover and MOG to pure cobs indicates two possibilities. Adding cob content to the briquetted material positively effects

durability, or adding stalk, leaf, and husk content to the material negatively impacts durability. Shifting across those materials from corn stover, to MOG, to pure cobs reduces the stalk and leaf content, and increases the cob content.

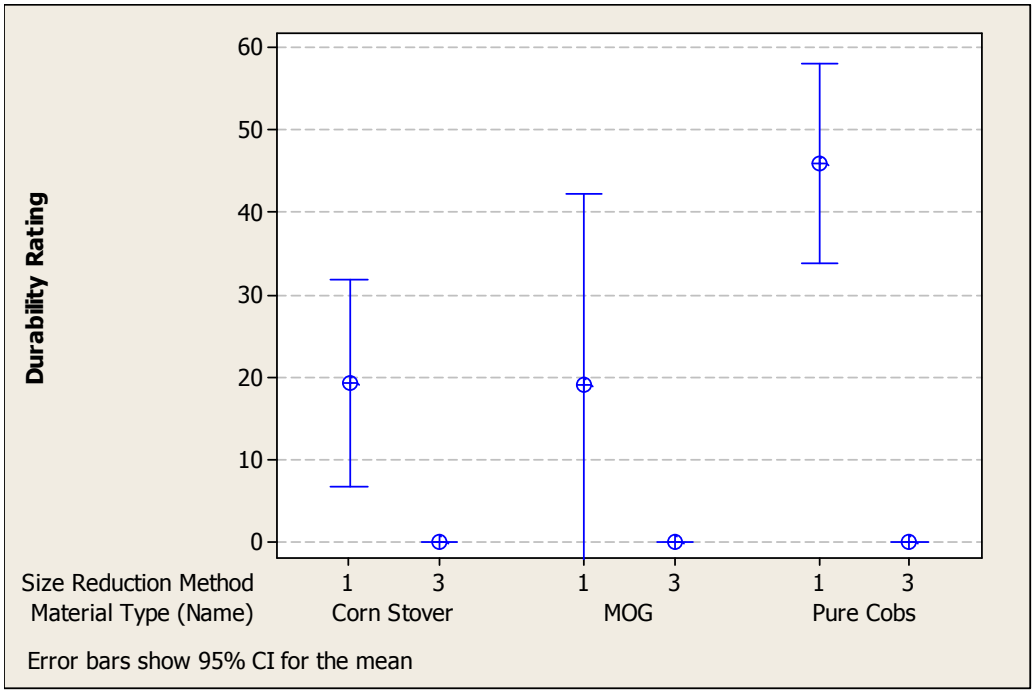

Figure 9.6. Treatment factor effects on durability rating (durability experiment)

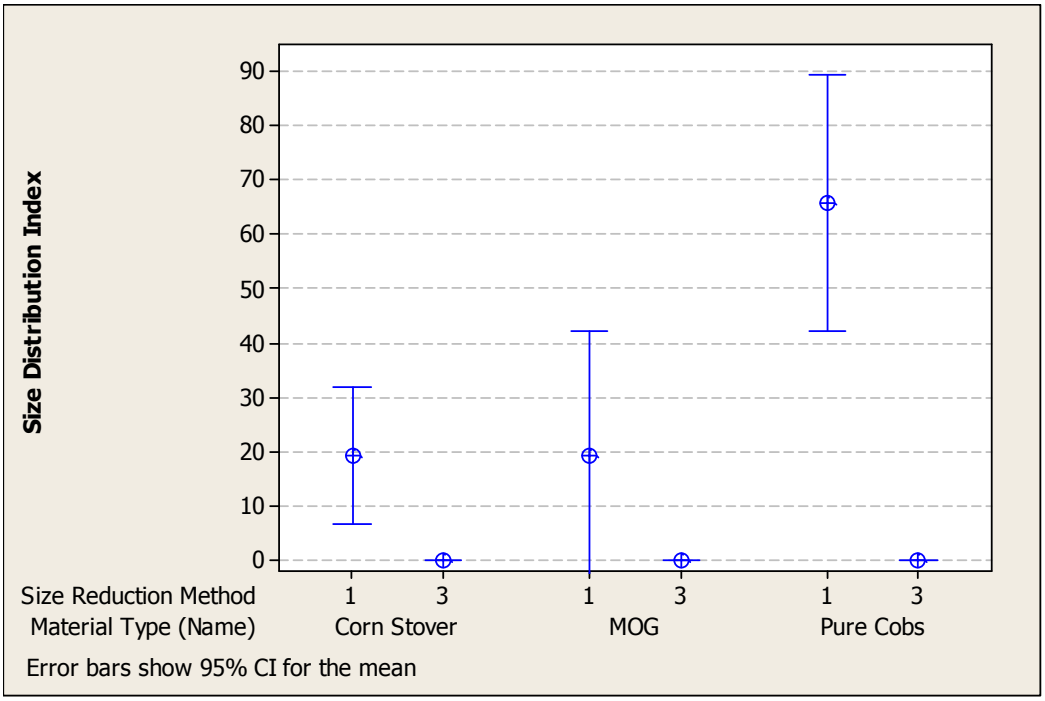

Figure 9.7. Treatment factor effects on size distribution index (durability experiment)

9.3.2. Qualitative Analysis

Tests that resulted in zero durability ratings had the same appearance after tumbling as the input product to the densification bench. Figure 9.8 shows a picture of a zero durability rating trial of hammer milled corn stover. All of the trials that resulted in a zero durability rating had about the same appearance.

Figure 9.8. Output product from a hammer milled corn stover tumbler test

The trials of 'as received' MOG briquettes showed improved durability ratings compared with the hammer milled samples, and this can be observed from the output sample from the tumbler (Figure 9.9). This material was able to retain a small amount of the original briquette mass and shape, with three remaining particles that were 20-40% of the original weight in this particular test. The remainder of the material either completely fractured back to loose material, or remained in single briquette flakes that were less than 20% of the original average briquette weight.

Figure 9.9. Output product from an 'as received' MOG tumbler test

The 'as received' pure cob briquettes demonstrated the best durability based on the output values, and this can also been seen in the output material (figure 9.10). This material was able to retain particles that weighed into the 20-40% and 40-60% mass class, and had very little product that was completely loose after the tumbling.

Figure 9.10. Output product from an 'as received' pure cob tumbler test

9.4. Comparisons

Comparing the results from these experiments to others found in the literature provides an indication of where these briquettes stand relative to other common briquetting and pelleting processes. The durability figures from the literature, however, utilize a different portion of the durability standard than the experiments conducted in this report, meaning the comparisons are not entirely equal.

The literature durability values were determined using the second portion of ASABE S269.4 (for pellets), which uses a similar tumbling apparatus, but calculates the durability rating in a different manner than the standard for cubes. Size Distribution Index is not calculated in this portion of the standard either. This portion of the standard is commonly used for densified particles with a much smaller volume than what is tested in this research. While this size difference made it unusable for this research, it provided good durability comparisons between other densified products. After the material is tumbled (in this portion of the standard), the output sample is screened with the top screen size having a diameter that is roughly 12-17% smaller than the mean geometric diameter of the pellets tested. The material that remains on the top screen is then weighed, and the durability rating is calculated using equation 9.3:

Equation 9.3. Durability rating for pellets

$$DR = \frac{M_{after}}{M_{before}} * 100$$

where

DR = Durability rating

M_{after} = Pellet mass on top screen after tumbling

M_{before} = Total pellet mass before tumbling

Table 9.4 shows the durability ratings across several studies identified through the literature search. The briquettes tested in the data found under (Sokhansanj, 2004), and (Kaliyan and Morey, 2008) were created using a uni-axial piston cylinder similar to the apparatus used in this research, although the material is pressed into a straight cylindrical die instead of a tapered cylindrical die. The materials used in (Kaliyan and Morey, 2009a) were created used pilot scale roll-press briquetting and ring-die pelleting mills.

Table 9.4. Durability comparisons with other experiments.

Experiment Information	Durability Rating	Input Material Details		
		Moisture Content (%wb)	Particle Size (mm)	Compression Pressure (MPa)
ISU Durability Testing				
Pure Cobs, Piston-Cylinder Briquetted	46	10%	39	14
MOG, Piston-Cylinder Briquetted	19	11%	31	14
Corn Stover, Piston-Cylinder Briquetted	19	8%	42	14
Sokhansanj, 2004				
Corn Stover, Piston Cylinder Briquetted	92	5-10%	5.6	15
Corn Stover, Piston Cylinder Briquetted	88	15%	5.6	15
Kaliyan and Morey, 2008				
Pure Cobs, Piston-Cylinder Briquetted	0	10-20%	0.9-2.8	150
Kaliyan and Morey, 2009a				
Corn Stover, Roll-Press Briquetted	67-88	7-17%	0.34-0.36	NA
Corn Stover, Ring-Die Pelleted	94-95	19-22%	0.34-0.36	NA

The durability levels of the all briquettes tested in this research are considerably lower than those observed in most of the other experiments from the literature. Some of the key differences that could cause this durability difference include:

- Briquettes tested in this research were considerably larger in mass and volume than all briquettes and pellets in the other experiments from the literature.
- The input material particle sizes used in this research were considerably larger than materials from other experiments in the literature.
- Durability testing experiments were different, and a direct comparison may not be entirely accurate.

9.5. Conclusions

Overall, the durability performance of the process variable combinations tested was quite low. Materials conditioned on a hammer mill to reduce particle size all had zero durability during tumbler testing. The best material in this testing (pure cobs) still had low durability ratings when compared with other densification experiments found in the literature

review. Based on both the tumbler data, and qualitative observations, the following setting changes will improve briquette durability (within the ranges specified)

- Increasing compression pressure (2.5 – 14.0 MPa)
- Decreasing moisture content (5-55% MCwb)
- Increasing particle size (2-39 mm)
- Increasing cob content of material

Even though the durability ratings of this type of material are quite low, a densified corn stover feedstock produced at these settings could still provide a good potential for in-field harvest systems. The handling operations required to get the material harvested, transported, and stored would likely be less intense and frequent than those simulated using this apparatus. Defining the durability requirements for a densified product produced using in-field biomass harvesting systems to deliver a feedstock to an upgrading or processing plant would provide a better idea of the potential of this type of briquetting for large scale biomass production.

Chapter 10. Power & Energy Analysis

10.1. Objectives

The previous chapters showed dry specific energy data for different treatment variable combinations, but this did not provide a complete illustration of the requirements for a briquetting process. The objective of this analysis was to compare the energy requirements of this system with other densification systems from the literature, and to determine the power requirements of a full-scale version of this system. To accomplish these goals, specific sub-objectives were developed:

- Determine optimal briquetting treatments based on briquette density and durability, and determine the specific energy requirements of those treatment combinations.
- Compare the specific energy requirements of the optimum briquetting treatments found in this research with other comparable briquetting processes.
- Compare the energy requirements of the optimum briquetting treatments found in this research with comparable single-pass baling energy requirements.
- Determine theoretical power requirements for a 'full-scale' briquetting system with optimized treatment variables for single-pass harvesting scenarios.

10.2. Materials and Methods

10.2.1. Optimum Briquetting Treatments

An optimum briquetting condition was selected for all three material types tested in this research. Based on analysis of the durability and density results, the following guidelines were developed for selecting the optimum briquette treatment variable combinations.

- Only 'as received' material particle sizes should be used to improve briquette durability.
- Maximum compression pressure (14.0 MPa) should be used to maximize particle density, and to ensure any kind of particle durability.
- Only moisture contents below 25%wb should be used to maximize briquette density and durability.

- Die geometry did not show any density effects on particles, and was not tested as a variable in the durability analysis, so no confident recommendations can be made regarding die geometry. Briquettes made with a 3.6^{O} die taper angle were used in the optimum briquette treatments.

Based on those guidelines, three optimum briquetting treatments were selected for the power and energy analysis, one for each material type tested. Table 10.1 shows the treatment variable combinations, and their respective specific energy requirements:

Table 10.1. Optimum briquetting treatments and specific energy requirements

Constants	Value	Units
Particle Size	As Received	
Compression Pressure	14	MPa
Die Taper Angle	3.6	deg

Material Type	Particle Size (mm)	Material Moisture Content (%wb)	Dry Particle Density (kg/m^3)	Estimated Dry Bulk Density (kg/m^3)	Wet Specific Energy (MJ/t)
Corn Stover	42	8.3	460	191	20.4
MOG	31	11.3	425	176	27.2
Pure Cobs	39	10.2	421	175	25.5

10.2.2. Calculations

The calculations for determining the specific energy of the briquetting process are found in section 3.3.3. While the specific energy value provided a means of comparing the energy requirements of different processes, it did not provide a complete description of the requirements of a densification system. Calculating the power requirement of a densification machine operating at a certain mass flow provided an idea of the size of the power supply needed to accomplish the process. Theoretical machine power can be calculated using a known process flow rate, and is shown in equation 10.1:

Equation 10.1. Theoretical Machine Power

$$P_{MACHINE} = \frac{SE_{BRICK} * MF}{E_{MACHINE}}$$

where

$P_{MACHINE}$ = Theoretical machine power requirement (power at engine crankshaft)

MF = Material mass flow

$E_{MACHINE}$ = Machine power efficiency (assumed)

SE_{BRICK} = Specific energy of briquetting treatment (from densification experiments)

Data shown in section 10.3.2 describes specific energy in terms of the amount of fuel consumed on a machine. Comparing specific energy based on fuel consumption to specific energy based on pure mechanical energy is not valid, and would create a biased comparison. To provide an equal comparison between the two sources of specific energy data, the efficiency of the engine and drivetrain must be accounted for. Equations 10.2 and 10.3 show the calculations used in this analysis to relate the specific energy based on fuel consumption to the specific energy based on pure mechanical energy:

Equation 10.2. Theoretical machine specific energy, based on engine fuel consumption

$$SE_{MACHINE} = SE_{FUEL} * E_{FUEL}$$

where

$SE_{MACHINE}$ = Specific energy requirement of the densification machine

SE_{FUEL} = Specific energy requirement of the densification machine (based on engine fuel consumption)

E_{FUEL} = Engine fuel energy efficiency

Equation 10.3. Theoretical mechanical specific energy, based on machine specific energy

$$SE_{MECHANICAL} = SE_{MACHINE} * E_{MACHINE}$$

10.2.3. Single-Pass Baling

Iowa State University has tested a single-pass baling system to simultaneously harvest corn grain and corn stover. The single-pass baler produced a high-quality densified stover product, and provided a good metric against the briquetting system for comparison. Baler energy data was collected based on engine fuel consumption during the fall 2010 harvest at Iowa State University. This data correlated the total diesel fuel consumption to the total weight of baled stover over time, so a specific energy requirement was known for a given harvesting system.

The single-pass baler was powered by a 4-cylinder, 4.4L turbocharged Perkins diesel engine rated at approximately 86 kW (115 Hp). The same engine is used in an AGCO Challenger MT465B tractor and rated at 84.3 kW (113 Hp) based on Nebraska OECD test 2527. At maximum power, this tractor is rated for a fuel efficiency of 3.28 kW*h/l (16.67 Hp*hr/gal), which equates to a fuel efficiency of about 31% (the efficiency of converting the specific energy of diesel fuel to shaft power at the PTO). To facilitate a relatively equal comparison between the briquetting and baling system, the following assumptions were used:

- The scaled-up briquetting system and single-pass baler are both continuously operated at maximum power, and the fuel efficiency of their power source is the same as that found on the MT465B at the PTO ($E_{FUEL} = 0.31$).
- The mechanical drive system efficiency of both the single-pass baler and scaled-up briquetting system was assumed to be 80% ($E_{MACHINE} = 0.8$)

10.3. Results

10.3.1. Specific Energy Comparisons to Briquetting Processes

Comparisons made in this section are drawn from briquetting experimental data collected at the University of Minnesota and the University of British Columbia. These experiments consisted of densification machines similar to the bench developed for this research, and some commercially available pelleting equipment. The experiment descriptions and treatment variable levels are all listed in table 10.2.

Figure 10.1 shows a chart of specific energy comparisons between comparable briquetting experiments. The number above each bar corresponds to a treatment combination from table 10.2. All specific energy values shown in figure 10.1 represent the energy required to accomplish the densification process, but do not include any energy required for initial material processing (mainly size-reduction processes). Several comparisons can be made from all these experiments:

- Corn stover can be densified to approximately 40% the density of a pellet from a ring-die pelleting mill, but at approximately 9% the energy requirement.

- Pure cobs can be densified to approximately 45% the density of the briquettes produced at 150 MPa, and at 50% the specific energy requirement, but without any additional particle size reduction processes.
- Reducing particle size from 42 to 5.6 mm will increase briquette density by about 75%, and energy consumption by about 30%, not including the energy required to size-reduce the material.

Table 10.2. Treatment variable list for specific energy comparisons

Number	Experiment Bibliographic Reference	Densification Machine	Compression Pressure (MPa)	Particle Size (mm)	Material Moisture Content (%wb)	Material Type (Name)	Dry Particle Density (kg/m^3)
1		ISU Densification Bench	14	42	8%	Corn Stover	460
2	2004, Mani	Hydraulic Press	15	5.6	10%	Corn Stover	810
3	2006, Kaliyan and Morey	INSTRON	100	0.8	10%	Corn Stover	1224
4	2006, Kaliyan and Morey	INSTRON	150	0.8	10%	Corn Stover	1220
5	2009, Kaliyan and Morey	Ring-Die Pelleting Machine	NA	0.34	20%	Corn Stover	1070
6		ISU Densification Bench	14	31	11%	MOG	425
7		ISU Densification Bench	14	39	10%	Pure Cobs	421
8	2008, Kaliyan and Morey	INSTRON	150	0.85	9%	Pure Cobs	942

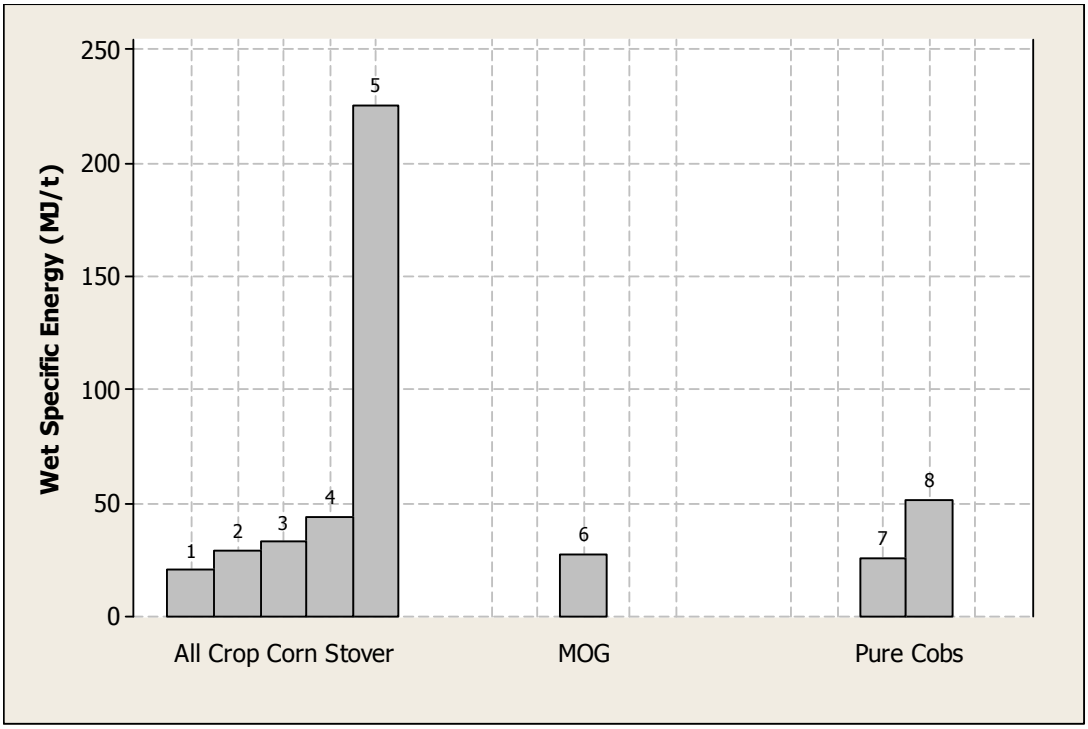

Figure 10.1. Specific energy comparison between briquetting processes

10.3.2. Specific Energy Comparison to Single-Pass Baling

Figure 10.2 shows the comparison of the specific energy requirements between the single-pass baling system and the scaled-up briquetting system. Based on the fuel consumption data, large square baling requires about 2.5 times less the specific energy requirement of briquetting corn stover with the treatment variables described in row 1 of table 10.1. Bales produced during this testing had a dry bale density of approximately 160 kg/m^3, while the briquettes produced at the treatment variables described had a dry bulk density of 190 kg/m^3.

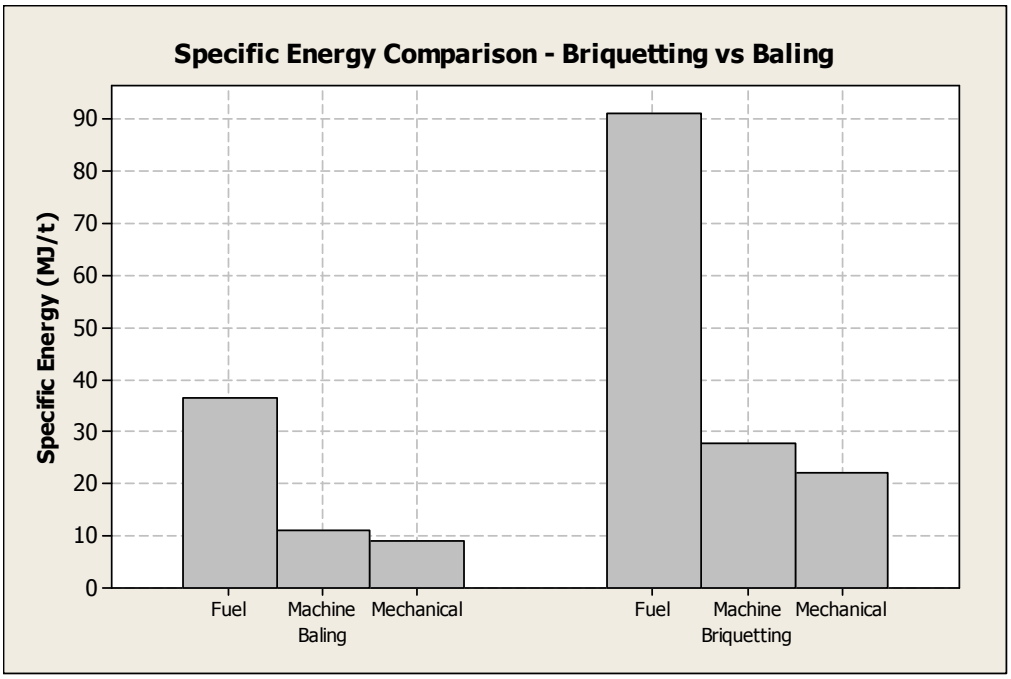

Figure 10.2. Specific energy comparison between single-pass baling and briquetting systems.

10.3.3. Scaled-Up Briquetting Power Requirements

Corn stover mass flow data was collected during the single-pass harvesting tests conducted in the fall 2009 and 2010 harvest at Iowa State University. The data collected showed corn stover flow from a class 8 combine can be sustained up to 4.5 kg/sec (10 lb/sec) when harvesting with a 12 row all-crop header. When harvesting corn with a conventional header the same class 8 machine could sustain MOG mass flows up to 2 kg/sec (4.5 lb/sec). Mass flow rates for a pure cob harvest are not known, but are likely less than the MOG mass

flow rate (based on a smaller mass yield of pure cobs compared with MOG). These mass flow rates can be related to specific power requirements for each harvesting type.

Power requirements for a full-scale briquetting system with mass flow rates up to 7 kg/sec (15 lb/sec) are shown in figure 10.3. Briquetting corn stover at 4.5 kg/sec theoretically requires 115 kW (154 Hp), while briquetting MOG at 2 kg/sec could theoretically be accomplished using 68 kW (91 Hp). The power requirements for a briquetting process will also likely be more consistent those for a baling process. The baler only allows material flow to the chamber when a specified amount is available. This helps maximize bale quality, but also creates an inconsistent power requirement for the system. Figure 10.4 shows the engine torque curve during a baling operation. The spikes from 115 to 184 seconds illustrate the points where material flow was allowed to the baling chamber. The torque requirement abruptly increases at the presence of material to densify, and then decreases until material is fed through again. Traditional briquetting equipment would likely not demonstrate this same trend, as the process is continuous.

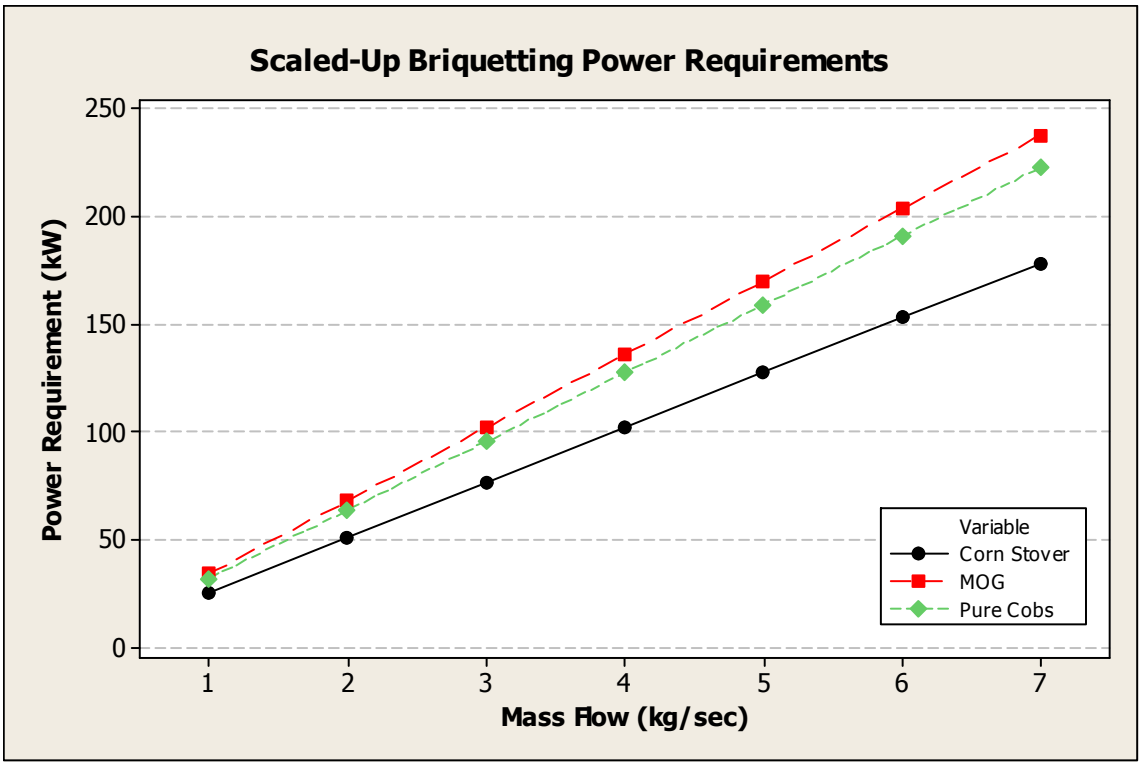

Figure 10.3. Scaled-up briquetting power requirements

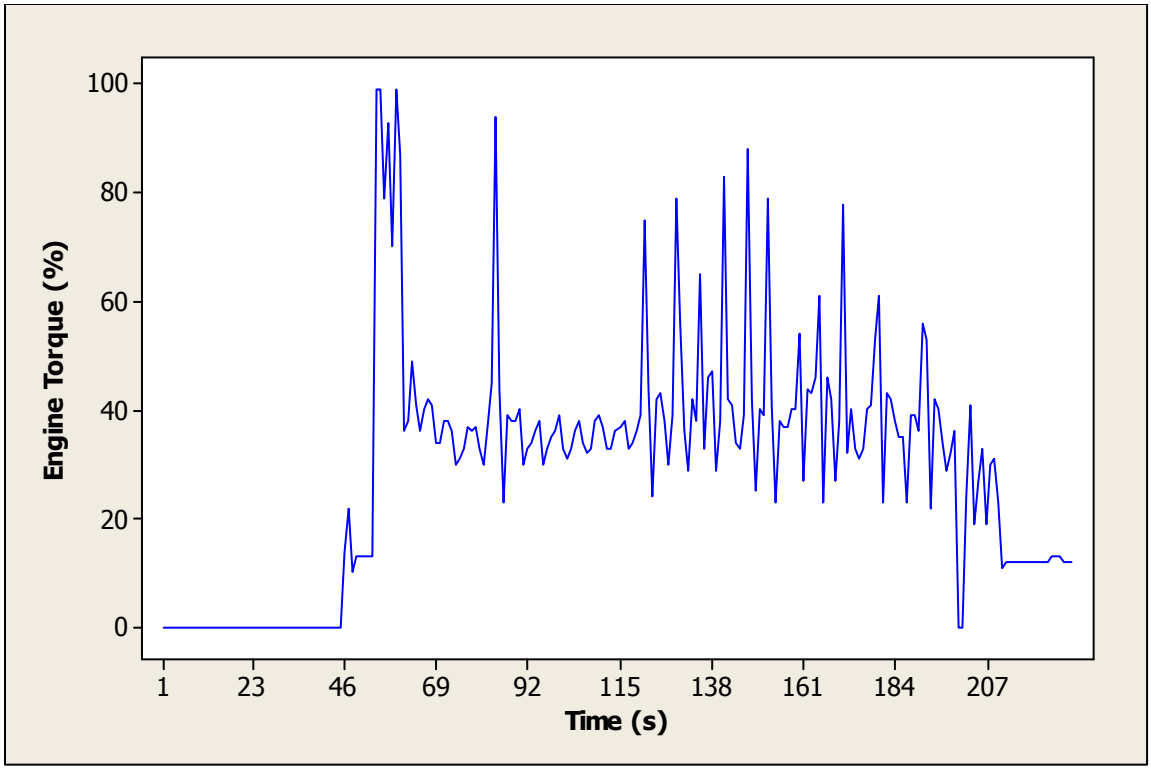

Figure 10.4. Baler engine torque curve during operation

10.4. Conclusions

The specific energy results gathered from the briquetting experiments described in this paper correlate very closely with relationships shown in similar experiments.

Data presented from other experiments showed that high-quality briquettes can be produced at higher compression pressures and smaller particle sizes than were tested in this research. The energy requirements, however, demonstrated that engine sizes traditionally used in agriculture today would not be sufficient to accomplish these briquetting processes in a single-pass system. Extreme particle size reduction would also be required to complete these densification processes, adding to the specific energy requirement of each process. Single-pass baling required about 60% less energy than this briquetting system, however, it produced bale densities about 20% lower than the bulk density of briquettes.

Key points that can be taken from these comparisons and scaled up power requirements include:

- Briquetting at the optimized settings found in this research requires significantly more energy than a comparable single-pass baling system, however, it can produce a more dense product that can be handled as a bulk material.
- Briquetting at lower compression pressures and higher particle sizes can produce briquettes with roughly 30-50% the density of the high pressure briquettes, and at 30-50% the energy requirement, but without any additional size reduction processes.

Chapter 11. Conclusions

11.1. Process Variable Summary

While each individual experiment did not reveal significant relationships with all of the process variables, between all of the experiments, distinct relationships for each process variable were identified. No consistently significant interaction effects were observed during any of the experiments. The following is a summary of the effects of each process variable. Data for each process variable was selected based on the optimal combination of the other process variables, so the data shown represents the best outputs a process variable level can achieve. Data for each treatment variable setting can be referenced back to the interval plots for each experiment in chapters 4-9.

Compression speed was tested for main and interaction effects (from 0.8 to 4.6 m/min) and demonstrated no significant effect on dry particle density or dry specific energy. Die taper angle was also tested at two levels (3.6, 7.2^{o}) during the testing period, and the two angles showed no significant differences or trends with respect to both dry particle density or dry specific energy.

Compression pressure demonstrated significant and predictable effects on the output factors (table 11.1). Compression pressure was tested from 7-14 MPa during the testing period, and positive, fairly linear trends were demonstrated with respect to dry particle density, dry specific energy, and durability rating. While the density values were excellent and specific energy requirements were good at 14 MPa compression pressure, the durability rating was poor at these compression pressure levels for corn stover. Pure cob briquettes produced significantly higher durability ratings at these same settings. If the positive trend continues past 14 MPa compression pressure for durability rating, increasing compression pressure may be a good method for obtaining acceptable durability levels for production.

Table 11.1. Compression pressure effects summary

Compression Pressure Effects			
Compression Pressure *(MPa)*	Particle Density *(kg/m^3)*	Specific Energy *(MJ/t)*	Durability Rating *(%)*
7	Good *(310)*	Very Good *(16.3)*	Very Poor *(0)*
10.5	Very Good *(370)*	Very Good *(20.7)*	Very Poor *(0)*
14	Excellent *(459)*	Good *(22.3)*	Poor *(19)*

The experiments showed the most extreme effects on all of the output factors were sourced from material moisture content (table 11.2). Material moisture content was tested on corn stover ranging from approximately 10-55%wb throughout the testing period, and between approximately 10-25%wb, briquette quality (namely durability) would translate from good to unacceptable. Material bulk density would significantly decrease due to extreme amount of briquette expansion at moisture contents greater than 25%wb, and product durability was completely nonexistent above 25%wb. This indicates that future in-field densification systems based from this research will require materials dryer than 25%wb. Current biomass harvesting research at Iowa State University suggests two methods for reducing harvested material moisture content. For corn stover, keep the harvesting cut height as high as possible, because the upper half of the plant tends to dry down sooner than the lower half. MOG and pure cob harvesting also tends to produce a dryer feedstock than corn stover, so focusing a harvesting method on those material types could provide a more suitable feedstock for this type of densification.

Table 11.2. Material moisture content effects summary

Material Moisture Content Effects			
Material Moisture Content *(%wb)*	Particle Density *(kg/m^3)*	Specific Energy *(MJ/t)*	Durability Rating *(%)*
13	Very Good *(368)*	Good *(27.7)*	Poor *(28)*
25	Good *(316)*	Good *(26.0)*	Very Poor *(0)*
48	Very Poor *(214)*	Poor *(30.2)*	Very Poor *(0)*

Material particle size was not identified in any of the experiments for having consistently significant effects on particle density or specific energy, however, an extreme relationship was identified during the durability test (table 11.3). Any briquettes tested using materials that were size-reduced using the hammer mill had zero durability ratings. This is counter intuitive to the research materials from the literature, where it is generally accepted that particle size reduction has a positive effect on particle density and briquette durability. Based on the data collected from this research, and the energy data collected in the literature review, particle size reduction in this type of densification system offers no benefit to the process, and has very significant energy requirements. For this type of densification, any particle size reduction beyond the integrated chopper on the combine is not recommended.

Table 11.3. Material particle size effects summary

Material Particle Size Effects			
Material Particle Size Reduction Method *(name)*	Particle Density *(kg/m^3)*	Specific Energy *(MJ/t)*	Durability Rating *(%)*
As Received	Excellent *(459)*	Good *(22.3)*	Poor *(28)*
Vermeer HG200	Very Good *(422)*	Good *(23.5)*	NA
Hammermill, 19 mm screen	Very Good *(417)*	Very Good *(20.8)*	Very Poor *(0)*

Material type had very drastic effects, and pointed toward many of the same harvesting recommendations as material moisture content (table 11.4). While no consistent differences were identified between material types with regards to dry particle density and dry specific energy, the durability and overall briquette quality was significantly improved with an increased cob content (cob content increasing from corn stover to MOG to pure cobs). With the briquette durability and quality of corn stover already in the poor category, this suggests that this system could perform optimally by harvesting the MOG or pure cob fraction of the corn stover.

Table 11.4. Material type effects summary

Material Type Effects			
Material Type *(Name)*	Particle Density *(kg/m^3)*	Specific Energy *(MJ/t)*	Durability Rating *(%)*
Corn Stover	Excellent *(460)*	Good *(22.3)*	Poor *(19)*
MOG	Very Good *(424)*	Poor *(30.7)*	Poor *(19)*
Pure Cobs	Very Good *(421)*	Poor *(28.4)*	Good *(46)*

11.2. Large Scale Implications

The theoretical scaled-up power requirements showed that this briquetting method was well within the power capabilities of engines powering traditional agricultural equipment. The energy requirements were significantly higher than traditional baling systems, but a large-scale system like this could also potentially reduce down-stream fuel costs by eliminating bale collection. operations. Full-scale logistical research would be required to determine the 'system energy' consumption. Depending on the type and moisture of corn stover harvested, material can be continuously densified to approximately 190 kg/m^3 dry bulk density (210 kg/m^3 wet) behind a class 8 combine harvester with a 68-115 kW (91-154 Hp) engine (theoretically). This output bulk density offers a small improvement over baling technologies offered today, but still falls short of optimizing the hauling efficiency of over the road trucks. Briquettes produced in this research had marginal durability ratings based on the ASABE standard tumbling method, however, it is unknown how well this method correlates with the actual handling and durability requirements of a large-scale biomass production system.

11.3. Recommendations for Further Densification Research

This research provided basic information on large particle size and low pressure corn stover densification, but much more research is required before it can be determined if this process is feasible for large scale, in-field briquette production. Continued bulk-flowable densification research should address the following areas:

Comparing the durability test from ASABE S269.4 to the handling requirements for single-pass corn stover harvesting systems will provide more information on the validity of this test to biomass harvesting technologies. Intuitively, it appears that the ASABE standard durability testing procedure is significantly more violent on briquettes than traditional handling operations would be. Conducting research to quantify the number of handling operations and the accelerations seen by densified materials during these operations would be valuable in determining if the standard provides a good representation of the durability needed for this type of product, or if a low durability rating is acceptable. It would also better demonstrate whether these briquetted corn stover products are capable of retaining their density prior to further processing.

This research demonstrated continuous trends in the pertinent outputs with respect to compression pressure. Further research should test a wider range of compression pressures to provide a wider range of density and energy requirements. This will provide a larger picture of the cost-benefit relationship compression pressure has with bulk density and specific energy, and determine the required increase in compression pressure to produce a product optimized for over the road transportation.

The densification bench provided a suitable platform for testing process variables on small amounts of stover in a non-continuous process. The specific energy values are calculated from the pure mechanical energy to produce the briquettes, which did not account for the energy required to operate a complete densification machine. The next step in determining the feasibility of this type of densification is to enlarge the scale and make the process continuous. A prototype continuous flow densification machine catered to the optimized settings illustrated in this work should be fabricated for further development work. This will provide continuous energy and power data which should more closely correlate with the characteristics of a full-scale machine, as well as produce large scale densified samples so the bulk characteristics of this product can be analyzed.

Once these earlier research steps are taken, further work should be done to determine the handling characteristics of these briquetted materials. Being less dense and significantly larger in volume than traditional briquettes and pellets makes it probable that these materials will handle much differently than briquettes or pellets. Quantifying angle of repose, flowability through orifices, and other handling characteristics of these densified materials will provide critical information to the feasibility of this densification process.

References

ASABE Standards. 2007. S269.4 - Cubes, Pellets, and Crumbles-Definitions and Methods for Determining Density, Durability, and Moisture Content. 624-626. St. Joseph, MI.: ASABE.

ASABE Standards. 2008. S358.2 - Moisture Measurement-Forages. 1. St. Joseph, MI.: ASABE

ASABE Standards. 2007. S424.1 – Method of Determining and Expressing Particle Size of Chopped Forage Materials by Screening. 663-665. St. Joseph, MI.: ASABE

ASTM Standards. 2006. E873 – 82: Standard Test Method for Bulk Density of Densified Particle Biomass Fuels. West Conschohocken, PA.: ASTM

DOE-USDA. 2005. Biomass as a Feedstock for a Bioenergy and Bioproducts Industry: The Technical Feasibility of a Billion-ton Annual Supply. Oak Ridge, TN.: U.S. DOE Office of Scientific and Technical Information.

Iowa DOT. 2011. Iowa Truck Information Guide. Des Moines, IA.: Iowa DOT.

Kaliyan, N. and V. R. Morey. 2008. Densification Characteristics of Corn Cobs. ASABE Paper No. 084267. St. Joseph, MI.: ASABE

Kaliyan, N. and V. R. Morey. 2006. Densification Characteristics of Corn Stover and Switchgrass. ASABE Paper No. 066174. St. Joseph, MI.: ASABE

Kaliyan, N., V. R. Morey, M.D. White, and A. Doering. 2009a. Roll Press Briquetting and Pelleting of Corn Stover and Switchgrass. *Transactions of the ASABE 52(2)*: 543-555

Kaliyan, N., V.R. Morey, M.D. White, and D. G. Tiffany. 2009b. A Tub-Grinding/Roll Press Compaction System to Increase Biomass Bulk Density: Preliminary Study. ASABE Paper No. 096658. St. Joseph, MI.: ASABE

Knutson, J. and G. E. Miller. 1982. Agricultural residues in California – factors affecting utilization. *Leaflet No. 21303*, Cooperative Extension, Berkeley, CA: University of California.

Mani, S., S. Sokhansanj, and B. Xiaotao. 2004. Compaction of Corn Stover. ASABE Paper No. 041160. St. Joseph, MI.: ASABE

Mani, S., L. G. Tabil, and S. Sokhansanj. 2002. Grinding Performance and Physical Properties of Selected Biomass. ASABE Paper No. 026175. St. Joseph, MI.: ASABE

NASS-USDA. 2011. Crop Production. Washington, D.C.: Agricultural Statistics Board.

Nebraska Tractor Test Lab. 2009. *Nebraska OECD Tractor Test 2527 – Summary 713*. Lincoln: Nebraska Tractor Test Lab, University of Nebraska, Lincoln.

Pordesimo, L. O., B. R. Hames, W. C. Edens, and S. Sokhansanj. 2003. Variation in Corn Stover Composition and Energy with Crop Maturity. ASABE Paper No. 036085. St. Joseph, MI.: ASABE

Shinners, K. J., B. N. Binversie, and P. Savoie. 2003. Harvest and Storage of Wet and Dry Corn Stover as a Biomass Feedstock. ASABE Paper No. 036088. St. Joseph, MI.: ASABE

Sokhansanj S., and A. F. Turhollow. 2004. Biomass Densification – Cubing Operations and Costs for Corn Stover. *Applied Engineering in Agriculture 20(4)*: 495-499

Appendices

A. Bench Operating Procedure

The following is a step-by-step process for producing a briquette for process variable testing on the densification bench.

1. Ensure all preparations from the previous section have been completed, start up the computer, log into windows, and open up the Macro Embedded Excel File title Small_Press_Control_ExperimentName.xlsm.
2. Enable embedded content on the interface, and click all the "Find Current…" sensor buttons to read all the sensors and ensure functionality.
3. Set the experiment number you would like to begin on, and click the "Start Sequence – Updated Settings" button to begin.
4. Read the material requirements from the "Experiment Settings" window and procure the proper stover sample for the experiment.
5. Read the die geometry requirements from the "Experiment Settings" window and procure the correct die for the experiment. Install the die and the instrumented die cap. Click "OK" on interface
6. Measure the weight of the empty extra stover tub in pounds and enter the value in the "Extra Stover Tub Empty" window. Click "OK".
7. Measure the weight of the empty briquette tub in pounds and enter the value in the "Empty Briquette Tub" window. Click "OK".
8. Measure the weight of the full input stover weight tub in pounds and enter the value in the "Initial Stover Weight" window. Click "OK". Leave the full input stover tub on the scale to measure each input sample.
9. Add the specified amount of stover to the chamber and ensure that the top level of the stover is at or below the top of the plunger head.
10. Place both hands on the safety switches and hold.

11. Wait until message window on the interface notifies you of the completed cycle. If the screen prompts you for more stover, repeat the last 3 steps again. If it says that desired compression pressure has been reached, proceed to the next step.
12. Remove hands from safety switches, and click “OK” on the desired compression pressure has been reached.
13. Remove the 6 bolts from the instrumented die cap and use the hoist to swing it out of the way of the die.
14. Measure the stover expansion from the end of the die in inches and enter the value in the Cap Axial Expansion window. Click “OK”.
15. Measure the weight of the input stover tub in pounds, and put the stover sample back into storage. Enter the weight into the “Final Stover Weight” window. Click “OK”.
16. Remove the 6 bolts attaching the die to the material chamber, and remove the die from the bench. Place the die in the briquette ejection press.
17. Remove any material remaining in the material chamber or anywhere else on the bench. Place all material in the extra stover tub.
18. Measure the weight of the extra stover tub in pounds, and enter the weight in the “Extra Stover Weight” window. Click “OK”. Empty the tub into a waste stover disposal and place empty tub under the bench.
19. Ensure the die is placed in the ejection press as shown in figure, and the empty briquette tub is beneath the press.
20. Apply pressure from a compressed air tank using the hand valve to eject the briquette. Once briquette falls out of die, release pressure screw to allow plunger to return to its starting position.
21. Place briquette in briquette tub and measure the weight in pounds of the combination. Enter the weight value into the “Final Briquette Tub Weight” window and click “OK”.
22. Place briquette on clean table and align lengthwise with a tape measure.
23. Measure the length of the briquette in inches and enter in the “Briquette Length” window. Click “OK”.
24. Take a picture of the briquette and tape measure together to provide a recording of the length measurement.

25. Empty all tubs containing stover or briquettes into waste material disposal and place them in their original location.

B. Moisture Conditioning Procedure

The procedure for adding moisture to a stover sample to reach a desired moisture content is as follows:

1. Determine the current moisture content of the sample to add moisture content to using ASABE S424.1.
2. Weigh the complete sample of material to add moisture to. Using that as WW in equation 3.4, and the moisture content determined in step 1, solve for DW.
3. Using equation 3.4 again, calculate the desired WW based on the new desired moisture content.
4. Determine the weight of water to be added to the sample by subracting the desired WW from the current WW.
5. In a plastic tub, mist the weight of water from step 4 over the material. If a large pile of material is being treated, pause regularly to shake up sample to improve water distribution.
6. Once the necessary water is added, cover sample and allow to sit for at least 24 hours before using to allow material to absorb the moisture.
7. During the briquetting trials with the moisture conditioned material, take regular samples for moisture content measurement to ensure the desired moisture content is obtained.